

THE SYNTHESIS AND CHARACTERIZATION OF
INORGANIC REDOX REAGENT-MODIFIED
CYTOCHROMES *C*

Thesis by
Kathryn Mary Yocom

In Partial Fulfillment of the Requirements
for the Degree of
Doctor of Philosophy

California Institute of Technology
Pasadena, California

1982

(Submitted December 11, 1981)

(C) 1981

Kathryn Mary Yocom

All Rights Reserved

To

Mother and Dad

ACKNOWLEDGEMENTS

I would like to acknowledge my "fearless leader", Harry B. Gray, for his support and enthusiasm. Thanks to his constant encouragement I, too, became attached to cytochrome *c*. I am also grateful to my unofficial advisors, Milo Bordignon, John Hopfield, Chuck Root, and Henrique Toma, for their invaluable contributions to this research project.

I gratefully acknowledge the HPLC and amino acid analysis expertise of Joan and Roger Shelton, respectively. But for their willingness to run "just a few more samples" this thesis would not have been completed. Vern Taniguchi, Walther Ellis, Vince Camarata, and Huey-jenn Chiang are thanked for their assistance with spectroelectrochemical measurements.

Members of the Gray group past are thanked for their wit and wisdom, especially Bob and Pom Scott, A. Grant Mauk, Steve Schichman, Cathy Coyle, Andy Maverick, Vanessa Lum, Barry Dohner, Dave Dooley, and Jim McArdle. Members of the Gray group present are thanked for more of the same.

Time and expertise were generously provided by innumerable members of the Caltech staff, for which I am grateful. Special thanks go to Charlie Beebe, Pat Bullard, Catherine May, and Rhonda Campbell. Mary Arguijo is thanked for her expert typing of this thesis, as is Valerie Purvis for drawing the figures.

Last, but not least, Michael Steigerwald, Penny Eidem, and Ann English are thanked for "the stuff lasting friendships are made of".

ABSTRACT

A stable complex is formed between pentaammineruthenium-(III) and the imidazole moiety of histidine-33 in cytochrome *c*. This complex is the major mono-substituted product of the reaction between aquopentaammineruthenium(II) and horse heart cytochrome *c* at pH 7. It is isolated and purified by ion exchange chromatography on CM-cellulose. High-pressure liquid chromatography of the tryptic hydrolysate of the modified cytochrome *c* is shown to be an effective method for the identification of the pentaammineruthenium binding site. The spectrum of the modified peptide mimics that of the pentaamminehistidineruthenium(III) model complex. Spectro-electrochemical and optical absorption measurements show that the integrity of the native structure in the vicinity of the heme *c* group is maintained in the ruthenium-modified protein. The reduction potentials of the two redox sites of the modified protein, derived from cyclic voltammetric measurements at a gold electrode in the presence of 4,4'-bipyridyl, are: heme *c* ($Fe^{3+}/2+$), 0.26 V; $Ru(NH_3)_5(His-33)^{3+/2+}$, 0.15 V (vs. NHE). A-15 \AA separation between the two redox sites in this system is estimated from molecular models of cytochrome *c*. It is suggested that the specificity, stability, and redox properties exhibited by aquopentaammineruthenium(II) render it an ideal protein modification reagent for the production of "synthetic" multisite metalloproteins.

The criterion of product stability is not met by the aquopentacyanoferate(II) ion. The products isolated from the reaction of this reagent with cytochrome *c* are believed to be a mixture of histidine and methionine substitution products, and ionic association complexes. The relatively rapid dissociation of the pentacyanoferate(II) moiety from the protein severely limits the extent to which the products can be characterized.

The synthesis of a cobalt(III)-cytochrome *c* complex is described. Tetrachloroplatinate(II) reacts specifically with methionine-65. Pyridine-4-carboxylatopentaamminecobalt-(III) is subsequently reacted with the platinum center. Unfortunately, the cobalt(II) form of the derivative is substitution labile, and the redox properties of the cobalt complex are highly unfavorable.

Intermolecular reductions of horse heart cytochrome *c*, *Pseudomonas aeruginosa* cytochrome *c*₅₅₁, *Pseudomonas aeruginosa* azurin, and *Rhus vernicifera* stellacyanin by hexaammine-ruthenium(II) are reported. Rate constants and activation parameters are presented. The results are discussed in terms of electron transfer distances for metalloprotein redox reactions.

TABLE OF CONTENTS

	<u>Page</u>
CHAPTER 1 - INTRODUCTION	1
References	17
CHAPTER 2 - KINETIC STUDIES OF THE REDUCTION OF SINGLE SITE METALLOPROTEINS BY HEXAAMMINERUTHENIUM(II)	
Introduction	21
Experimental Section	23
Results	33
Discussion	40
Appendix	48
References	49
CHAPTER 3 - SYNTHESIS OF A PYRIDINE-4-CARBOXYLATO- PENTAAMMINECOBALT(III) COMPLEX OF FERROCYTOCHROME C	
Introduction	54
Experimental Section	59
Results	69
Discussion	75
References and Notes	79
CHAPTER 4 - SYNTHESIS OF PENTACYANOFERRATE(II) COMPLEXES OF FERROCYTOCHROME C	
Introduction	82
Experimental Section	85
Results	89
Discussion	101
References and Notes	104

	<u>Page</u>
CHAPTER 5 - SYNTHESIS AND CHARACTERIZATION OF PENTAAMMINERUTHENIUM(III) COMPLEXES OF FERRICYTOCHROME <i>C</i>	
Introduction	108
Experimental Section	118
Results	146
Discussion	205
Appendices	213
References and Notes	229

CHAPTER 1

INTRODUCTION

The specificity of metalloprotein electron transfer reactions is largely a result of the environment imposed on the redox-active prosthetic group by the polypeptide chain. In simpler inorganic systems electron transfer can occur by direct interaction of the reactive species. When an electron is transferred between metalloproteins, or between prosthetic groups within a multisite protein, direct interaction of the redox sites is often precluded by the intervening protein material. The distance over which electron transfer occurs becomes an important consideration in understanding the mechanisms of metalloprotein redox reactions. This subject has received increased attention in recent years, and the approaches taken in addressing it have been varied.

Using kinetic data for the reactions of metalloproteins with inorganic complexes, Mauk, Scott, and Gray¹ have developed a method for determining the distance of electron transfer between the reactive metal centers, as well as the protein redox site-to-protein surface distance. The disposition of redox sites is illustrated in Figure 1.1. The total intersite distance, R , is a sum of the contributions from the protein, R_p , and from the inorganic reagent, R_r . ΔR_p is the protein redox site-to-surface distance. A modified form of Hopfield's² equation is used to calculate these distances from the experimental rate constants. ΔR_p values for several of the metalloproteins studied in our laboratory are listed in Table 1.1. The relatively

Figure 1.1. Components of the intermolecular electron transfer distance for the reaction of a single site metalloprotein (M_1) with an inorganic complex (M_2).

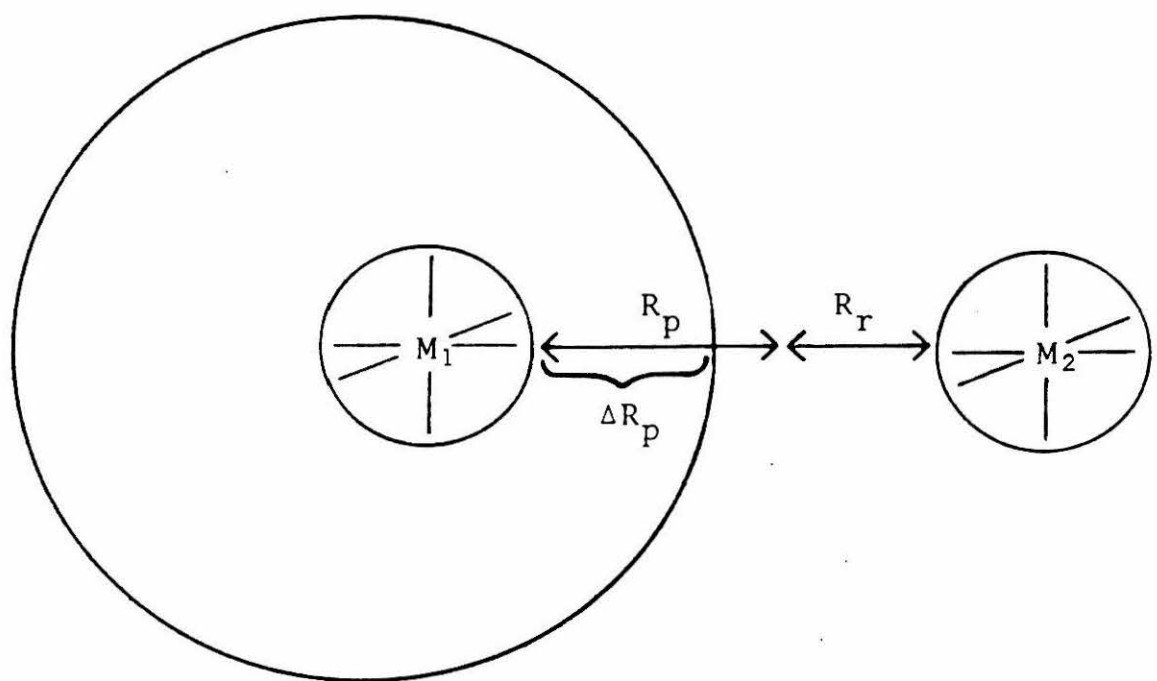


Table 1.1. Metalloprotein ΔR_p Values^a

Protein	ΔR_p (Å) ^b
stellacyanin	0
plastocyanin	2.6
cytochrome <i>c</i>	3.4
cytochrome <i>c</i> ₅₅₁	4.0
azurin	5.5
HiPIP	5.8

^aReference 1. ^bBased on $\text{Fe}(\text{EDTA})^{2-}$.

short distances obtained suggest that small inorganic reagents are limited only by how buried the redox site is in the protein; they are able to seek out the shortest electron transfer distance available. Inorganic reagents with hydrophobic, π -conducting ligands find even shorter transfer distances owing to their ability to penetrate the hydrophobic region of the protein.¹

The data base on which the above conclusions rest is fairly large. Inorganic complexes possessing assorted charges, reduction potentials, and ligand structures were reacted with a variety of single site metalloproteins. It was noted, though, that surprisingly few kinetic studies made use of positively charged, hydrophilic reagents. The hexaammineruthenium(II) ion is representative of this class of inorganic complexes. A kinetic study of the reduction of single site metalloproteins by hexaammineruthenium(II) is presented in Chapter 2. The results suggest that the assumptions made in the calculation of electron transfer distances for these systems are, in fact, assumptions, and that admission of slightly larger uncertainties in the values obtained is warranted. Nonetheless, the basic conclusions regarding metalloprotein-inorganic complex reactivity remain intact, *i.e.*, electron transfer between sites is a relatively short range phenomenon, occurring over distances on the order of eight Å or less.

There are exceptions to, and arguments with, the close contact mechanism for metalloprotein-inorganic complex reactions. Highly charged inorganic complexes are known to bind electrostatically to oppositely charged regions on the surface of proteins. For example, NMR evidence shows that $\text{Cr}(\text{CN})_6^{3-}$ binds to a positive region of cytochrome *c* about 10 Å from the heme group;³ $\text{Cr}(\text{phen})_3^{3+}$ binds to a negative patch on plastocyanin about 10 Å from the copper atom of the active site.⁴⁻⁶ Apparent rate saturation is observed in the kinetics of the redox active analogs of these reagents, *i.e.*, in the $\text{Fe}(\text{CN})_6^{4-}$ reduction of cytochrome *c*,⁷ and in the $\text{Co}(\text{phen})_3^{3+}$ oxidation of plastocyanin.⁸⁻¹⁰ The kinetics have been analyzed⁷⁻¹⁰ in terms of a precursor complex mechanism - the small molecule reagent binds to the protein with a binding constant, *K*, then transfers an electron intramolecularly with a rate constant, k_{et} . Alternatively, rate saturation at high reagent concentration can be analyzed in terms of a close contact mechanism^{11,12} - electron transfer occurs bimolecularly via a close contact pathway with formation of a dead-end complex at the more distant binding site accounting for the rate saturation. Evidence exists which supports both mechanistic arguments.¹² Furthermore, one cannot rule out the possibility that both pathways could contribute to the observed electron transfer reactivity.¹² The direct observation of electron transfer across known distances of 10 Å or greater in metalloprotein-small molecule precursor complexes has not yet been realized.

The distance question has also been addressed in purely physiological systems. Electron transfer between metalloproteins involves the interaction of two macromolecules. Often one, or both, of these molecules is membrane-bound. Given these constraints, it is not unrealistic to propose that the interacting redox sites are separated by long distances. Estimates of intersite distances in protein-protein systems obtained by a variety of techniques are shown in Table 1.2. Note that distances in excess of 10 Å predominate, in sharp contrast to the close contact distances calculated for metalloprotein-small molecule reactions.

Multisite metalloenzymes have received increased attention in recent years, owing in part to the importance of the reactions which they catalyze, *e.g.*, the reductions of molecular oxygen and nitrogen. In addition to their redox interactions with external reagents and/or proteins, electrons are shuttled intramolecularly between the various prosthetic groups within the macromolecule. Estimates of intramolecular electron transfer distances in multisite enzymes are given in Table 1.3.

Note that in Tables 1.2 and 1.3 a distinction is made between heme-edge-to-heme-edge distances and metal-to-metal distances. Electrons are readily transferred through heme groups and other π -conducting ligands (*e.g.*, imidazole). Thus, the important distance with respect to the determination

Table 1.2. Intermolecular Site-to-Site Distances in Metalloprotein Systems

Interacting Proteins	Distance	Experimental Technique	Reference
cytochrome <i>c</i> -cytochrome <i>c</i> peroxidase	7 Å ^a (15-20 Å ^c)	photoinduced electron transfer	13
	15-20 Å ^c	19 ^f NMR	14
	16.5 Å ^a	X-ray structure model	15
	19 Å ^b	resonance energy transfer	16
	>25 Å ^a	NMR linewidth	17
			Ω
cytochrome <i>c</i> -cytochrome <i>c</i> oxidase ($\alpha\alpha_3$)	15-18 Å ^{b,d}	resonance energy transfer	18
	25 Å ^{b,e}	resonance energy transfer	19
	35 Å ^{b,e}	resonance energy transfer	20
	18 Å ^b	resonance energy transfer	21
cytochrome <i>c</i> -cytochrome <i>b</i> ₂	8.4 Å ^a	X-ray structure model	22
cytochrome <i>c</i> -cytochrome <i>b</i> ₅	8 Å ^c	EPR	23
cytochrome <i>c</i> ₅₅₃ -cytochrome <i>c</i> ₅₅₅			

^aHeme edge-to-edge distance.^bHeme center-to-center distance.^cFe-to-Fe distance.^dCytochrome *c* to Cu of oxidase.^eCytochrome *c* to heme *a* of oxidase.

Table 1.3. Intramolecular Site-to-Site Distances in Multisite Metalloproteins

Protein	Distance	Experimental Technique	Reference
cytochrome <i>cd</i>	13-15 \AA ^a	kinetics analysis	24
cytochrome <i>c</i> ₃	10.9 \AA ^b 17.3 \AA ^c	X-ray crystal structure	25
xanthine oxidase	20-25 \AA ^d	EPR	26

^aHeme edge-to-edge distance. ^bShortest Fe-to-Fe distance in the 4-heme protein.

^cLongest Fe-to-Fe distance in the 4-heme protein. ^dMo-to-FeSI center distance.

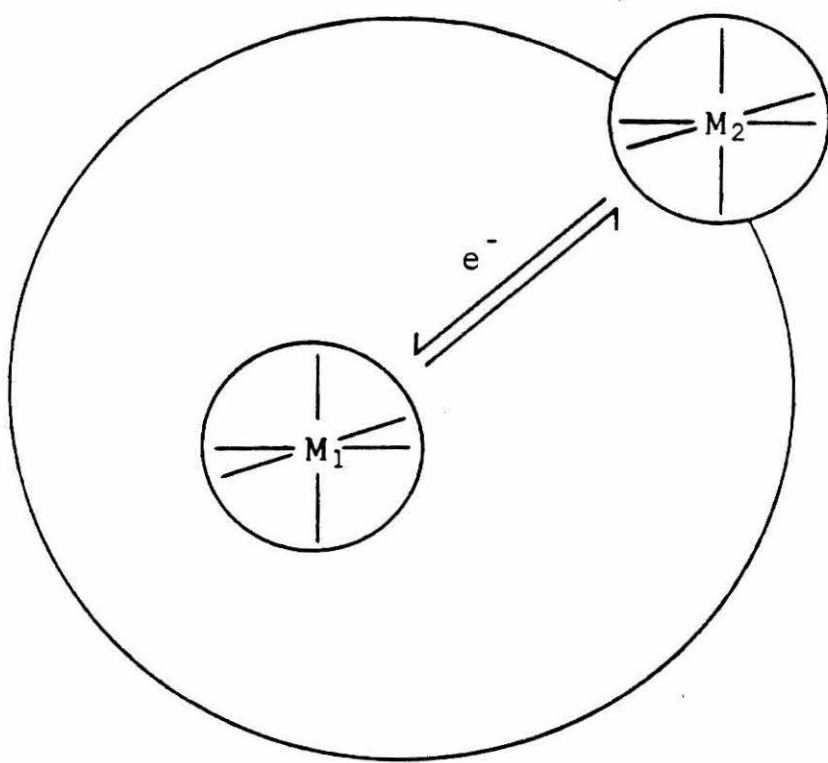
of the electron transfer barrier height is the *intersite* distance (*e.g.*, heme-edge-to-heme-edge), not the distance between metal atoms.

The information compiled in Tables 1.2 and 1.3 illustrates several problems. First, there is a high degree of variability (and often uncertainty) in the distances obtained by the various techniques listed. In the case of a single system, for example, cytochrome *c*-cytochrome *c* peroxidase, the range of heme-to-heme distances spanned is 7 to 25 Å. Second, many of the experimental techniques cited are capable only of measuring intersite distances in equilibrium situations. Depending on the mechanism, the actual distance between, and orientation of redox sites may differ in the dynamic situation. Third, the electron transfer theories and mechanisms presently being discussed in the literature are not compatible with the large intersite distances determined experimentally. The inner sphere and outer sphere electron transfer mechanisms so familiar to inorganic chemists²⁷⁻³⁰ are essentially short range phenomena. (Intramolecular electron transfer has been observed over metal-to-metal distances up to 15 Å in transition metal systems, however, the bridging ligands in these systems possess delocalized π orbitals which mediate the electron transfer.³¹ The *intersite* distance is therefore essentially zero.) Hopfield² and Jortner³² have formulated electron

tunneling theories to deal with biological electron transfer processes, but these too predict a low probability of electron transfer between sites separated by greater than 10 Å.

The studies to be described in Chapters 3-5 are designed to directly address the rate-distance question in metalloprotein electron transfer reactions. The approach taken is illustrated in Figure 1.2. A structurally well characterized protein containing a single metal redox center (M_1) is chosen. A second redox center (M_2) in the form of an inorganic complex is covalently attached to the surface of the metalloprotein. This produces a system in which two redox active metal centers are fixed at a known distance in a protein environment. Such a derivative is a synthetic multisite metalloprotein that should be a good model for intraprotein electron transfer. In intermolecular reactions, just such a fixed-site situation is created physiologically when electrostatic binding occurs between two proteins prior to electron transfer, or when the interacting proteins are membrane-bound. A redox reagent-derivatized protein is also a way to deal directly with the questions being raised in the interpretation of metalloprotein-inorganic complex kinetic data. By defining the intersite distance restrictions for metalloprotein electron transfer, the feasibility of various suggested intramolecular/precursor complex mechanisms may be assessed more critically.

Figure 1.2. Covalent attachment of a redox-active inorganic complex (M_2) to the surface of a metalloprotein (M_1).



The generality of the synthetic approach outlined above makes it adaptable to variations of the single site metalloprotein and variations of the attached redox reagents. The result is a range of intersite distances and molecular properties ideally suited to addressing important mechanistic questions: Can electron transfer occur efficiently over long distances, *i.e.*, 10, 20, 30 Å? Are large protein conformational changes necessary to bring the two metal centers together prior to electron transfer? Is electron transfer between sites a sensitive function of the nature of the intervening protein material? Are the electron transfer theories currently available adequate to describe the observed reactivity or are new theories demanded?

In this thesis the synthesis and characterization of three protein-metal complex derivatives will be described. The metalloprotein employed in all three cases is horse heart cytochrome *c*, a heme-containing, mitochondrial electron transport protein. The three different coordination complexes, chosen for their favorable substitution and redox properties, are pyridine-4-carboxylatopentaamminecobalt(III), aquopentacyanoferrate(II), and aquopentaammineruthenium(II).

Cytochrome *c* was the metalloprotein of choice for these studies for several reasons. Most important, it is structurally well characterized.³³⁻³⁹ Therefore, once the site of attachment of the inorganic complex is identified the distance between the two metal centers can be determined

from the crystal structure data. Second, there is a large body of information in the literature on the intermolecular electron transfer reactivity of cytochrome *c* with small molecule reagents, as well as with other metalloproteins. Lastly, a more practical aspect, cytochrome *c* is commercially available in the quantities required for protein modification studies.

REFERENCES

1. Mauk, A.G.; Scott, R.A.; Gray, H.B. *J. Am. Chem. Soc.* 1980, 102, 4360.
2. Hopfield, J.J. *Proc. Natl. Acad. Sci. USA* 1974, 71, 3640.
3. Hopfield, J.J.; Ugurbil, K. *Ayrlie House Symposium*, 1980, in press.
4. Cookson, D.J.; Hayes, M.T.; Wright, P.E. *Nature* 1980, 283, 682.
5. Cookson, D.J.; Hayes, M.T.; Wright, P.E. *Biochim. Biophys. Acta* 1980, 591, 162.
6. Handford, P.M.; Hill, H.A.O.; Lee, R.W.; Henderson, R.A.; Sykes, A.G. *J. Inorg. Biochem.* 1980, 13, 83.
7. Miller, W.G.; Cusanovich, M.A. *Biophys. Struct. Mech.* 1975, 1, 97.
8. Segal, M.G.; Sykes, A.G. *J.C.S. Chem. Comm.* 1977, 21, 764.
9. Segal, M.G.; Sykes, A.G. *J. Am. Chem. Soc.* 1978, 100, 4585.
10. Lappin, A.G.; Segal, M.G.; Weatherburn, D.C.; Sykes, A.G. *J. Am. Chem. Soc.* 1979, 101, 2297.
11. Yoneda, G.S.; Holwerda, R.A. *Bioinorg. Chem.* 1978, 8, 139.
12. Mauk, A.G.; Bordignon, E.; Gray, H.B., submitted for publication in *J. Am. Chem. Soc.*
13. Potasek, M.J. *Science* 1978, 201, 151.

14. Smith, M.B.; Millett, F. *Biochim. Biophys. Acta* 1980, 626, 64.
15. Poulos, T.L.; Kraut, J. *J. Biol. Chem.* 1980, 255, 10322.
16. Leonard, J.J.; Yonetani, T. *Biochemistry* 1974, 13, 1465.
17. Gupta, R.K.; Yonetani, T. *Biochim. Biophys. Acta* 1973, 292, 502.
18. Glatz, P.; Chance, B.; Vanderkooi, J.M. *Biochemistry* 1979, 18, 3466.
19. Dockter, M.E.; Steinemann, A.; Schatz, G. *J. Biol. Chem.* 1978, 253, 311.
20. Vanderkooi, J.M.; Landesberg, R.; Hayden, G.W.; Owen, C.S. *Eur. J. Biochem.* 1977, 81, 339.
21. Vanderkooi, J.M.; Glatz, P.; Casadei, J.; Woodrow, G.V. *Eur. J. Biochem.* 1980, 110, 189.
22. Salemme, F.R. *J. Mol. Biol.* 1976, 102, 563.
23. Tiede, D.; Leigh, J.S.; Dutton, P.L. *Biochim. Biophys. Acta* 1979, 503, 524.
24. Schichman, S.A. Ph.D. Dissertation, University of Chicago, 1981.
25. Haser, R.; Pierrot, M.; Frey, M.; Payan, F.; Astier, J.P.; Bruschi, M.; LeGall, J. *Nature* 1979, 282, 806.
26. Lowe, D.J.; Bray, R.C. *Biochem. J.* 1978, 169, 471.
27. Reynolds, W.L.; Lumry, R.W. "Mechanisms of Electron Transfer"; Ronald Press: New York; 1966.
28. Basolo, F.; Pearson, R.G. "Mechanisms of Inorganic Reactions", 2nd ed.; Wiley: New York, 1967; Chapter 6.

29. Taube, H. "Electron Transfer Reactions of Complex Ions in Solution"; Academic Press: New York, 1970.
30. Linck, R.G. *Survey of Progress in Chemistry* 1976, 7, 89.
31. Fischer, H.; Tom, G.M.; Taube, H. *J. Am. Chem. Soc.* 1976, 98, 5512.
32. Jortner, J. *J. Chem. Phys.* 1976, 64, 4860.
33. Dickerson, R.E.; Timkovich, R. In "The Enzymes", 3rd ed.; Boyer, P.D., Ed.; Academic Press: New York, 1975; Vol. 11, Chapter 7.
34. Dickerson, R.E.; Takano, T.; Eisenberg, D.; Kallai, O.B.; Samson, L.; Cooper, A.; Margoliash, E. *J. Biol. Chem.* 1971, 246, 1511.
35. Swanson, R.; Trus, B.L.; Mandel, N.; Mandel, G.; Kallai, O.B.; Dickerson, R.E. *J. Biol. Chem.* 1977, 252, 759.
36. Takano, T.; Trus, B.L.; Mandel, N.; Mandel, G.; Kallai, O.B.; Swanson, R.; Dickerson, R.E. *J. Biol. Chem.* 1977, 252, 776.
37. Mandel, N.; Mandel, G.; Trus, B.L.; Rosenberg, J.; Carlson, G.; Dickerson, R.E. *J. Biol. Chem.* 1977, 252, 4619.
38. Takano, T.; Dickerson, R.E. *Proc. Natl. Acad. Sci. USA* 1980, 77, 6371.
39. Takano, T.; Kallai, O.B.; Swanson, R.; Dickerson, R.E. *J. Biol. Chem.* 1973, 248, 5234.

CHAPTER 2

KINETIC STUDIES OF THE REDUCTION OF
SINGLE SITE METALLOPROTEINS BY
HEXAAMMINERUTHENIUM(II)

INTRODUCTION

Marcus theory has been used effectively in our laboratory to assess the factors which govern electron transfer reactions between inorganic complexes and metalloproteins.¹⁻¹⁹ Reactivity patterns have emerged based on the comparison of electron transfer self-exchange rate constants (k_{11}) in a series of single site metalloproteins. Once corrected for electrostatic interactions between reactants, k_{11}^{∞} (∞ designates correction to infinite ionic strength) can be used to calculate the distance over which electron transfer occurs.¹⁸ The calculations employ a modified form of Hopfield's vibronically-coupled electron tunneling theory.²⁰

The major conclusions drawn from these studies are^{8,18}:

- 1) the reactivity of a metalloprotein redox site is strongly dependent on the location of the site relative to the protein surface;
- 2) the enhanced reactivity of reagents possessing hydrophobic, π -conducting ligands arises from their ability to penetrate the protein interior; and
- 3) hydrophilic reagents apparently cannot penetrate hydrophobic protein interiors and are forced to transfer electrons over longer distances by less efficient nonadiabatic pathways.

The inorganic redox complexes studied most extensively to date include hydrophobic, negatively charged reagents ($\text{Fe}(\text{dipic})_2^{2-}$,^{16,19} $\text{Co}(\text{dipic})_2^{-}$,^{16,19}), hydrophobic, positively charged reagents ($\text{Co}(\text{phen})_3^{3+}$,^{1,3,9,14,17,21-24}

$\text{Ru}(\text{NH}_3)_5\text{py}^{3+}$ ^{13, 23}), and hydrophilic, negatively charged reagents ($\text{Fe}(\text{EDTA})^{2-}$,^{2, 3, 5, 10, 12, 15, 25} $\text{Co}(\text{EDTA})^{-}$ ^{26, 27}).

The hydrophilic, positively charged complex chosen to complete this study of single site metalloprotein reactivity was the hexaammineruthenium(II) ion. The kinetics of reduction of horse heart cytochrome *c*, *Pseudomonas aeruginosa* cytochrome *c*₅₅₁, *Pseudomonas aeruginosa* azurin, *Phaseolus vulgaris* plastocyanin, and *Rhus vernicifera* stellacyanin by hexaammineruthenium(II) are presented here.

The reaction of cytochrome *c* with hexaammineruthenium(II) is also relevant to the chemical modification studies to be presented in Chapter 5. The hexaammineruthenium(II) reduction of pentaammineruthenium-modified cytochrome *c* exhibits kinetic behavior markedly different from that of native cytochrome *c*.

EXPERIMENTAL SECTIONMaterials

Horse heart cytochrome *c* (type VI) was purchased from Sigma Chemical Co. and used without further purification. *Pseudomonas aeruginosa* cytochrome *c*₅₅₁ and azurin, *Phaseolus vulgaris* plastocyanin, and *Rhus vernicifera* stellacyanin were isolated and purified by methods employed previously in this laboratory.^{2,12} The samples used for kinetics experiments had the following ratios: cytochrome *c*₅₅₁, A₅₅₁/A₂₈₀ = 1.2; azurin, A₆₂₅/A₂₇₈ = 0.47; plastocyanin, A₂₇₈/A₅₉₇ = 1.2; stellacyanin, A₂₈₀/A₆₀₄ = 7.8, 6.0. Disposable Millex-GS 0.22 μ m filter units used for filtration of protein solutions were obtained from Millipore Corp.

Ruthenium(III) chloride (RuCl₃•3H₂O) used in the preparation of hexaammineruthenium(II) chloride was obtained from Johnson Matthey, Inc. (through Alfa). All other chemicals were reagent grade and were used as supplied.

Rubber serum stoppers were cleaned before use either by boiling in solutions of 1 M NaOH and 1 M HCl, or by soaking in solutions of ethanolic-KOH and ethanolic-HCl.

Distilled water was purified by passage through a Barnstead Nanopure water purification system (Model D1974). A series of scrubbing devices (one MnO/vermiculite column²⁸ followed by two proflavin/methylviologen towers²⁹) was used to remove oxidizing impurities from the argon used in

kinetics experiments. Argon used in the synthesis of hexaammineruthenium(II) chloride was passed through two vanadous scrubbing towers.

Methods

Hexaammineruthenium(II) Chloride. The chloride salt of hexaammineruthenium(II) was prepared according to the method of Lever and Powell.³⁰ It was recrystallized in the following manner. Two grams of crude product were dissolved in 20 mL boiling aqueous ammonia (15%). Zinc powder (*ca.* 0.5 g) was added to insure complete reduction of the ruthenium. The hot solution was filtered through a sintered glass funnel to remove the zinc. All operations subsequent to the filtration were carried out under a stream of argon. Solid ammonium chloride (or a saturated solution thereof) was added to reprecipitate the product. After cooling in an ice bath, the solution was filtered. The yellow-orange crystalline product was washed with cold aqueous ammonia (29%) followed by cold acetone. The complex was dried in a vacuum desiccator. Yield *ca.* 1 g. Anal. Calcd.: Ru, 36.87; N, 30.65; H, 6.62; Cl, 25.86. Found: Ru, 36.93; N, 30.91; H, 6.52; Cl, 25.1.

Analysis of the % Ru reported above was carried out spectrophotometrically using a modification of literature procedures^{31,32} based on the oxidation of ruthenium to ruthenate (RuO_4^{2-}) and perruthenate (RuO_4^-). A sample of

ruthenium complex (*ca.* 5 mg) was dissolved in 5 mL of 2 M KOH. 0.1 g potassium persulfate ($K_2S_2O_8$) was added and the solution was boiled for 5-10 min. After allowing to cool, the solution was diluted to 25 mL with 2 M KOH.

The absorbance at 415 nm (isobestic wavelength of RuO_4^{2-} and RuO_4^-) was recorded against a solution blank. Ruthenium concentration was calculated using $\epsilon_{415} = 1047 M^{-1} cm^{-1}$.³²

Solutions of hexaammineruthenium(II) ion for use in kinetics experiments were prepared by dissolving a weighed amount of hexaammineruthenium(II) chloride in deoxygenated buffer (pH 7.0 phosphate, $\mu = 0.1$ M). The quantity of ruthenium complex desired was weighed on a Cahn Gram Electrobalance (Model G) and placed in a stopped serum bottle. The bottle was flushed with argon via a platinum needle for a minimum of 0.5 hour before addition of deoxygenated buffer. The buffer was bubbled with argon for at least one hour before use and was transferred to the ruthenium-containing serum bottles via a Hamilton gas-tight syringe. A continuous stream of argon was maintained through the ruthenium(II) solutions and each solution was used within one hour of preparation. The ruthenium(II) solution was transferred to the stopped-flow apparatus through a platinum needle and Teflon tubing. Generating a range of ruthenium(II) concentrations by the preparation of each solution individually was found to be preferable to the method of stock solution

dilution. Stock solutions of hexaammineruthenium(II) ion showed signs of decomposition several hours after preparation based on observed spectral changes.

Protein Solutions. Solutions of ferricytochrome *c* were prepared for kinetics measurements by dissolving the lyophilized protein in a few mL of buffer, passing the solution through a Millipore filter, and diluting to the desired concentration with pH 7.0 phosphate buffer. The remaining proteins studied are stored as concentrated solutions at -60°C. After thawing, the protein solutions were Millipore-filtered and diluted with pH 7.0 phosphate buffer. Alternatively, more dilute protein solutions were dialyzed into phosphate buffer, filtered, and diluted to the final volume desired. Protein concentrations generally fell in the 4-6 μ M range for the cytochrome solutions and in the 10-20 μ M range for the blue copper protein solutions. Concentrations were determined spectrally on a Cary 219 UV-Vis spectrophotometer. A Brinkman Model 101 pH meter was used for all pH measurements.

Prior to kinetics measurements the protein solution was placed in a serum-capped bottle and deoxygenated by bubbling with argon for 15-20 min via a stainless steel needle. A constant flow of argon over the protein solution was maintained; direct bubbling of the solution was discontinued after the initial deoxygenation period to avoid protein

denaturation. The protein solution was transferred to the stopped-flow syringe through a stainless steel needle and Teflon tubing.

Kinetic Measurements. All kinetic measurements were made with a Durrum Model D-110 spectrophotometer. Several parts of the Durrum flow system have been modified for anaerobic work as described elsewhere.^{33,34} These modifications allowed nitrogen to be flushed through the space behind the plunger tips as well as over the valve tips. This minimized solution oxidation once the reactants had been transferred to the Durrum drive syringes. The additional anaerobic options designed for use with our Durrum^{33,34} (*i.e.*, Lucite bath cover, specially designed reagent flasks, methylviologen preflush of the flow system) were not deemed necessary for the reactions described here.

Temperature control was obtained with a circulating constant temperature bath (Forma Scientific bath, Gorman-Rupp pump). The temperature of the bath surrounding the syringe barrels was maintained to within $\pm 0.1^{\circ}\text{C}$. Reactant solutions were allowed to equilibrate in the syringes for a minimum of 15 minutes before use.

The rates of metalloprotein reduction were monitored at the following wavelengths: cytochrome *c*, 550 nm ($\Delta\epsilon = 18.5 \times 10^3 \text{ M}^{-1} \text{ cm}^{-1}$); cytochrome *c*₅₅₁, 551 nm ($\Delta\epsilon = 19 \times 10^3 \text{ M}^{-1} \text{ cm}^{-1}$); azurin, 625 nm ($\Delta\epsilon = 5.7 \times 10^3 \text{ M}^{-1} \text{ cm}^{-1}$); plastocyanin, 597 nm ($\Delta\epsilon = 4.5 \times 10^3 \text{ M}^{-1} \text{ cm}^{-1}$); stellacyanin,

604 nm ($\Delta\epsilon = 4.1 \times 10^3 \text{ M}^{-1} \text{ cm}^{-1}$). An absorbance change of 0.05 to 0.10 was monitored in all cases. Reductant concentrations were in pseudo-first-order excess over the oxidant and were varied over as wide a range as experimentally possible.

The rates of reduction of cytochrome *c*, cytochrome *c*₅₅₁, azurin, and stellacyanin by hexaammineruthenium(II) were studied as a function of ruthenium concentration, and also as a function of temperature at a fixed concentration of ruthenium. All the kinetic measurements were carried out in phosphate buffer at pH 7.0 with a total ionic strength of 0.1 M.

Data Collection and Analysis. A representation of the absorbance *vs.* time curve for each run was displayed on a Tektronix 564B storage oscilloscope. Simultaneously the corresponding data set was stored in an analog input buffer (with built-in ADC). Prior to triggering the next run, the data was sent under software control to a VAX 11/780 computer system. The analog input buffer was designed by J.P. Elliot of the Caltech Computing Center. The computer program used for data acquisition and processing (entitled Interactive Data Collector, or IDC) was written by T. Dailey, modified by H.V. Derby, and recently translated into Fortran by J. Hershberger. IDC was used to collect and store data sets, and to generate plots of $\ln|A-A_\infty|$ *vs.* time and weighted

linear least squares slopes of the plots. These plots and the respective calculated rate constants were useful in verifying first order kinetic behavior throughout the course of the experiment. Final calculation of k_{obsd} values employed a program written by R.A. Scott entitled KINPRO.³³ KINPRO utilizes an iterative nonlinear least squares method based on the Newton-Gauss approach. The k_{obsd} values reported at each reductant concentration represent the average of at least four reproducible kinetic runs. A weighted linear least squares program (K12FIT³³) was used to calculate the second order rate constant from k_{obsd} vs. concentration data. The dependence of rate on temperature was fit to the Eyring expression by a weighted linear least squares program (EYRFIT³³) to yield values of ΔH^\ddagger and ΔS^\ddagger .

Electron Transfer Distance Calculations. The rationale for the calculation of metalloprotein electron transfer distances is described by Mauk, Scott, and Gray.¹⁸ The computational procedure is summarized below for the purposes of this chapter. In the subscript notation used, reactant 1 refers to the protein and reactant 2 is the inorganic complex. The Marcus relationships for adiabatic (or uniformly non-adiabatic) electron transfer reactions are used to correct for the thermodynamic driving force of the redox reaction and for the reactivity properties of the inorganic complex:^{35,36}

$$k_{12} = (k_{11} k_{12} f K_{12})^{\frac{1}{2}} \quad (2.1)$$

$$\log(f) = [\log(K_{12})]^2 / [4 \log(k_{11} k_{22} / Z^2)] \quad (2.2)$$

In our case the known experimental values are k_{12} , the rate constant for the cross reaction between protein and inorganic complex; k_{22} , the self-exchange electron transfer rate constant for the inorganic complex; and ΔE_{12}° , the driving force of the cross-reaction. K_{12} is calculated from ΔE_{12}° :

$$\ln K_{12} = \frac{nF}{RT} \Delta E_{12}^\circ \quad (2.3)$$

Consequently k_{11} , the protein self-exchange rate, can be calculated by rearrangement of equations (2.1) and (2.2):

$$k_{11} = k_{12}^2 / (k_{22} K_{12}^f) \quad (2.4)$$

$$4[\log(f)]^2 - 4 \log[k_{12}^2 / (K_{12} Z^2)] [\log(f)] + [\log(K_{12})]^2 = 0 \quad (2.5)$$

Z , the collision frequency, is taken to be $10^{11} \text{ M}^{-1} \text{ s}^{-1}$.

The experimental values used to calculate k_{11} are first corrected for nonspecific electrostatic effects using Debye-Hückel theory.⁶ The equations below essentially correct the experimental quantities to infinite ionic strength:

$$k_{12}^\infty = \exp \left[\ln(k_{12}) + 3.576 \right. \\ \left. \times \left(\frac{\exp(-\kappa R_1)}{1 + \kappa R_2} + \left(\frac{\exp(-\kappa R_2)}{1 + \kappa R_1} \right) \left(\frac{Z_1 Z_2}{R_1 + R_2} \right) \right) \right] \quad (2.6)$$

$$k_{22}^\infty = \exp \left[\ln(k_{22}) + 3.576 \left(\frac{2 \exp(-\kappa R_2)}{1 + \kappa R_2} \right) \left(\frac{Z_2 Z'_2}{2 R_2} \right) \right] \quad (2.7)$$

$$\Delta E_{12}^\infty = \Delta E^\circ + \left[0.09182 \right. \\ \left. \times \left(\frac{\exp(-\kappa R_1)}{1 + \kappa R_2} + \frac{\exp(-\kappa R_2)}{1 + \kappa R_1} \right) \left(\frac{Z_1 Z_2 - Z'_1 Z'_2}{R_1 + R_2} \right) \right] \quad (2.8)$$

where,

Z_1, Z_2 = charges on reactants

Z'_1, Z'_2 = charges on products

R_1, R_2 = radii of reactants

at 25°C , $\kappa = 0.329 \mu^{\frac{1}{2}} \text{ \AA}^{-1}$

(μ = experimental ionic strength)

Thus, k_{11}^∞ , the protein self-exchange rate at infinite ionic strength, is calculated from k_{12}^∞ , k_{22}^∞ , and ΔE_{12}^∞ .

R_p , defined as one-half the intersite distance for the protein self-exchange reaction, can be calculated from k_{11}^∞ using the following equation:¹⁸

$$R_p = 6.2 = 0.35 \ln(k_{11}^\infty) \quad (2.9)$$

ΔR_p , the shortest distance from the active site to the protein surface is just R_p minus the van der Waals contact (1.85 Å). The total intersite distance (R) between protein active site and inorganic reagent is the sum of the protein distance contribution (R_p) and the reagent contribution (R_r). R_r , the reagent van der Waals contact distance, is also on the order of 2 Å for the small molecules studied.

RESULTS

First-order plots of absorbance *vs.* time data for the reductions of cytochrome *c*, cytochrome *c*₅₅₁, azurin, and stellacyanin were found to be linear for greater than 90% of the reaction in all cases. The dependences of the observed first-order rate constants on hexaammineruthenium(II) concentration are shown in Figure 2.1. The rate law for the reduction of these four proteins by Ru(NH₃)₆²⁺ is therefore

$$\frac{-d[\text{Protein(ox)}]}{dt} = k_{12} [\text{Ru}(\text{NH}_3)_6^{2+}] [\text{Protein(ox)}]$$

At 25°C in phosphate buffer, pH 7.0, $\mu = 0.10$ M, the second-order rate constants (k_{12}) for reduction by Ru(NH₃)₆²⁺ are: cytochrome *c*, $6.70 (\pm 0.14) \times 10^4 \text{ M}^{-1} \text{ s}^{-1}$; cytochrome *c*₅₅₁, $5.17 (\pm 0.17) \times 10^5 \text{ M}^{-1} \text{ s}^{-1}$; azurin, $6.78 (\pm 0.11) \times 10^4 \text{ M}^{-1} \text{ s}^{-1}$; stellacyanin, $6.63 (\pm 0.11) \times 10^4 \text{ M}^{-1} \text{ s}^{-1}$. Eyring plots for these reactions are shown in Figure 2.2. The activation parameters obtained from the fits of the temperature dependence data are: cytochrome *c*, $\Delta H^\ddagger = 0.91 (\pm 0.15)$ kcal/mol, $\Delta S^\ddagger = -34 (\pm 1)$ eu; cytochrome *c*₅₅₁, $\Delta H^\ddagger = -0.02 (\pm 0.28)$ kcal/mol, $\Delta S^\ddagger = -33 (\pm 1)$ eu; azurin, $\Delta H^\ddagger = 0.22 (\pm 0.24)$ kcal/mol, $\Delta S^\ddagger = -36 (\pm 1)$ eu; stellacyanin, $\Delta H^\ddagger = 4.4 (\pm 0.2)$ kcal/mol, $\Delta S^\ddagger = -22 (\pm 1)$ eu.

The reduction of plastocyanin by Ru(NH₃)₆²⁺ was too fast to measure by our stopped-flow techniques. At 10°C and [Ru(II)] = 0.1 mM, a $t_{\frac{1}{2}}$ of less than 5 ms was estimated.

Figure 2.1. The dependences of the observed rate constants on the concentration of $\text{Ru}(\text{NH}_3)_6^{2+}$ at 25°C, $\mu = 0.1$ M, pH 7.0 (phosphate). (a) cytochrome *c*. (b) cytochrome c_{551} . (c) azurin. (d) stellacyanin.

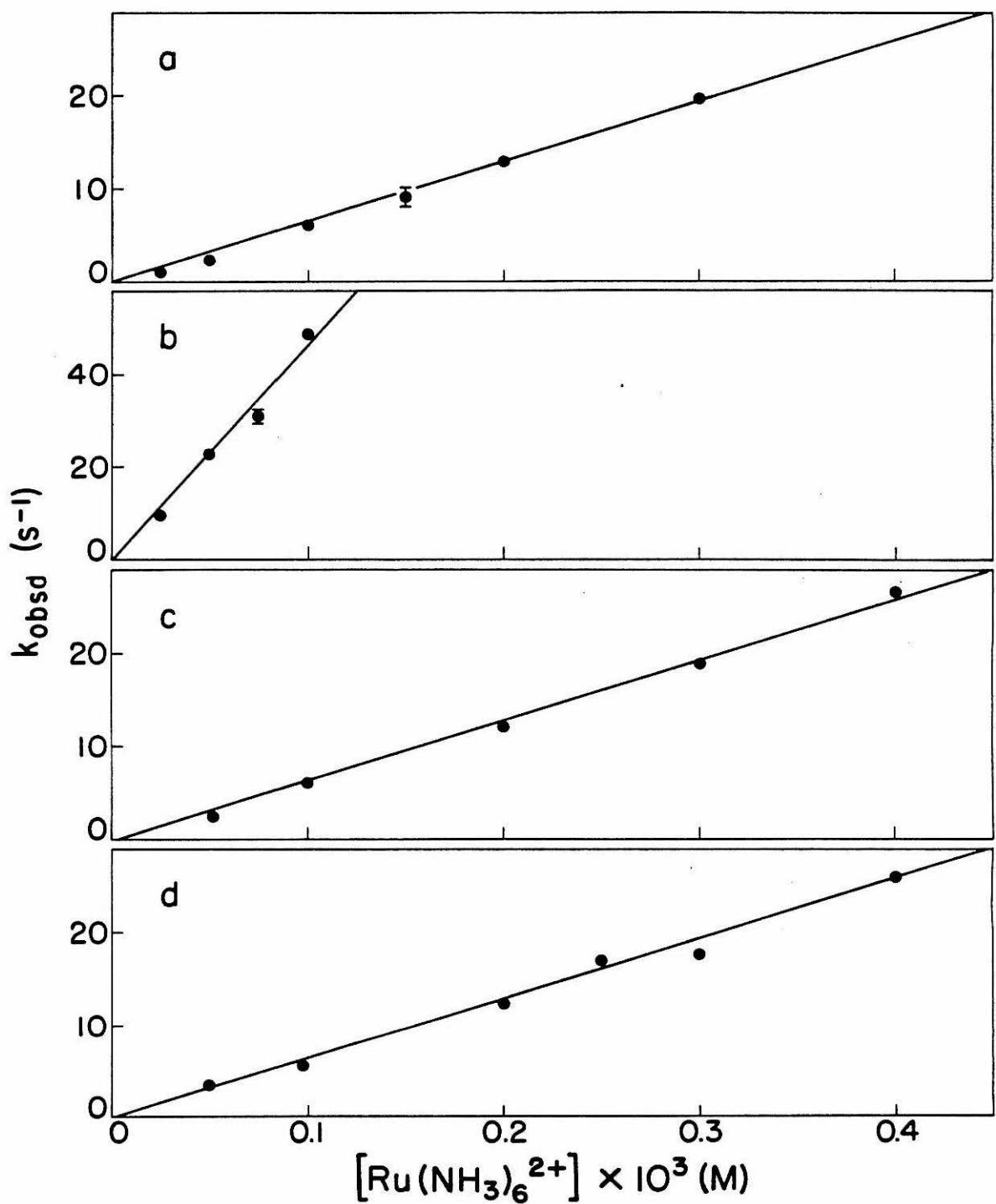
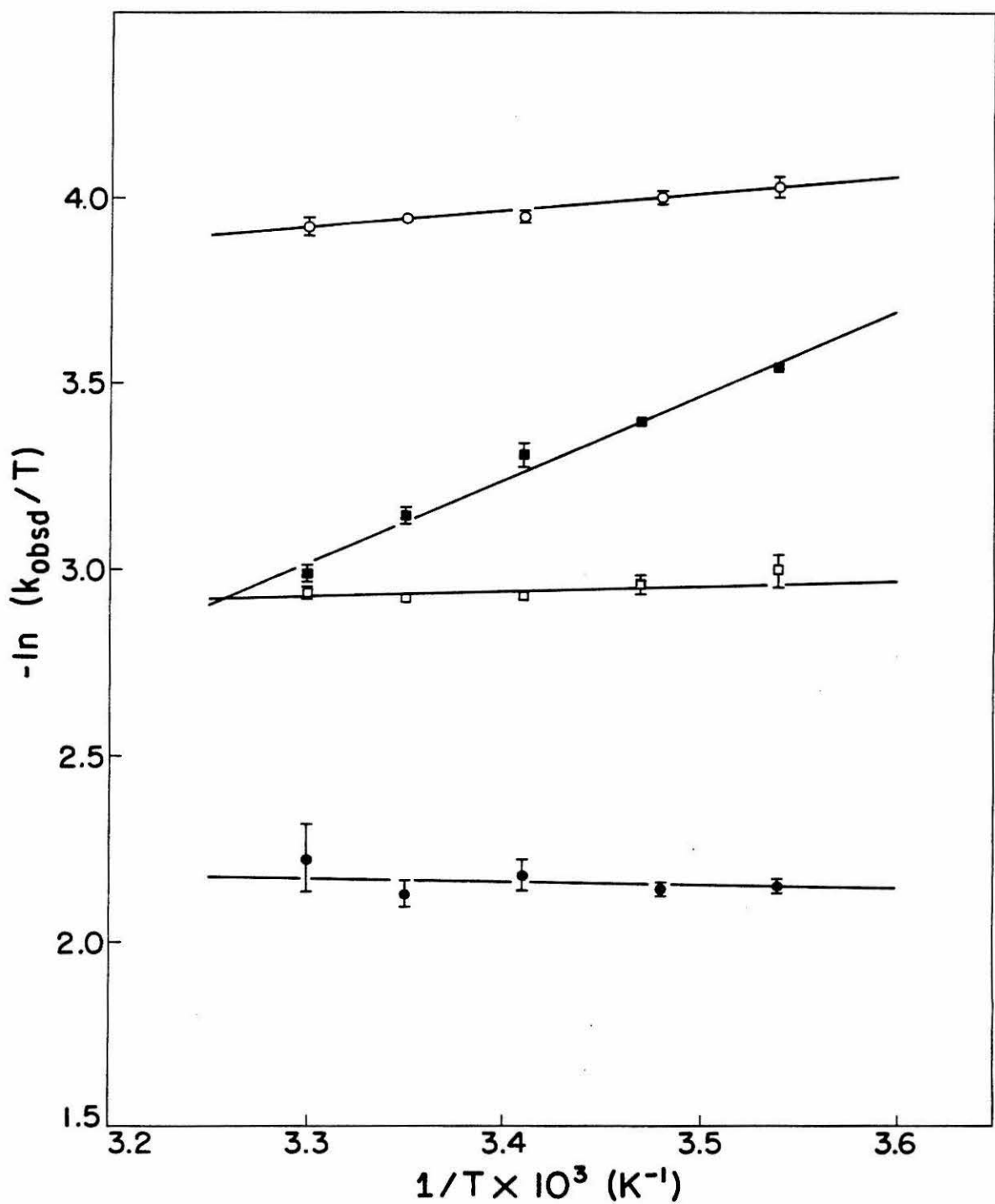


Figure 2.2. Eyring plots of the rate constant data (pH 7.0 phosphate, $\mu = 0.1$ M): (○) cytochrome *c*, $[Ru] = 1.0 \times 10^{-4}$ M; (●) cytochrome c_{551} , $[Ru] = 7.5 \times 10^{-5}$ M; (□) azurin, $[Ru] = 2.5 \times 10^{-4}$ M; (■) stellacyanin, $[Ru] = 2.0 \times 10^{-4}$ M.



This translates to a second-order rate constant on the order of $1 \times 10^6 \text{ M}^{-1} \text{ s}^{-1}$ or greater. At 5°C in pH 7.0 Tris buffer, Segal and Sykes²³ have reported a rate constant for this reaction of $2.4 \times 10^6 \text{ M}^{-1} \text{ s}^{-1}$.

Protein electron transfer distances were calculated from k_{11}^∞ 's, the electrostatics-corrected protein self-exchange rates. The results for the five proteins studied are set out in Table 2.1, along with the relevant input parameters for the Marcus calculations. The protein E° values (vs. NHE) employed were:¹⁸ cytochrome *c*, 260 mV; cytochrome *c*₅₅₁, 260 mV; azurin, 304 mV; plastocyanin, 347 mV; stellacyanin, 184 mV. The properties of $\text{Ru}(\text{NH}_3)_6^{2+}$ required were available in the literature. The values chosen were those determined under conditions most closely resembling the kinetics conditions utilized here. They are: $k_{22} = 3.2 \times 10^3 \text{ M}^{-1} \text{ s}^{-1}$ (0.1 M $\text{CF}_3\text{SO}_3\text{H}$, 25°C);³⁷ $E^\circ = 67 \text{ mV}$ (0.1 M NaClO_4 , 25°C);³⁸ and $R_2 = 3.3 \text{ \AA}$.³⁷

Table 2.1. Calculated Protein Self-Exchange Rate Constants and Electron Transfer Distances for the Reduction of Single Site Metalloproteins by $\text{Ru}(\text{NH}_3)_6^{2+}$

protein	$k_{12}(\text{M}^{-1} \text{s}^{-1})^a$	$\Delta E_{12}^\circ(\text{V})$	$R_1(\text{\AA})/R_2(\text{\AA})$	Z_1/Z_1'	Z_2/Z_2'
cytochrome <i>c</i>	6.70×10^4	0.193	16.6/3.3	7.5/6.5	2/3
cytochrome <i>c551</i>	5.17×10^5	0.193	14.4/3.3	-2/-3	2/3
azurin	6.78×10^4	0.237	17.2/3.3	-1/-2	2/3
plastocyanin	2.4×10^6 ^b	0.280	15.8/3.3	-9/-10	2/3
stellacyanin	6.63×10^4	0.117	19.5/3.3	0/0	2/3

protein	$k_{12}^\infty(\text{M}^{-1} \text{s}^{-1})$	$k_{22}^\infty(\text{M}^{-1} \text{s}^{-1})$	$\Delta E_{12}^\infty(\text{V})$	$k_{11}^\infty(\text{M}^{-1} \text{s}^{-1})$	$R_p(\text{\AA})$
cytochrome <i>c</i>	1.93×10^5	9.91×10^4	0.185	4.15×10^2	4.1
cytochrome <i>c551</i>	3.59×10^5	9.91×10^4	0.205	7.33×10^2	3.9
azurin	5.94×10^4	9.91×10^4	0.244	4.89×10^0	5.6
plastocyanin	5.98×10^5	9.91×10^4	0.304	7.18×10^1	4.7
stellacyanin	6.63×10^4	9.91×10^4	0.117	5.46×10^2	4.0

^aAt 25°C in pH 7.0 phosphate, $\mu = 0.10 \text{ M}$.

^bAt 5°C; reference 23.

DISCUSSION

The hexaammineruthenium(II) ion has been used extensively as an outer sphere electron transfer reagent in inorganic redox studies. The study of $\text{Ru}(\text{NH}_3)_6^{2+}$ reactivity with metalloproteins has been comparatively limited.^{23,39-43} Results obtained by Ewall³⁹ and Adegit⁴⁰ on cytochrome *c* and by Segal²³ on plastocyanin are in close agreement with the values reported here.

Hexaammineruthenium(II), like $\text{Fe}(\text{EDTA})^{2-}$, is a hydrophilic, outer sphere redox reagent. Relatively small k_{11}^∞ 's, small enthalpies of activation, and large negative activation entropies characterize the reactions of both these reagents with most of the single site metalloproteins.⁸ This is consistent with a mechanism involving nonadiabatic electron transfer from the protein surface to the redox site. On the other hand, complexes possessing hydrophobic, π -conjugated ligands can penetrate into the protein interior to facilitate electron transfer reactions with the protein active site. Thus when $\text{Co}(\text{phen})_3^{3+}$ ^{1,9,11} and $\text{Ru}(\text{NH}_3)_6\text{py}^{3+}$ ^{13,23} oxidize the single site proteins this enhanced reactivity is reflected in higher k_{11}^∞ 's.^{8,18} Also, the more positive ΔH^\neq and ΔS^\neq values observed are suggestive of protein conformational changes and/or loss of ordered water molecules from the protein surface, both consistent with the proposed penetration mechanism.^{9,11,13}

The protein site-to-surface distances (ΔR_p 's) calculated from the metalloprotein- $\text{Ru}(\text{NH}_3)_6^{2+}$ reactions are compared in Table 2.2 to the ΔR_p 's obtained from $\text{Fe}(\text{EDTA})^{2-}$ kinetic studies.¹⁸ Also included in the table are estimates of site-to-surface distances taken from protein molecular models for those proteins that have been characterized crystallographically. Detailed mechanistic arguments should not be sustained on differences of about 1 \AA or less in the values listed.¹⁸ The agreement between the distances calculated from the $\text{Ru}(\text{NH}_3)_6^{2+}$ experiments and the structural ΔR_p 's is reasonably good.

Several points of interest are raised by the comparison of calculated ΔR_p 's based on $\text{Fe}(\text{EDTA})^{2-}$ with those based on $\text{Ru}(\text{NH}_3)_6^{2+}$. If $\text{Fe}(\text{EDTA})^{2-}$ and $\text{Ru}(\text{NH}_3)_6^{2+}$ are both hydrophilic, nonpenetrating electron transfer reagents their distances of approach to the protein active site should be comparable, once charge interactions are factored out. That azurin has the most buried redox center is strongly suggested by the low reactivity of both reagents with the blue copper site. This postulate is gaining credibility as more refined data continues to emerge from azurin's crystallographers.⁴⁴ The relative ordering of cytochrome *c*, cytochrome *c*₅₅₁, and plastocyanin with respect to redox site accessibility differs between $\text{Ru}(\text{NH}_3)_6^{2+}$ and $\text{Fe}(\text{EDTA})^{2-}$, but the magnitude of the differences involved (all ≤ 2 \AA) is too small to be

Table 2.2. Site-to-Surface Distances for Single Site Metalloproteins

Protein	Redox Site	$\Delta R_p (\text{\AA})$; ^a Fe(EDTA) ²⁻ _b	$\Delta R_p (\text{\AA})$; ^a $\text{Ru}(\text{NH}_3)_6^{2+}$	$\Delta R_p (\text{\AA})$; ^a Structural ^c
cytochrome <i>c</i>	heme <i>c</i>	3.4	2.2	3 ± 1
cytochrome <i>c</i> ₅₅₁	heme <i>c</i>	4.0	2.0	3 ± 1
azurin	blue Cu	5.5	3.8	c
plastocyanin	blue Cu	2.6	2.9	1 ± 1
stellacyanin	blue Cu	0	2.1	c

^a $\Delta R_p = R_p - 1.85 \text{ \AA}$. ^bReference 18.

^cStructural estimate not available.

considered mechanistically significant. Furthermore, in the case of plastocyanin the k_{12} value used in the calculations is the cross reaction rate constant at 5°C.²³ Depending on the magnitude of the temperature dependence of the rate, and the accuracy of the measurements, a significantly larger k_{12} at 25°C is probably more realistic. This would translate into a larger k_{11}^∞ and smaller ΔR_p , thus bringing the $\text{Ru}(\text{NH}_3)_6^{2+}$ and $\text{Fe}(\text{EDTA})^{2-}$ results into closer agreement. The kinetically determined ΔR_p of plastocyanin would also converge on the structural estimate.

The distance discrepancy in the case of stellacyanin, however, merits closer examination. The reactions of stellacyanin with $\text{Fe}(\text{EDTA})^{2-}$, $\text{Co}(\text{phen})_3^{3+}$, and $\text{Ru}(\text{NH}_3)_5\text{py}^{3+}$ are considered to be essentially adiabatic; stellacyanin is well-behaved within the Marcus theory framework.⁸ The k_{11}^∞ values for the reactions are all high - about $10^5 \text{ M}^{-1} \text{ s}^{-1}$. Coupled with the observation that stellacyanin can interact with an electrode, unaided by redox mediators,⁴⁵ stellacyanin's active site has been deemed accessible. It is in fact the reference point on which the calculation of R_p values is based.¹⁸ The equation which relates the electron transfer rate constant, k , to the intersite distance, R , is given by:⁴⁶

$$k = Ce^{-2aR} \quad (2.10)$$

Using Hopfield's estimate of 0.72 \AA^{-1} for a ,²⁰

$$R = -0.694 \ln (k/C) \quad (2.11)$$

In order to obtain a value of C (a function of numerous donor and acceptor site properties), it was assumed that the average value of k_{11}^{∞} for stellacyanin ($2.4 \times 10^5 \text{ M}^{-1} \text{ s}^{-1}$) was associated with a close contact electron transfer distance of 3.7 \AA (*i.e.*, redox site separation is limited only by van der Waals contact, or $\Delta R_p = 0$). Thus, equation (2.9) is obtained, relating R_p and k_{11}^{∞} . In light of the results obtained from the reduction of stellacyanin by $\text{Ru}(\text{NH}_3)_6^{2+}$, the assumptions involved here should be reexamined.

It is perhaps fortuitous that the k_{11}^{∞} values for most of the reagents studied to date with stellacyanin express such high reactivities. Indeed the reagents studied possess hydrophobic ligands capable of protein penetration (*e.g.*, $\text{Co}(\text{phen})_3^{3+}$, $\text{Ru}(\text{NH}_3)_5 \text{ py}^{3+}$), are negatively charged (*e.g.*, $\text{Fe}(\text{EDTA})^{2-}$, $\text{Co}(\text{ox})_3^{3-}$, $\text{Co}(\text{EDTA})^-$), or both (*e.g.* $\text{Co}(\text{dipic})_2^-$, $\text{Fe}(\text{dipic})_2^{2-}$). The Marcus calculations carried out on stellacyanin rate data include no protein-based electrostatics corrections due to the fact that the charge on the protein is assumed to be zero at pH 7.⁸ This assumption rests on the basis that the rate of oxidation of stellacyanin by $\text{Co}(\text{phen})_3^{3+}$ was independent of ionic strength.^{6,9} If in fact the mechanistic importance of hydrophobic penetration by $\text{Co}(\text{phen})_3^{3+}$ outweighs the importance of electrostatic interactions, the assumption of zero charge is invalid. The

calculation of protein charge from the reaction of a hydrophilic, nonpenetrating reagent would provide a more acceptable estimate. The ionic strength dependence of the stellacyanin- Fe(EDTA)^{2-} reaction was not reported.² If stellacyanin is actually positively charged, as estimated from sequence data^{6,17} and pI determinations,⁴⁷ its apparent enhanced reactivity with negatively charged reagents is not surprising. The somewhat lower reactivity observed here for $\text{Ru}(\text{NH}_3)_6^{2+}$ follows, in that it is the only positively charged, hydrophilic reagent examined.

The analysis offered above suggests that the question of the charge on stellacyanin, and its ensuing effects on the Marcus and distance calculations, be explored further. It should be noted that the charge situation is more complex in the case of stellacyanin than it is for the other proteins examined. This is related to the fact that, as isolated, stellacyanin contains about 20% carbohydrate (and 20% hexosamine) by weight.^{48,49} The nature of the protein-carbohydrate interactions is unknown, complicating the estimation of charge from sequence data. The presence of the carbohydrate has also made stellacyanin essentially intractable to crystallization. (Structural estimates of redox site accessibility for stellacyanin will be long in coming.) Also, implicit in the comparisons made here is the assumption of prep-to-prep reproducibility, *i.e.*, all of

the data obtained in our laboratory on stellacyanin represents the same protein-carbohydrate entity. (There is reason to believe that lab-to-lab reproducibility cannot always be assumed.⁵⁰)

It should be emphasized that a calculated ΔR_p of 2 Å for stellacyanin, contrasted with the previously assumed value of 0 Å, does not represent a serious departure from the conclusions drawn to date for metalloprotein-small molecule redox reactions. The model employed still clearly distinguishes an inaccessible active site (*e.g.*, azurin) from a fairly accessible site (*e.g.*, cytochrome *c*, stellacyanin). The $\text{Ru}(\text{NH}_3)_6^{2+}$ results do suggest, though, that some of the assumptions implicit in these calculations translate to larger uncertainties in the final distances than previously thought. It appears that hydrophilic reagents may be more sensitive to the electrostatic environment in the vicinity of the active site than hydrophobic reagents. Thus the small inconsistencies observed in the R_p 's calculated from metalloprotein-hydrophilic reagent reactions could also be, in part, a reflection of the fact that a spherical distribution of total protein charge is assumed in the calculations.⁸

The big picture remains the same for metalloprotein-small molecule reactions. The $\text{Ru}(\text{NH}_3)_6^{2+}$ study, along with the other kinetic studies cited herein, strongly supports a mechanism involving the close approach of inorganic

reagents to metalloprotein redox sites. Clearly electron transfer over a total intersite distance of 8 Å or less ($R = R_p + R_r$; $R_r \approx 2 \text{ } \text{Å}$) is common for this type of metalloprotein reaction. Systems designed to determine if metalloprotein electron transfer distances of 10-15 Å are equally feasible are described in the following chapters.

Appendix 2.1. Supplementary Data. First-Order Rate Constants
for the Reduction of Single Site Metalloproteins by $\text{Ru}(\text{NH}_3)_6^{2+}$ ^a

Protein	T(°C) ^b	$[\text{Ru}(\text{NH}_3)_6^{2+}] \times 10^4$ (M)	$k_{\text{obsd}}(\text{s}^{-1})$ (SD)
cytochrome <i>c</i>	25.0	0.25	1.05 (0.02)
		0.51	2.27 (0.13)
		1.0	5.88 (0.24)
		1.5	9.00 (1.09)
		2.0	12.8 (0.3)
		3.0	19.6 (0.2)
	30.0	1.0	6.02 (0.15)
		1.0	5.79 (0.08)
		1.0	5.67 (0.11)
		1.0	5.27 (0.10)
cytochrome <i>c</i> ₅₅₁	25.0	1.0	5.03 (0.14)
		0.25	9.68 (0.31)
		0.50	22.8 (0.8)
		0.75	31.0 (1.3)
		1.0	48.7 (0.4)
	29.7	0.75	32.7 (3.1)
		0.75	35.3 (1.3)
		0.75	33.0 (1.4)
		0.75	33.8 (0.5)
azurin	25.0	0.75	32.8 (0.6)
		0.52	2.40 (0.08)
		1.0	6.06 (0.10)
		2.0	12.2 (0.2)
		3.0	18.9 (0.2)
		4.0	26.6 (0.2)
	30.0	6.0	39.5 (0.6)
		2.5	16.1 (0.3)
		2.5	16.0 (0.2)
		2.5	15.6 (0.1)
stellacyanin	25.0	14.8	14.9 (0.4)
		9.6	14.1 (0.6)
	30.2	2.5	
		2.5	
		3.0	
		4.1	
	25.0	2.0	2.51 (0.03)
		0.50	5.59 (0.02)
		2.0	12.4 (0.05)
		2.5	16.9 (0.2)
25.0	19.7	3.0	17.6 (0.4)
		4.1	25.9 (0.4)
		2.0	15.3 (0.3)
		2.0	12.8 (0.3)
	14.8	2.0	10.7 (0.3)
		2.0	9.63 (0.04)
	9.6	2.0	8.20 (0.11)

^aIn pH 7.0 phosphate buffer, $\mu = 0.10$ M. ^b $\pm 0.1^\circ\text{C}$.

REFERENCES

1. McArdle, J.V.; Gray, H.B.; Creutz, C.; Sutin, N. *J. Am. Chem. Soc.* 1974, 96, 5737.
2. Wherland, S.; Holwerda, R.A.; Rosenberg, R.C.; Gray, H.B. *J. Am. Chem. Soc.* 1975, 97, 5260.
3. Rawlings, J.; Wherland, S.; Gray, H.B. *J. Am. Chem. Soc.* 1976, 98, 2177.
4. Holwerda, R.A.; Wherland, S.; Gray, H.B. *Ann. Rev. Biophys. Bioeng.* 1976, 5, 363.
5. Rosenberg, R.C.; Wherland, S.; Holwerda, R.A.; Gray, H.B. *J. Am. Chem. Soc.* 1976, 98, 6364.
6. Wherland, S.; Gray, H.B. *Proc. Natl. Acad. Sci. USA* 1976, 73, 2950.
7. Gray, H.B.; Coyle, C.L.; Dooley, D.M. *et al.* In "Bioinorganic Chemistry-II", Adv. Chem. Ser., No. 162; Raymond, K.N., Ed.; ACS: Washington, DC, 1977; p. 145.
8. Wherland, S.; Gray, H.B. In "Biological Aspects of Inorganic Chemistry"; Addison, A.W.; Cullen, W.; James, B.R.; Dolphin, D., Eds.; Wiley: New York, 1977; p. 289.
9. McArdle, J.V.; Coyle, C.L.; Gray, H.B.; Yoneda, G.S.; Holwerda, R.A. *J. Am. Chem. Soc.* 1977, 99, 2483.
10. Rawlings, J.; Wherland, S.; Gray, H.B. *J. Am. Chem. Soc.* 1977, 99, 1968.
11. McArdle, J.V.; Yocom, K.; Gray, H.B. *J. Am. Chem. Soc.* 1977, 99, 4141.

12. Coyle, C.L.; Gray, H.B. *Biochem. Biophys. Res. Commun.* 1976, 73, 1122.
13. Cummins, D.; Gray, H.B. *J. Am. Chem. Soc.* 1977, 99, 5158.
14. Holwerda, R.A.; Read, R.A.; Scott, R.A.; Wherland, S.; Gray, H.B.; Millett, F. *J. Am. Chem. Soc.* 1978, 100, 5028.
15. Mauk, A.G.; Gray, H.B. *Biochem. Biophys. Res. Commun.* 1979, 86, 206.
16. Mauk, A.G.; Coyle, C.L.; Bordignon, E.; Gray, H.B. *J. Am. Chem. Soc.* 1979, 101, 5054.
17. Holwerda, R.A.; Knaff, D.B.; Gray, H.B.; Clemmer, J.D.; Crowley, R.C.; Smith, J.M.; Mauk, A.G. *J. Am. Chem. Soc.* 1980, 102, 1142.
18. Mauk, A.G.; Scott, R.A.; Gray, H.B. *J. Am. Chem. Soc.* 1980, 102, 4360.
19. Mauk, A.G.; Bordignon, E.; Gray, H.B., submitted for publication in *J. Am. Chem. Soc.*
20. Hopfield, J.J. *Proc. Natl. Acad. Sci. USA* 1974, 71, 3640.
21. Lappin, A.G.; Segal, M.G.; Weatherburn, D.C.; Sykes, A.G. *J. Am. Chem. Soc.* 1979, 101, 2297.
22. Lappin, A.G.; Segal, M.G.; Weatherburn, D.C.; Henderson, R.A.; Sykes, A.G. *J. Am. Chem. Soc.* 1979, 101, 2302.
23. Segal, M.G.; Sykes, A.G. *J. Am. Chem. Soc.* 1978, 100, 4585.
24. Segal, M.G.; Sykes, A.G. *J.C.S. Chem. Comm.* 1977, 21, 764.
25. Hodges, H.L.; Holwerda, R.A.; Gray, H.B. *J. Am. Chem. Soc.* 1974, 96, 3132.
26. Coyle, C.L. Ph.D. Dissertation, California Institute of Technology, 1977.

27. Yoneda, G.S.; Holwerda, R.A. *Bioinorg. Chem.* 1978, 8, 139.
28. Shriver, D.F. "The Manipulation of Air Sensitive Compounds"; McGraw-Hill: New York, 1969; p. 199.
29. Sweetser, P.B. *Anal. Chem.* 1967, 39, 979.
30. Lever, F.M.; Powell, A.R. *J. Chem. Soc. (A)* 1969, 1477.
31. Woodhead, J.L.; Fletcher, J.M. *J. Chem. Soc.* 1961, 5039.
32. Marchant, J.A.; Matsubara, T.; Ford, P.C. *Inorg. Chem.* 1977, 16, 2160.
33. Scott, R.A. Ph.D. Dissertation, California Institute of Technology, 1980.
34. Schichman, S.A. Ph.D. Dissertation, University of Chicago, 1981.
35. Marcus, R.A. *J. Phys. Chem.* 1963, 67, 853.
36. Marcus, R.A.; Sutin, N. *Inorg. Chem.* 1975, 14, 213.
37. Brown, G.M.; Sutin, N. *J. Am. Chem. Soc.* 1979, 101, 883.
38. Yee, E.L.; Cave, R.J.; Guyer, K.L.; Tyma, P.D., Weaver, M.J. *J. Am. Chem. Soc.* 1979, 101, 1131.
39. Ewall, R.X.; Bennett, L.E. *J. Am. Chem. Soc.* 1974, 96, 940.
40. Adegbite, A.; Okpanachi, M.I. *J. Am. Chem. Soc.* 1980, 102, 2832.
41. Bennett, L.E. *Prog. Inorg. Chem.* 1973, 18, 1.
42. Scott, R.A.; Gray, H.B. *J. Am. Chem. Soc.* 1980, 102, 3219.
43. Jacks, C.A.; Bennett, L.E.; Raymond, W.N.; Lovenberg, W. *Proc. Natl. Acad. Sci. USA* 1974, 71, 1118.
44. Adman, E.T.; Jensen, L.H. *Isr. J. Chem.* 1981, 21, 8.
45. Sailsuta, N.; Anson, F.C. Gray, H.B. *J. Am. Chem. Soc.* 1979, 101, 455.

46. Gamov, G. *Z. Phys.* 1928, 51, 204.
47. Reinhammer, B. *Biochim. Biophys. Acta* 1970, 205, 35.
48. Peisach, J., Levine; W.G.; Blumberg, W.E. *J. Biol. Chem.* 1967, 242, 2847.
49. Bergman, C.; Gandvik, E.-K.; Nyman, P.; Strid, L. *Biochem. Biophys. Res. Commun.* 1977, 77, 1052.
50. Peisach, J., personal communication, 1981.

CHAPTER 3

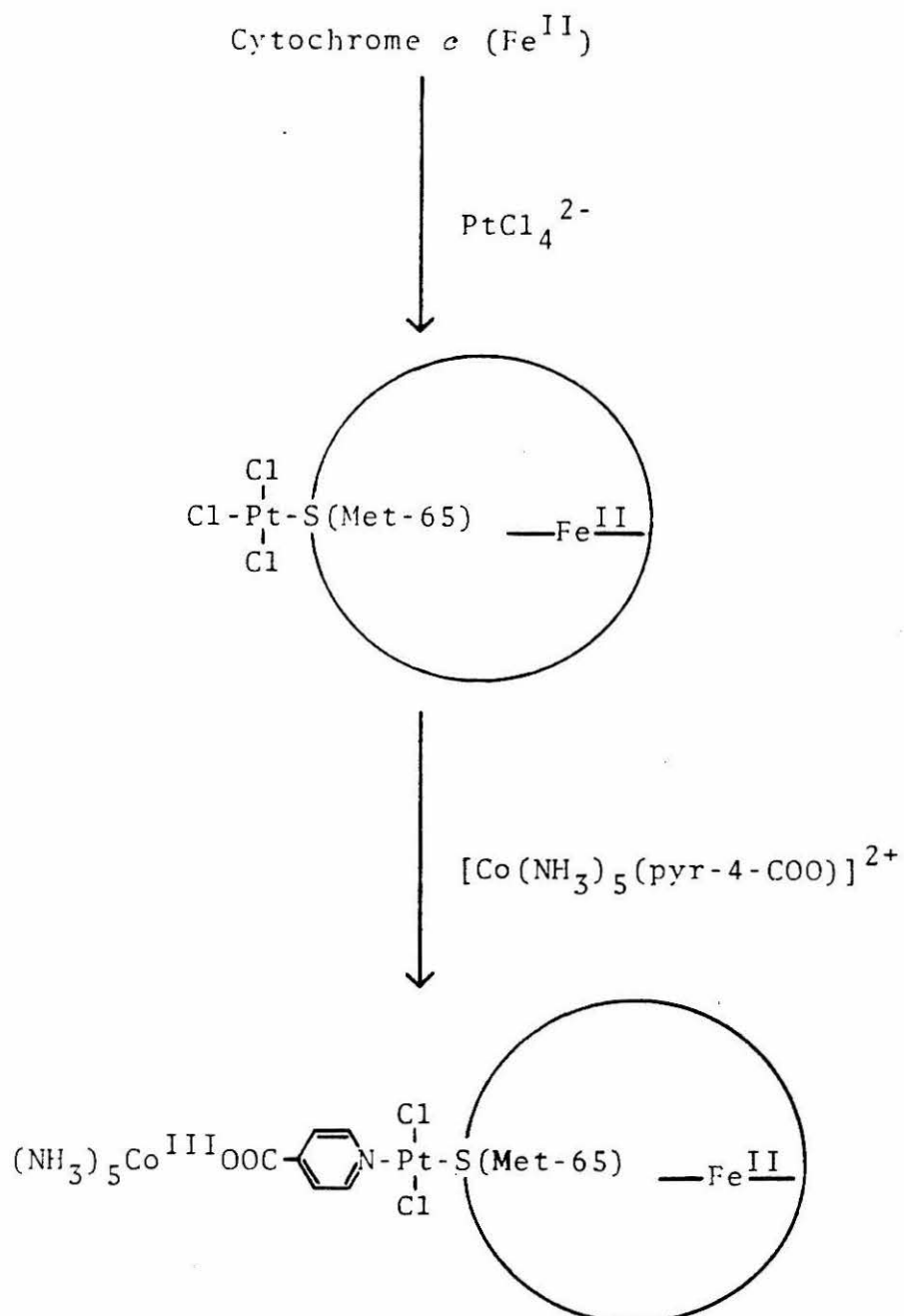
SYNTHESIS OF A PYRIDINE-4-CARBOXYLATO-
PENTAAMMINECOBALT(III) COMPLEX OF
FERROCYTOCHROME *c*

INTRODUCTION

In order to generate a synthetic multisite metalloprotein suitable for intramolecular electron transfer studies, several conditions must be met. First, the single site metalloprotein employed must be available in large quantities and must be structurally well characterized. Cytochrome *c* meets these criteria as discussed earlier (Chapter 1). Secondly, a pure one-to-one, redox reagent-to-metalloprotein, derivative must be isolable. The derivative must be stable with respect to dissociation of the inorganic complex. The location of the attached redox reagent must be known. Finally, the thermodynamics of the system must be favorable for the observation of electron transfer processes between the two sites.

The pyridine-4-carboxylatopentaamminecobalt(III) complex of cytochrome *c* described herein is the first of three systems designed to meet these criteria. The desired complex is one in which tetrachloroplatinate(II) is covalently bound to the sulfur of methionine-65 on the surface of ferrocyanocytocrome *c*, and the pyridine-4-carboxylatopentaamminecobalt(III) complex is subsequently bound to platinum through its free pyridine nitrogen. The sulfur atom of Met-65 is located about 11 Å from the closest aromatic carbon of the heme *c*.¹ The attachment scheme is depicted in Figure 3.1.

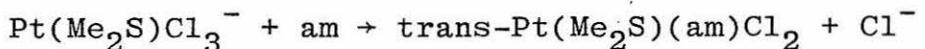
Figure 3.1. Method of attachment of Co(III) redox probe to ferrocyanochrome *c*.



This approach appeared promising for several reasons. Dickerson and coworkers have shown that PtCl_4^{2-} binds specifically to Met-65 in both tuna ferro- and ferricytochrome *c* crystals.² Earlier work on horse heart ferricytochrome *c* crystals also showed the major binding site to be Met-65.³ (A minor second site which contributed little to the phase analysis was located near His-33.) Preparation of these derivatives involved soaking the crystals for several days in a solution of the heavy atom reagent to allow the reagent to diffuse through solvent channels and gain access to the protein binding site.⁴ The reaction of PtCl_4^{2-} with cytochrome *c* in solution should be much more rapid.

Free methionine reacts quite rapidly with PtCl_4^{2-} in solution.⁵

The reaction of the cobalt(III) complex with the PtCl_4^{2-} -cytochrome *c* derivative should be similar to simple square planar substitution reactions. Tobe and coworkers have looked at the kinetics of the reaction



where am represents an amine.⁶ These reactions follow the usual two-term rate law for square planar substitution reactions, namely,

$$\text{rate} = k_1 [\text{Pt}] + k_2 [\text{Pt}] [\text{am}]$$

so that under pseudo-first-order conditions (excess am),

$$k_{\text{obsd}} = k_1 + k_2 [\text{am}]$$

Of interest here is the case where $\text{am} = \text{pyridine}$. In methanol, $k_1 = 1.8 \times 10^{-3} \text{ s}^{-1}$ and $k_2 = 6.71 \times 10^{-2} \text{ M}^{-1} \text{ s}^{-1}$. In the case where $\text{am} = 3,4\text{-dimethylpyridine}$ an equilibrium constant of greater than 10^5 was estimated. Thus the formation of a stable one-to-one $\text{Co(III)-cytochrome } c$ complex appeared thermodynamically and kinetically feasible. The synthetic procedure developed for the generation of the $\text{Co-Pt-cytochrome } c$ complex is outlined in the following section.

For the approach we have outlined it is important to characterize the intermolecular redox reactions of the probe reagent with cytochrome c before turning to the intramolecular electron transfer systems. Unfortunately, the reduction potential of the pyridine-4-carboxylatopentaamminecobalt(III) complex is unknown. Due to the substitutional lability of cobalt(II), electrochemical measurements are plagued by irreversibility problems. Aquopentaamminecobalt(III), however, has an estimated reduction potential of +330 mV (*vs.* NHE),⁷ suitable for the oxidation of ferrocyanochrome c ($E^\circ = +260 \text{ mV } vs. \text{ NHE}$).⁸ Based on the fact that the coordination environment of the pyridine-4-carboxylato-pentaamminecobalt(III) complex is quite similar to the aquo complex, it was predicted that the former should prove to be redox active with cytochrome c . Intermolecular kinetic studies of the reaction of the cobalt(III) complex with ferrocyanochrome c are reported here.

EXPERIMENTAL SECTIONMaterials

Isonicotinic acid (4-pyridinecarboxylic acid) is commercially available and was used as supplied. K_2PtCl_4 (Matthey Bishop) and horse heart cytochrome *c* (Sigma, type VI) were also used without further purification. All other chemicals were reagent grade.

Argon gas was passed through two vanadous towers to remove oxidizing impurities. When the use of Millipore water is indicated this refers to low conductivity water purified by a Millipore Milli-Q system. Otherwise deionized distilled water was utilized.

MethodsSynthesis of Cobalt(III) Pentaammine Complexes.

Aquopentaamminecobalt(III) perchlorate, $[Co(NH_3)_5H_2O](ClO_4)_3$. This complex was used as the starting material for the synthesis of the carboxylato complex. It was prepared from carbonatopentaamminecobalt(III) nitrate, $[Co(NH_3)_5CO_3]NO_3$, which was prepared by air oxidation of a solution of $Co(NO_3)_2 \cdot 6H_2O$, $(NH_4)_2CO_3$, and NH_4OH .⁹ Contamination by the carbonatotetraammine complex can be avoided by slow oxidation.¹⁰ The solution was not directly bubbled with air but left standing in air until the brick-red product precipitated (*ca.* 10 days). The carbonato nitrate was

converted to the aquo perchlorate by treatment with concentrated perchloric acid.¹⁰

Pyridine-4-carboxylatopentaamminecobalt(III) perchlorate, $[\text{Co}(\text{NH}_3)_5(\text{Hpyr-4-COO})](\text{ClO}_4)_3$. The hydroperchlorate form (ring nitrogen protonated) of this complex was isolated as it proved more amenable to purification. The procedure used was basically that of Gould and Taube¹⁰ with several modifications. Five grams of isonicotinic acid (40 mmol) were dissolved in 1.75 N NaOH (*ca.* 25 mL) and heated at 75°C for 10 min. The solution was filtered. Two grams of aquopentamminecobalt(III) perchlorate (4 mmol) were dissolved in hot water (*ca.* 10 mL) and added to the ligand solution. The reaction mixture was heated at 75°C with stirring for 2 hours. The solution was filtered and cooled. Some product and/or excess parent carboxylic acid may precipitate upon cooling. Concentrated HClO_4 was added to the solution until no more precipitate formed. The product was filtered. Additional product could be obtained by rotary evaporation of the filtrate at 50°C. The combined solids were redissolved in hot water (70°) and saturated NaHCO_3 was added dropwise to pH 8. Rotary evaporation of the solution at 50°C gave mainly a pink precipitate. Most of the excess ligand remained solubilized as the sodium salt. At this point the product is fairly pure. Final purification was carried out by redissolving the product in water and adding Bio-Rad AG50W-X2 cation exchange resin (200-400 mesh, H^+ form) until

the solution was colorless.¹¹ The resin was filtered and washed extensively with water. The complex was eluted from the resin with concentrated HCl. The perchlorate salt was isolated from this solution by addition of concentrated HClO_4 , followed by rotary evaporation. The product was recrystallized from 0.1 N HClO_4 and dried in a vacuum desiccator. The spectrum of the pure complex agreed with that reported in the literature;¹⁰ absorption maxima were observed at 502 nm ($\epsilon \sim 80 \text{ M}^{-1} \text{ cm}^{-1}$) and 350 nm ($\epsilon \sim 65 \text{ M}^{-1} \text{ cm}^{-1}$). Elemental analyses were done by the Caltech Analytical Laboratory. Calcd.: C, 12.7; H, 3.6; N, 14.8. Found: C, 12.8; H, 3.5; N, 14.7.

Attachment of the Cobalt(III) Pentaammine Complex to Cytochrome *c*. All reactions were carried out at room temperature in phosphate buffer, $\mu = 0.1 \text{ M}$. The concentrations of ferrocytochrome *c* solutions were determined spectrally using $\epsilon_{550} = 29.5 \times 10^3 \text{ M}^{-1} \text{ cm}^{-1}$.¹²

Formation of the PtCl_4^{2-} -ferrocytochrome *c* derivative. Ferrocytochrome *c* solutions in phosphate buffer, pH 6.0, were prepared by dissolving the oxidized protein in a few mLs of buffer and adding excess $\text{Fe}(\text{EDTA})^{2-}$. Excess $\text{Fe}(\text{EDTA})^{2-}$ and $\text{Fe}(\text{EDTA})^-$ were removed from the ferrocytochrome *c* solution using a Sephadex G-25 gel filtration column equilibrated with deoxygenated buffer. The reduced protein was eluted from the column, and diluted to the desired volume, with deoxygenated buffer. The solution was stored

in a serum-capped bottle under constant flow of argon prior to use. Concentration of the reduced cytochrome *c* was 0.1-0.2 mM.

The $\text{Fe}(\text{EDTA})^{2-}$ used in the preparation of the ferro-cytochrome *c* solutions was made by combining a solution of ferrous ammonium sulfate with a buffered solution (phosphate, pH 7) containing a 20% excess over the stoichiometric amount of $\text{Na}_2\text{H}_2\text{EDTA}$. This was done anaerobically, and the solution was stored under argon, as $\text{Fe}(\text{EDTA})^{2-}$ is rapidly destroyed by oxygen.

A 10 mM solution of K_2PtCl_4 was prepared in water, and deoxygenated by bubbling with argon. A 10-fold excess of K_2PtCl_4 was added dropwise to the cytochrome *c* solution with stirring. The solution was stirred slowly under argon for periods ranging from three to seven hours. After the specified reaction time the excess PtCl_4^{2-} was removed by running the solution down a Sephadex G-25 gel filtration column equilibrated with deoxygenated phosphate buffer at pH 7.0. This treatment removed the unreacted platinum and reequilibrated the protein into the medium desired for reaction with the cobalt(III) complex. Ferrocyanocytocrome *c* concentration after elution from the column was in the range of 0.03-0.10 mM. When a sample was to be analyzed at this point for iron and platinum content, the sample was dialyzed into Millipore water. The dialysis was done either in dialysis tubing or in a hollow fiber beaker dialyzer

(Dow Bio-Fiber 50). Cytochrome *c* tends to adhere to dialysis tubing when dialyzed at low ionic strengths. This problem could be minimized by acetylating the dialysis tubing. This was done by soaking it overnight in 10% acetic anhydride in pyridine, followed by thorough washings with sodium bicarbonate solution and deionized distilled water.¹³ The solution was then concentrated by N_2 pressure in an Amicon concentrator equipped with a UM-2 membrane to a concentration acceptable for atomic absorption, *i.e.*, 0.02-0.10 mM. Solutions which were to be reacted with the cobalt complex remained in buffer and were concentrated to 0.1-0.9 mM.

Formation of the cytochrome *c*-platinum-cobalt complex. A concentrated solution (10.0 or 40.0 mM) of $[\text{Co}(\text{NH}_3)_5(\text{Hpyr-4-COO})(\text{ClO}_4)_3$ was prepared in phosphate buffer (pH 7.0, $\mu = 0.1$ M). At pH 7 the pyridine nitrogen is deprotonated; $pK_a = 4.8$.¹⁰ A 50- or 100-fold excess of cobalt(III) complex was added dropwise with stirring under argon to the Pt-ferrocytochrome *c* solution. The solution was then run down a Sephadex G-25 gel filtration column equilibrated with deoxygenated pH 7.0 phosphate buffer. The cytochrome *c* band elutes first, and a clean separation between the protein and excess cobalt complex was observed. The concentration of eluted cytochrome *c* was 0.04-0.10 mM. Samples to be used for atomic absorption analysis of metal content were dialyzed into Millipore water (and concentrated

if necessary) as described above. Samples to be monitored for oxidation of ferrocyanochrome *c* remained in buffer and were diluted to about 0.02 mM.

A control was done in which the procedure outlined above was carried out except that no PtCl_4^{2-} was added. This was done to check for any nonspecific covalent binding of the cobalt(III) complex to ferrocyanochrome *c* in the absence of platinum.

Atomic absorption (AA) analyses. Analysis of the Fe, Pt, and Co content of the modified cytochrome *c* samples was done on a flame atomic absorption spectrophotometer (Instrumentation Laboratories, Inc.; Model 151). Standard solutions of 1000 ppm Fe (FeCl_3 in dilute HCl) and 1000 ppm Co (CoCl_2 in dilute HCl) are commercially available. These were used to prepare standard solutions at 2, 3 and 4 ppm for both elements by pipetting the appropriate amount of concentrated standard and diluting with Millipore water. $(\text{NH}_4)_2\text{PtCl}_4$ purchased from Alfa was used to prepare a 1000 ppm Pt solution. This solution was then used to prepare standard solutions at the following concentrations: 2, 5, 10, 20, 30, 40 ppm. The concentrations of the standard solutions were chosen in the range where linear absorbance *vs.* concentration plots are expected: Fe, 0-5 ppm; Co, 0-5 ppm; Pt, 0-150 ppm. Each day a sample was to be analyzed, new standard plots were determined for each element. A minimum of ten absorbance readings was taken on each

standard and sample solution measured, and the values averaged. The instrument was zeroed with Millipore water. A linear regression program was used to fit the standard solution data and to determine the metal concentrations in the protein samples from the absorbance readings.

It was necessary to dialyze all samples into Millipore water and to use $(\text{NH}_4)_2\text{PtCl}_4$ (rather than K_2PtCl_4) as the Pt standard because Na^+ from the buffer and K^+ both significantly suppress the Pt absorbance in atomic absorption measurements. Cobalt is also listed as an interference for Pt so that the Pt content obtained by AA for the totally labeled samples should be taken as a lower limit on the amount of Pt actually present. Attempts to quantitate the magnitude of Pt signal suppression at the level of Co present in these samples were unsuccessful. It is suggested that making the samples 2% in La should help eliminate the interferences.¹⁴ Controls done to test this gave Pt contents above the amount actually present in the sample when 2% La was added.

Kinetics Measurements. All kinetics runs done at pH 7 were in phosphate buffer with final ionic strength of 0.1 M. Kinetics at pH 4 were in acetate buffer, $\mu = 0.1$ M.

Intermolecular oxidation of cytochrome *c* by $[\text{Co}(\text{NH}_3)_5(\text{Hpyr-4-COO})](\text{ClO}_4)_3$. Ferrocytochrome *c* solutions were prepared as described above. Stock solutions of the pyridine-4-carboxylopentaamminecobalt(III) perchlorate were made up in phosphate (or acetate) buffer. Solutions

of the desired concentrations were prepared by diluting the appropriate amount of stock solution with buffer. The Co(III) solutions were deoxygenated by bubbling with argon for a minimum of 15 minutes prior to use in a kinetics run.

A Cary 15 spectrophotometer was used in all kinetics experiments. A 1-cm cell with two side chambers was used in these experiments. The cell was purged with argon and equal volumes of oxidant and reductant were introduced into the two sidearm chambers via Hamilton gastight syringes. The cell was closed off under a positive flow of argon. The reactants could then be mixed at time zero, and the cell transferred to the spectrophotometer immediately. Alternatively, the ferrocytochrome *c* aliquot was transferred via gastight syringe to a regular serum-capped 1-cm Cary cell under a positive flow of argon. The oxidant was then introduced into the cell at time zero via gastight syringe and the cell transferred to the Cary. All kinetics runs were carried out at 25°C, maintained by a thermostatted cell holder in the Cary 15.

The oxidation of ferrocytochrome *c* was monitored at 550 nm ($\Delta\epsilon = 18.5 \times 10^3 \text{ M}^{-1} \text{ cm}^{-1}$).¹⁵ The initial concentration of oxidant was varied between $1 \times 10^{-4} \text{ M}$ and $1 \times 10^{-2} \text{ M}$ and was always kept in pseudo-first-order excess over reductant.

Log $(A_t - A_\infty)$ vs. time plots were checked for several preliminary kinetics runs on the oxidation of cytochrome *c*

by $[\text{Co}(\text{NH}_3)_5(\text{Hpyr-4-COO})(\text{ClO}_4)_3$ at pH 7 to verify first-order kinetic behavior. The plots appeared linear over greater than 90% of the reaction. The k_{obsd} values reported here for this reaction were calculated by the Guggenheim method.¹⁶ A minimum of 70 absorbance *vs.* time data points were used in the calculation of each k_{obsd} value.

Reactivity of the Co(III)-Pt-modified ferrocyanochrome *c*. The sample of Co(III)-Pt-modified ferrocyanochrome *c* used for this experiment was prepared as described above. After the excess cobalt complex was separated from the protein complex by gel filtration, the concentration of reduced protein was about 0.1 mM. A fraction of this solution was diluted approximately five-fold with phosphate buffer (pH 7.0, $\mu = 0.1$ M) and transferred to a special 1-cm quartz cell equipped with a side-chamber, needle valve, and sidearm for attachment to a vacuum line. The solution was subjected to three freeze-pump-thaw degassing cycles to remove any oxygen, and the cell was sealed under an atmosphere of argon. The first spectrum was recorded 0.5 h after the sample was eluted from the Sephadex G-25 column.

All spectra were recorded on a Cary 17 spectrophotometer. The reaction was monitored for greater than eight weeks. The solution was reduced with dithionite after the reaction was terminated, and total cytochrome concentration determined using $\epsilon_{550} = 29.5 \text{ mM}^{-1} \text{ cm}^{-1}$.

The remainder of the undiluted sample eluted from the column was subsequently dialyzed into Millipore water and analyzed by atomic absorption.

RESULTSAttachment of Pyridine-4-carboxylatopentaamminecobalt(III)
to Ferrocytochrome *c*

The atomic absorption results obtained for a number of modified cytochrome *c* samples are given in Table 3.1. The reaction conditions used in the preparation of the samples are also summarized in the table. In the samples containing both Pt and Co the value obtained for the Pt concentration may be low due to suppression of the Pt absorbance by Co. Although the extent of the suppression has not been quantified in this particular system, estimates based on measurements made by Pitts, Van Loon, and Beamish¹⁴ suggest that the absorbance readings should not be suppressed by more than 25% at the Pt:Co ratios studied here.

Samples 4A through 4C indicate that the initial attachment of PtCl_4^{2-} is slower than would be predicted by model complex studies.⁵ Using a ten-fold excess of PtCl_4^{2-} , cytochrome *c* is still only 90% modified after seven hours. This result is not surprising in view of the fact that Met-65 is located in a region of negative charge on cytochrome *c*.³ Results on sample 2 show that once PtCl_4^{2-} is bound to cytochrome *c*, addition of 100 equivalents of the cobalt(III) reagent results in nearly optimal binding of cobalt to platinum in 0.5 h. In the absence of bound PtCl_4^{2-} essentially no cobalt(III) reagent binds to the protein (sample 5).

Table 3.1. Metal Content of Modified Ferrocyanochrome *c* Samples

Reaction Conditions:		cyt <i>c</i> + PtCl ₄ ²⁻		Co(III) + cyt <i>c</i>	
Sample	[PtCl ₄ ²⁻]/[cyt <i>c</i>]	rxn. time (h)	[Co(III)]/[cyt <i>c</i>]	rxn. time (h)	[Fe] : [Pt] : [Co]
1	10	4.6 - 6.8 ^a	50	0.5 - 1.0	
2	10	3.0	100	0.5	
3	10	3.0	-	-	
4A	10	3.0	-	-	
4B	10	5.0	-	-	
4C	10	7.0	-	-	
5	10	-	100	0.5	

Atomic Absorption Results:					
Sample	[Fe] x 10 ⁴ (M)	[Pt] x 10 ⁴ (M)	[Co] x 10 ⁴ (M)	[Fe] : [Pt] : [Co]	[Fe] : [Pt] : [Co]
1	1.5 ± 0.1	1.2 ± 0.1 ^b	0.64 ± 0.02	1.0 : 0.80 : 0.43	
2	1.1 ± 0.04	0.54 ± 0.06 ^b	0.55 ± 0.02	1.0 : 0.49 : 0.50	
3	1.6 ± 0.04	0.52 ± 0.05	-	1.0 : 0.33 : -	
4A	0.34 ± 0.02	0.16 ± 0.01	-	1.0 : 0.47 : -	
4B	0.32 ± 0.02	0.22 ± 0.04	-	1.0 : 0.69 : -	
4C	0.34 ± 0.02	0.31 ± 0.04	-	1.0 : 0.91 : -	
5	1.4 ± 0.04	-	0.002 ± 0.001	1.0 : - : 0.001	

^aSolution volume and column capacity prevented column purification of total sample at one time.

^b[Pt] reported is minimum value due to suppression by Co.

No samples exhibiting the desired Fe:Pt:Co ratio of 1:1:1 were obtained. Based on the results which were obtained, it is predicted that the following reaction sequence would produce such a fully labeled species: react cytochrome *c* with a ten-fold excess of PtCl_4^{2-} for eight to ten hours; remove excess PtCl_4^{2-} ; react the PtCl_4^{2-} -cytochrome *c* solution with a 100-fold excess of Co(III) reagent for 0.5 hour; remove the excess cobalt reagent. In light of the kinetics results discussed below, this route to the desired species was not pursued.

Intermolecular Oxidation of Cytochrome *c* by $[\text{Co}(\text{NH}_3)_5$ -
 $(\text{Hpyr-4-COO})](\text{ClO}_4)_3$

The k_{obsd} values obtained in pH 7 phosphate buffer, $\mu = 0.1$ M, for the oxidation of ferrocyanochrome *c* by pyridine-4-carboxylatopentaamminecobalt(III) perchlorate at four different oxidant concentrations are listed in Table 3.2. The k_{obsd} values presented here represent only one kinetics run at each concentration, as it required more than 20 hours to carry each reaction to completion. Essentially, no dependence of the rate on Co(III) concentration was observed over the 100-fold range of oxidant concentration examined. Thus, at pH 7, the rate law is given by

$$\frac{-d[\text{cyt } c(\text{II})]}{dt} = k [\text{cyt } c(\text{II})]$$

where $k \approx 4 \times 10^{-5} \text{ s}^{-1}$.

Table 3.2. Kinetic Parameters for the Oxidation of Ferrocyanochrome *c* by
 $[\text{Co}(\text{NH}_3)_5(\text{Hpyr-4-COO})_3(\text{ClO}_4)_3$ (25°C, phosphate, $\mu = 0.1 \text{ M}$)

$[\text{Co}(\text{III})] \times 10^4 \text{ (M)}$	$k_{\text{obsd}} \times 10^5 \text{ (s}^{-1}\text{)}$	pH 7.0		pH 4.0	
		$[\text{Co}(\text{III})] \times 10^4 \text{ (M)}$	$t_{\frac{1}{2}} \text{ (min)}$	$[\text{Co}(\text{III})] \times 10^4 \text{ (M)}$	$t_{\frac{1}{2}} \text{ (min)}$
0.5	3.2	5.0	301		
1.5	4.4	25.0	74		
2.6	4.4	50.0	31		
5.2	3.4				

Whereas at pH 7 the pyridine nitrogen of the cobalt(III) complex is deprotonated, at pH 4 the complex is 86% protonated; $pK_a = 4.8$.¹⁰ At pH 4 the oxidation of cytochrome *c* by $[\text{Co}(\text{NH}_3)_5(\text{Hpyr-4-COO})](\text{ClO}_4)_3$ gave nonlinear first-order plots but the rate did show a dependence on Co(III) concentration. The half-lives for the reaction measured at three different oxidant concentrations are given in Table 3.2. The nonlinearity of the first-order plots at pH 4 may be due to the presence of two forms of the cobalt complex (protonated and deprotonated) as well as two forms of cytochrome *c*. Ferrocytochrome *c* exhibits a pK_a of about 4, below which the protein begins to unfold.⁸

Reactivity of Co(III)-Pt-Modified Ferrocytochrome *c*

An aliquot of the solution designated sample 2 in Table 3.1 was used for the initial kinetic study aimed at probing the electron transfer reactivity of the Co(III)-modified ferrocytochrome *c*. Based on the total cytochrome concentration in the sample (0.019 mM), the cytochrome *c* eluted from the column after attachment of the cobalt(III) reagent was about 80% reduced (Fe(II)), 20% oxidized (Fe(III)). Atomic absorption results on this sample indicated that the molar ratio of total cytochrome *c* to cobalt was two to one. Assuming that all the cobalt present after column elution was cobalt(III), the cobalt(III)

concentration at time zero was about 0.009 mM. Thus 63% of the reduced cytochrome in the sample was capable of being oxidized intermolecularly. Assuming that some of the cobalt(III) complex was attached to cytochrome molecules which became oxidized during sample preparation, the fraction of reduced cytochrome *c* molecules capable of being oxidized intramolecularly was less than 63%. Since only 63% of the reduced cytochrome *c* present could be oxidized by the cobalt(III) (the only oxidant present, assuming no O_2 leakage), the total absorbance change observable was 0.15. Over a period of 8.4 weeks $\Delta A_{\text{obsd}} = 0.05 \pm 0.02$, accounting for the oxidation of $33 \pm 10\%$ of the reduced cytochrome *c* present at time zero. The scatter in the absorbance *vs.* time curve was too large to warrant further manipulation of the data.

This preliminary kinetics study was far from extensive enough to assess whether the limited oxidation observed was attributable to purely second-order intermolecular electron transfer, first-order intramolecular transfer, or a combination of the two.

DISCUSSION

A procedure has been developed here which can be used to attach an inorganic redox reagent to the surface of cytochrome *c*. The specificity desired was achieved by exploiting the fact that PtCl_4^{2-} is known to bind almost exclusively to methionine 65 of cytochrome *c*.^{2,3} The redox active cobalt(III) pentaammine reagent employed has a sixth ligand with a free deprotonated pyridine nitrogen at pH 7 which subsequently reacts with the attached PtCl_4^{2-} . The observation that no cobalt complex bound to cytochrome *c* in the absence of platinum confirmed that this reaction also proceeded with the desired specificity.

The intermolecular oxidation of cytochrome *c* by $[\text{Co}(\text{NH}_3)_5(\text{Hpyr-4-COO})](\text{ClO}_4)_3$ was extremely slow. It is quite possible that the thermodynamic driving force for the reaction is very low. This cannot be confirmed as the redox potential of the cobalt complex is unknown. Unlike the reactions of most inorganic redox reagents with cytochrome *c*, the rate of cytochrome *c* oxidation was independent of oxidant concentration at pH 7. One mechanism consistent with such an observation involves rapid binding (noncovalent) of the cobalt reagent to cytochrome *c* followed by slow intramolecular electron transfer. If it is postulated that the free deprotonated nitrogen of the pyridine-4-carboxylate ligand is involved in the formation of a protein-oxidant complex, protonation of the nitrogen should inhibit the binding.

At pH 4, where the pyridine ring is 86% protonated, the observed cytochrome *c* oxidation rates were dependent on Co(III) concentration, although simple pseudo-first-order kinetic behavior was not observed. The proposed mechanism is indeed speculative. A more extensive kinetic study would have to be undertaken to elucidate the details of the mechanism which is operative in this system.

The slow rate of intermolecular cytochrome *c* oxidation at pH 7 ($t_{\frac{1}{2}} \approx 5$ hr) did prove experimentally advantageous in the formation of a mixed valence Co(III)-Fe(II) cytochrome *c* derivative. The cobalt(III) complex could be attached to the PtCl_4^{2-} -modified ferrocytochrome *c* without substantial loss of reduced cytochrome *c* to intermolecular oxidation by free cobalt(III) reagent. In actuality, though, the slow rate of cytochrome *c* oxidation by the cobalt(III) complex severely limited the utility of this reagent as a probe of intramolecular electron transfer reactivity in metalloproteins. In the Co(III)-Pt-ferrocytochrome *c* derivative the distance between the pyridine nitrogen of the cobalt site and the closest aromatic carbon of the heme group is about 15 Å.^{1,17} It is unrealistic to expect the rate of intramolecular electron transfer over such a distance to be readily observable in a system where the intermolecular reactivity of the two redox species is so low. If investigated more thoroughly, the slow oxidation of the heme iron in the

Co(III)-Pt-modified ferrocytocchrome *c* sample would, no doubt, prove to be an intermolecular, rather than intramolecular, process.

The results of this initial protein modification study were encouraging in that the generation of a redox reagent-modified metalloprotein was realized by simply applying the principles of inorganic substitution chemistry. The modification procedure was specific for a single site on the protein, and the derivative was stable as isolated.

(It should be noted here that although stable in the cobalt(III) form, the cobalt-cytochrome *c* derivative was not stable to external reductants due to the substitutional lability of cobalt(II) ammine complexes. Thus the number of redox manipulations which could be carried out on the derivative was extremely limited.) Unfortunately, the cobalt complex chosen did not possess the properties required to effectively probe intramolecular electron transfer reactivity in metalloproteins.

A synthetic multisite metalloprotein more conducive to the study of intramolecular electron transfer could be generated by simply utilizing a more reactive inorganic redox reagent in the procedure developed here for the attachment of the cobalt(III) pentaammine complex to cytochrome *c*. This approach was not taken, however, owing to the realization that the specificity required in the modification of a metalloprotein could also be achieved by

the direct attachment of redox reagents to the surface of the protein. The need for initial attachment of PtCl_4^{2-} to cytochrome *c* was eliminated in the production of the pentacyanoferrate- and pentaammineruthenium-cytochrome *c* derivatives to be described in the following chapters.

REFERENCES AND NOTES

1. Estimate from 3-D model of tuna cytochrome *c* is 11 Å.
Distance calculated from tuna cytochrome *c* atomic coordinates is 11.5 Å.
2. Takano, T.; Kallai, O.B.; Swanson, R.; Dickerson, R.E. *J. Biol. Chem.* 1973, 248, 5234.
3. Dickerson, R.E.; Takano, T.; Eisenberg, D.; Kallai, O.B.; Samson, L.; Cooper, A.; Margoliash, E. *J. Biol. Chem.* 1971, 246, 1511.
4. Blundell, T.L.; Johnson, L.N. "Protein Crystallography"; Academic Press: New York, 1976.
5. Volshtein, L.M.; Mogilevskina, M.F. *Russ. J. Inorg. Chem. (English Transl.)* 1963, 8, 304.
6. Kennedy, B.P.; Gosling, R.; Tobe, M.L. *Inorg. Chem.* 1977, 16, 1744.
7. Yalman, R.G. *Inorg. Chem.* 1962, 1, 16.
8. Dickerson, R.E.; Timkovich, R. In "The Enzymes", 3rd ed.; Boyer, P.D., Ed.; Academic Press: New York, 1975; Vol. 11, Chapter 7.
9. Basolo, F.; Murmann, R.K. *Inorg. Syn.* 1953, 4, 171.
10. Gould, E.S.; Taube, H. *J. Am. Chem. Soc.* 1964, 86, 1318.
11. Thamburaj, P.K.; Loar, M.K.; Gould, E.S. *Inorg. Chem.* 1977, 16, 1946.
12. Van Gelder, B.F.; Slater, E.C. *Biochim. Biophys. Acta* 1962, 58, 593.
13. Peterman, B.F.; Morton, R.A. *Can. J. Biochem.* 1977, 55, 796.

14. Pitts, A.E.; Van Loon, J.C.; Beamish, F.E. *Anal. Chim. Acta* 1970, 50, 181.
15. Margoliash, E.; Frohwirt, N. *Biochem. J.* 1959, 71, 570.
16. Frost, A.A.; Pearson, R.G. "Kinetics and Mechanisms", 2nd ed.; Wiley: New York, 1961; p. 49.
17. Dickerson, R.E.; Eisenberg, D.; Varnum, J.; Kopka, M.L. *J. Mol. Biol.* 1969, 45, 77.

CHAPTER 4

SYNTHESIS OF PENTACYANOFERRATE(II)

COMPLEXES OF FERROCYTOCHROME *c*

INTRODUCTION

The pentacyanoferrate(II) ion exhibits a marked affinity for imidazole¹ and thioether² moieties. In a recent investigation³ of an extensive series of aminoacidpentacyanoferrate(II) complexes the methionine and histidine complexes were found to be the most stable, with association constants of $1.2 \times 10^6 \text{ M}^{-1}^2$ and $5.9 \times 10^5 \text{ M}^{-1}^1$, respectively. The rate of formation of the methionine complex is $5.35 \times 10^2 \text{ M}^{-1} \text{ s}^{-1}$; the rate of dissociation is $4.4 \times 10^{-4} \text{ s}^{-1}$.² For histidinepentacyanoferrate(II), $k^f = 3.15 \times 10^2 \text{ M}^{-1} \text{ s}^{-1}$; $k^d = 5.3 \times 10^{-4} \text{ s}^{-1}$.¹ The specificity of $\text{Fe}(\text{CN})_5^{3-}$ with respect to methionine and histidine residues renders it an attractive reagent for protein modification. An exploration of the possibility of obtaining a stable $\text{Fe}(\text{CN})_5^-$ -cytochrome *c* derivative was undertaken.

Horse heart cytochrome *c* has within its single polypeptide chain a total of two methionines and three histidines. Met-80 and His-18 act as axial ligands to the heme iron.⁴ Met-65, His-26, and His-33 are located on the surface of the protein, well removed ($>10 \text{ \AA}$) from the active site heme group.⁵ Therefore, assuming the integrity of the active site is not disrupted, a maximum of three covalently bound pentacyanoferrate(II) groups is predicted in the reaction of $\text{Fe}(\text{CN})_5\text{H}_2\text{O}^{3-}$ with ferrocyanocytocrome *c*. The possibility of $\text{Fe}(\text{CN})_5^{3-}$ attachment to the axial ligands in ferricytochrome *c*

cannot be ruled out in view of the greater substitutional lability of the heme iron in its oxidized state.⁴

The electron transfer reactivity of cyanoferates with cytochrome *c* is well documented.⁶⁻³¹ Both ferri- and ferrocyanide exchange electrons rapidly with cytochrome *c*.^{6,7} The rates of oxidation of ferrocyanide by a number of pentacyanoferate(III) complexes are also quite high.^{15,30,31} In the cytochrome *c* derivatives proposed here the reactive species, with respect to the intramolecular oxidation of cytochrome *c*, will be methioninepentacyanoferate(III) and histidinepentacyanoferate(III). In each case the driving force for the oxidation of cytochrome *c* is favorable; the reduction potentials of these two ions are 575 mV and 355 mV (vs. NHE), respectively.³ ($E^\circ = 260$ mV for cytochrome *c*).⁴ The potential of the aquopentacyanoferate ion is 390 mV.³²

The substitution and redox properties which render the pentacyanoferate ion an attractive protein modification reagent also place restrictions on the preparative methods which can be utilized in obtaining the desired derivative. Substitution kinetics dictate the use of pentacyanoferate(II) in the initial attachment reaction with cytochrome *c*. Based on the redox potentials noted above, this reaction will produce a species which is redox inert regardless of the oxidation state of the cytochrome *c*. This is, in fact, a desirable situation in that the production of a stable

species for initial purification and characterization studies is necessary. The generation of a redox active mixed valence species ($\text{Fe}^{\text{III}}(\text{CN})_5\text{Met-cyt c}^{\text{II}}$ and/or $\text{Fe}^{\text{III}}(\text{CN})_5\text{His-cyt c}^{\text{II}}$) is subsequently required in order to probe the intramolecular electron transfer reactivity of the $\text{Fe}(\text{CN})_5$ -labeled protein.

This chapter presents the results obtained for the reaction of the aquopentacyanoferate(II) ion with ferro-cytochrome *c*. The utility of the $\text{Fe}(\text{CN})_5^{3-}$ ion as a redox active protein modification reagent is evaluated.

EXPERIMENTAL SECTIONMaterials

Horse heart cytochrome *c* (type VI) and Sephadex G-25-150 gel filtration beads were obtained from Sigma. DEAE-52 (≡DE-52) anion exchange cellulose was obtained from Whatman. All other chemicals were reagent grade and were used as supplied.

$\text{Na}_3[\text{Fe}(\text{CN})_5\text{NH}_3] \cdot 3\text{H}_2\text{O}$ was prepared from nitroprusside, $\text{Na}_2[\text{Fe}(\text{CN})_5\text{NO}] \cdot 2\text{H}_2\text{O}$, by the standard procedure.³³ The product was recrystallized three times from 28% ammonia, washed with ethanol and ether, and dried in a vacuum desiccator. It was stored under vacuum at room temperature in the dark. The procedure of Bahner and Norton³⁴ was used in the preparation of N-methyl pyrazinium iodide from pyrazine (Aldrich, gold label) and methyl iodide.

Argon gas was passed through two chromous towers prior to use to remove oxidizing impurities. Distilled water was purified by a Barnstead Nanopure system (Model D1794).

Methods

The preparative and analytical procedures outlined below are variations on procedures initially worked out by Henrique E. Toma.³⁵ Changes in reagent concentrations, reaction times, and ionic strength were made from run to run, but only two basic procedural methods were used throughout. A typical example of each is given below.

Method 1. Ferrocytochrome *c* (1.0 μmol) and ascorbic acid (20 μmol) were placed in a serum-capped bottle. The bottle was purged with argon for 15 minutes after which 1.0 mL deoxygenated phosphate buffer (pH 7, $\mu = 0.5$ M) was added to dissolve the contents. After 30 minutes the cytochrome *c* was totally reduced by the ascorbate and solid $\text{Na}_3[\text{Fe}(\text{CN})_5\text{NH}_3] \cdot 3\text{H}_2\text{O}$ (11 μmol) was added to the ferrocytochrome *c* solution with stirring. The reaction was allowed to proceed for one hour at room temperature under argon.

Aquation of $\text{Fe}(\text{CN})_5\text{NH}_3^{3-}$ to give $\text{Fe}(\text{CN})_5\text{H}_2\text{O}^{3-}$ is rapid, but at the concentration employed here (11 mM) the formation of dimeric species (*e.g.* $\text{Fe}_2(\text{CN})_{10}^{6-}$) cannot be neglected.³⁶ Prior to chromatographic separation of the excess pentacyano-ferrate ions from the cytochrome *c*, an excess (100 μmol) of N-methyl pyrazinium iodide (MPzI) was added to the reaction mixture. The MPz⁺ reacts with the excess monomeric $\text{Fe}(\text{CN})_5\text{H}_2\text{O}^{3-}$, as well as the dimeric species, to form $\text{Fe}(\text{CN})_5\text{MPz}^{2-}$, a bright blue complex. After 35 minutes the reaction mixture was transferred anaerobically to a Sephadex G-25 column (1.5 x 80 cm) equilibrated with deoxygenated phosphate buffer (pH 7, $\mu = 0.05$ M). Elution with deoxygenated buffer at 4°C resulted in clean separation of the cytochrome *c* (red), $\text{Fe}(\text{CN})_5\text{MPz}^{2-}$ (blue), and excess MPz⁺ (yellow) bands. The separation was complete within about 30 minutes. The cytochrome *c* band was collected and maintained under a flow of argon. Analysis of the $\text{Fe}(\text{CN})_5^{3-}$ content was subsequently carried out.

Method 2. The initial steps of the procedure were the same as in Method 1, through the addition of $\text{Na}_3[\text{Fe}(\text{CN})_5\text{NH}_3] \cdot 3\text{H}_2\text{O}$. The reaction was allowed to proceed for about 1.3 hours at room temperature. Chromatographic separation of excess reagent was carried out on DEAE-52 cellulose, an anionic ion exchange material. The column bed was $\sim 2 \times 8$ cm. The column was equilibrated with deoxygenated phosphate buffer (pH 7, $\mu = 0.05$ M), and the separation procedure was carried out as anaerobically as possible. Eluting with the same buffer, the negative ions $(\text{Fe}(\text{CN})_5\text{H}_2\text{O})^{3-}$ and $\text{Fe}_2(\text{CN})_{10}^{6-}$ bound tightly to the top of the column. The ferrocytocchrome *c* species (net charge of unmodified ferrocytocchrome *c* at pH 7 is $+6.5^{37}$) passed through the column and was collected within five minutes of loading. The modified cytochrome *c* was maintained under argon and subsequently analyzed for $\text{Fe}(\text{CN})_5^{3-}$ content.

Analysis of the $\text{Fe}(\text{CN})_5^{3-}$ content of a modified cytochrome *c* solution was carried out by adding excess (>350-fold) N-methyl pyrazinium iodide to the cytochrome *c* solution. As the $\text{Fe}(\text{CN})_5^{3-}$ attached to the cytochrome *c* dissociated, formation of the $\text{Fe}(\text{CN})_5\text{MPz}^{2-}$ complex was monitored at 655 nm in a deoxygenated, serum-capped spectrophotometer cell. When the reaction was complete (usually <1 day), the total $\text{Fe}(\text{CN})^{3-}$ content was calculated using $\epsilon_{655}(\text{Fe}(\text{CN})_5\text{MPz}^{2-}) = 12.3 \times 10^3 \text{ M}^{-1} \text{ cm}^{-1}^{38}$. The cytochrome *c* concentration was calculated from A_{550}^{reduced} ($\epsilon = 29.5 \times 10^3 \text{ M}^{-1} \text{ cm}^{-1}^{39}$) measured prior to the addition of MPzI. All

spectral measurements were carried out on a Cary 219 UV-Vis spectrophotometer.

Analyses of the total iron content of the cytochrome *c* samples were done by atomic absorption (Caltech Analytical Laboratory).

RESULTS

Two different methods were employed in the generation of pentacyanoferate(II) complexes of ferrocyanochrome *c*. The preparative sequence of Method 1 is outlined in Figure 4.1. The $\text{Fe}(\text{CN})_5^{3-}$ content of a series of modified ferrocyanochrome *c* samples prepared by Method 1 is given in Table 4.1. The reaction conditions utilized in the preparation of each sample are also summarized in the table. Several generalizations can be made concerning the results; these are discussed below. The term "bound $\text{Fe}(\text{CN})_5$ groups" is used loosely in the following paragraphs. It refers to the number of $\text{Fe}(\text{CN})_5^{3-}$ groups present, and analyzable, in the solution that is obtained after the chromatographic separation is complete. It does not necessarily imply covalent bonding, as will be discussed. (The term covalent itself requires explanation - it refers to strong attachment of a protein ligand directly to the iron atom in $\text{Fe}(\text{CN})_5^{3-}$.)

Changes in the concentrations of reactants affected the product in the following manner. As the ratio of $\text{Fe}(\text{CN})_5\text{H}_2\text{O}^{3-}$ to cytochrome *c* in the reaction mixture is lowered, the number of bound $\text{Fe}(\text{CN})_5^{3-}$ groups decreases (samples 7, 8, 9). The dependence of the product on methyl pyrazinium ion concentration was puzzling. Increasing the amount of MPz^+ which was added to the reaction mixture prior to chromatography resulted in fewer bound $\text{Fe}(\text{CN})_5^{3-}$'s if the MPz^+ reaction time

Figure 4.1. Method 1 for the preparation, purification, and analysis of $\text{Fe}(\text{CN})_5^{3-}$ derivatives of ferrocytocchrome *c*.

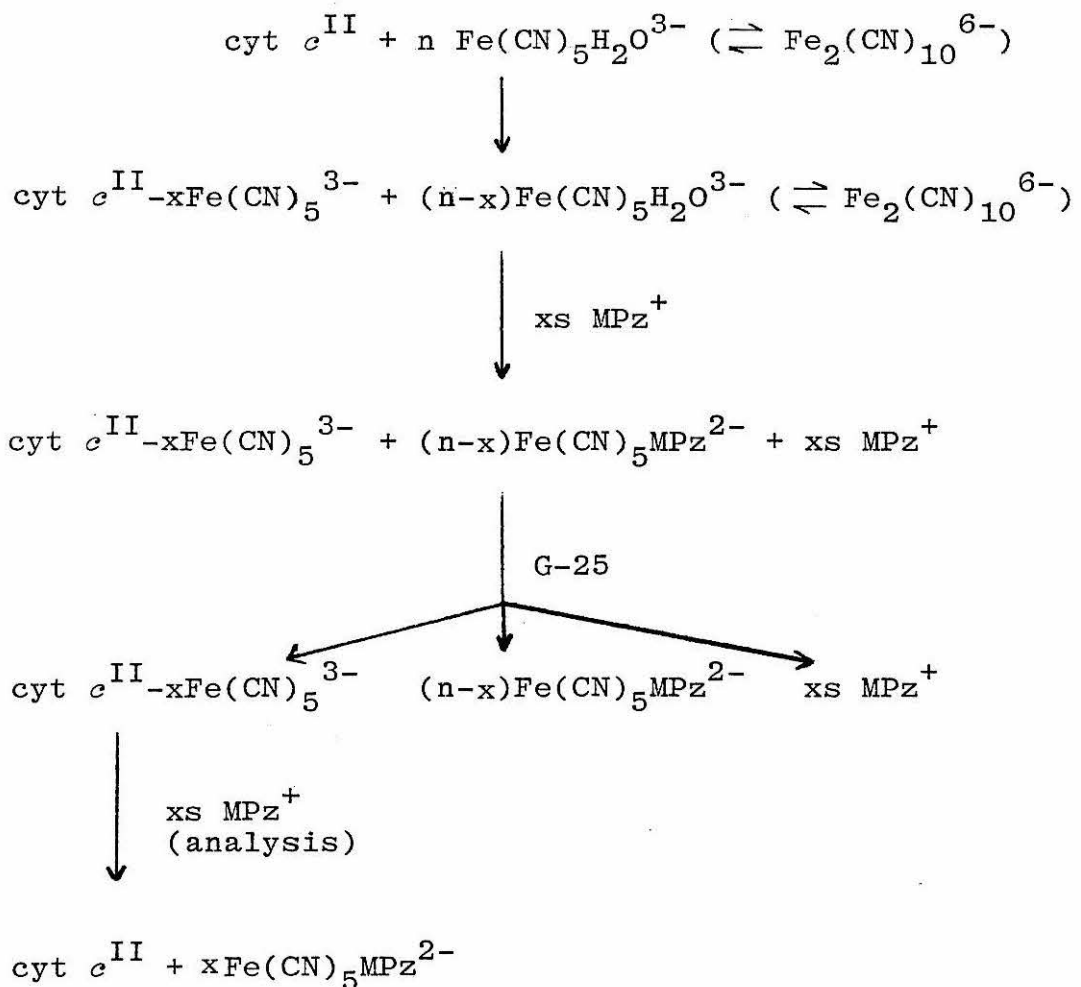


Table 4.1. Method 1 - Reaction Conditions and $[\text{Fe}(\text{CN})_5]^{3-}$ Content of Modified Ferrocyanochrome *c* Samples

Samples	Reaction Conditions ^a					Chromatography ^b $[\text{Fe}(\text{CN})_5]^{3-}$ / [cyt <i>c</i>]			
	[cyt <i>c</i>] (mM)	$[\text{Fe}(\text{CN})_5]^{3-}$ (mM)	$\text{Fe}(\text{CN})_5$ time (h)	[MPz ⁺] (mM)	MPz ⁺ rxn. time (min)	μ_{rxn} (M)	μ_{column} (M)	Spectral Analysis	AA ^d Analysis
1	1.0	21	2.0	181	10	0.1	0.1	4.6	
2	1.0	21	1.0	1800	6	0.1	0.1	2.8	
3	1.0	20	1.0	1800	5	1.1	0.1	0.25	
4	1.0	20	1.0	100	4	1.1	0.1	0.40	
5	1.0	20	2.0	100	3	1.1	0.1	0.45	
6	1.1	20	1.0	50	4	0.5	0.05	6.3	
7	1.0	19	1.0	50	35	0.5	0.05	4.5	
8	1.0	11	1.0	50	35	0.5	0.05	2.3	
9	1.0	5	1.0	50	35	0.5	0.05	0.91	
10	1.0	10	1.0	50	45	0.5	0.05	1.4	
11	1.1	10	1.0	50	45	0.5	0.05	1.7	
12	1.0	11	1.0	50	38	0.5	0.05	2.1	
13	1.0	11	1.0	100	35	0.5	0.05	2.2	
14	1.0	11	1.0	100	37	0.5	0.05	1.2	
15	1.0	11	1.0	100	35	0.5	0.05	1.4	
16	1.0	11	1.0	100	36	0.5	0.05	1.4	
17	1.0	11	1.0	100	25	0.5	0.05	2.1	
18	1.0	11	1.0	100	27	0.5	0.05	2.7	
19	1.0	11	1.0	100	33	0.5	0.05	1.5	2.3
20	1.0	11	1.0	100	31	0.5	0.05	2.2	2.7
21	1.0	11	1.0	100	28	0.5	0.05	1.9	

^aAscorbic acid present in all reaction solutions at 20 mM. ^bSephadex G-25. ^cPhosphate buffer, pH 7. ^dAtomic absorption.

was short (samples 1, 2; 3,4). At longer MPz^+ reaction times little, if any, dependence of $\text{Fe}(\text{CN})_5^{3-}$ content on MPz^+ concentration was noted (samples 12,13).

Increasing the cytochrome *c* + $\text{Fe}(\text{CN})_5\text{H}_2\text{O}^{3-}$ reaction time from one hour to two hours did not significantly increase the number of bound $\text{Fe}(\text{CN})_5^{3-}$ groups (samples 4,5). Increasing the length of time the MPz^+ was allowed to react with the cytochrome *c*- $\text{Fe}(\text{CN})_5^{3-}$ solution prior to chromatography did, however, result in fewer bound $\text{Fe}(\text{CN})_5^{3-}$'s (samples 6, 7; 16, 17).

Ionic strength was an important variable in these reactions. The reaction between positively charged ferro-cytochrome *c* (+6.5 at pH 7³⁷) and negatively charged $\text{Fe}(\text{CN})_5\text{H}_2\text{O}^{3-}$ should be most favorable at low ionic strengths. Indeed, increasing the ionic strength of the reaction buffer from 0.1 M to 1.1 M resulted in a significant drop in cytochrome *c*-bound $\text{Fe}(\text{CN})_5^{3-}$ (samples 2,3).

The iron content of samples 19 and 20 was checked by atomic absorption. The concentration of heme iron was determined spectrally and subtracted from the total iron content to obtain the number of bound $\text{Fe}(\text{CN})_5^{3-}$ groups. In both cases the number determined by atomic absorption exceeded that determined by the MPz^+ analytical procedure. Partial oxidation of the bound $\text{Fe}(\text{CN})_5^{3-}$ groups could account for such a discrepancy; once oxidized, the $\text{Fe}(\text{CN})_5^{3-}$ ion no longer reacts with MPz^+ to give $\text{Fe}(\text{CN})_5\text{MPz}^{2-}$.

The results obtained on several samples prepared by Method 1 suggest that the analytical number of $\text{Fe}(\text{CN})_5^{3-}$ groups per cytochrome *c* molecule does not actually represent the number of $\text{Fe}(\text{CN})_5^{3-}$ groups covalently bound to cytochrome *c*. Given that there are only three attachment sites (Met-65, His-33, His-26) on the surface of cytochrome *c*, $[\text{Fe}(\text{CN})_5^{3-}] / [\text{cyt c}]$ ratios of 6.3, 4.6, and 4.5 are immediately called into question (samples 1, 6, 7). It is postulated that excess $\text{Fe}(\text{CN})_5^{3-}$ and $\text{Fe}_2(\text{CN})_{10}^{6-}$ ions bind electrostatically to the positively charged protein surface. (There is precedent for this in the binding of $\text{Fe}(\text{CN})_6^{4-}$ to cytochrome *c*.^{13,17}) It appears that treatment of the reaction mixture with methyl pyrazinium ion prior to separation on G-25, and the actual gel filtration chromatography itself, are not totally effective in removing the electrostatically bound species from the cytochrome *c*.

In an attempt to minimize the retention of electrostatically bound pentacyanoferrates by cytochrome *c*, Method 2 was instituted. The procedure is outlined in Figure 4.2. The use of an anion exchange column for product purification eliminates the need for pretreatment of the reaction mixture with methyl pyrazinium ion. The anion exchange column should bind all the excess $\text{Fe}(\text{CN})_5^{3-}$ and $\text{Fe}_2(\text{CN})_{10}^{6-}$, while the cytochrome *c* species is eluted from the column. The results obtained using Method 2 are summarized in Table 4.2.

Figure 4.2. Method 2 for the preparation, purification, and analysis of $\text{Fe}(\text{CN})_5^{3-}$ derivatives of ferrocytocchrome *c*.

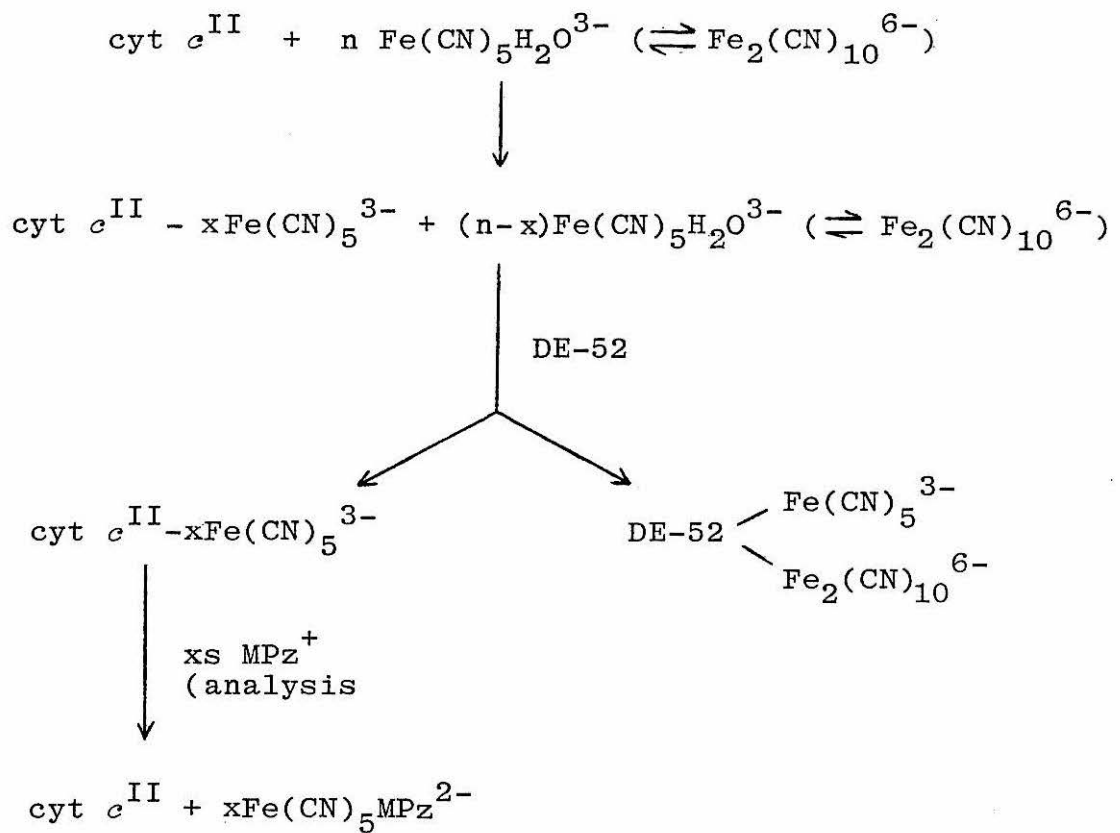


Table 4.2. Method 2 - Reaction Conditions and $\text{Fe}(\text{CN})_5^{3-}$ Content of Modified Ferrocyanochrome *c* Samples

Table 4.2 (cont.)

^a Ascorbic acid present in all reaction solutions at 20[cyt c].	^b DEAE-52 anion exchange.	^c Phosphate buffer,
^d Atomic absorption.	^e Aliquot of 5A kept at r.t. for 2 days, repurified on DE-52.	^f Aliquot of 6A kept at 4°C for 1 day, repurified on DE-52.
^g Aliquot of 7A kept at 4°C for 1 day, repurified on DE-52.	^h Aliquot of 8A lyophilized, redissolved after 1 day, analyzed without further purification.	ⁱ Aliquot of 8A lyophilized, redissolved after 6 days, analyzed without further purification.
^j Aliquot of 10A lyophilized, redissolved after 1 day, analyzed without further purification.	^k Aliquot of 10A lyophilized, redissolved after 1 day, repurified on DE-52.	^l Aliquot of 10A lyophilized, redissolved after 4 days, repurified on DE-52.
^m Aliquot of 10A lyophilized, redissolved after 4 days, repurified on DE-52.	ⁿ Aliquot of 11A repurified on DE-52 1 hour after initial DE-52.	^o Aliquot of 11A kept at -60°C for 1 day, analyzed without further purification.
^q Aliquot of 11A kept at -60°C for 1 day, repurified on DE-52.	^p Aliquot of 11A kept at -60°C for 1 day, repurified on DE-52.	^q Aliquot of 11A kept at -60°C for 1 day, repurified on G-25.

Note that under similar conditions of reagent concentration, reaction time, and ionic strength, the samples generated by Method 2 contained significantly fewer $\text{Fe}(\text{CN})_5^{3-}$ groups than did those generated by Method 1. Method 2 appeared to be fairly reproducible, yielding a cytochrome *c* derivative with $1 \pm 0.2 \text{ Fe}(\text{CN})_5^{3-}$ group per protein molecule. Atomic absorption results were also in good agreement with the spectral analyses. Rather than continuing the investigation of the effects of varied reaction conditions, the emphasis in the Method 2 studies was on the exploration of the stability and properties of the derivatives obtained.

Once the modified cytochrome *c* species was eluted from the anion exchange column, dissociation of the bound $\text{Fe}(\text{CN})_5^{3-}$ groups was monitored by the addition of methyl pyrazinium iodide and subsequent spectral observation of $\text{Fe}(\text{CN})_5^{\text{MPz}2-}$ formation. At 25°C dissociation was complete in less than 24 hours, with $t_{\frac{1}{2}}$ less than one hour in most cases. Although a detailed study of the dissociation kinetics was not made, first order plots were nonlinear. This suggests that a $[\text{Fe}(\text{CN})_5^{3-}] / [\text{cyt } c]$ ratio of one does not necessarily mean that only one site on the protein is modified. Most likely several sites are partially substituted, giving rise to a dissociation rate which is actually a composite of at least two different k^d 's.

The stability of the modified cytochrome *c* samples was tested under various conditions. As noted above, the

cytochrome *c* derivative was not stable for long periods of time at room temperature. An aliquot of a sample with an initial analysis of 1.1 $\text{Fe}(\text{CN})_5^{3-}$ per molecule was left under argon at room temperature for two days. It was then repurified on DE-52 and analyzed. No $\text{Fe}(\text{CN})_5^{3-}$ remained bound to the cytochrome *c* (sample 5C). Results on sample 11B are consistent with an estimated $t_{\frac{1}{2}} < 1$ hour at 25°C: one hour after the initial DE-52 column the sample was subjected to a second DE-52 purification, then analyzed. Only one-half the original amount of bound $\text{Fe}(\text{CN})_5^{3-}$ remained. Storage of a sample at 4°C, or -60°C, improved the stability; $t_{\frac{1}{2}}$ increased to about 1 day (samples 6B, 7B, 11D, 11E). Once the initial purification was carried out on DE-52, the second purification could be done on either DE-52 or G-25, with similar results on each (samples 6B, 7B; 11D, 11E). Thus it did not appear that the anion exchange material promoted the dissociation of the bound $\text{Fe}(\text{CN})_5^{3-}$.

Attempts to determine where the $\text{Fe}(\text{CN})_5^{3-}$ groups were attached to the protein were made using cyclic voltammetry. Solutions directly off the DE-52 column were concentrated to ≥ 0.2 mM and used within several hours of preparation. Platinum and gold electrodes were utilized. Reproducible results were not obtained.

DISCUSSION

The reaction of aquopentacyanoferate(II) with ferrocytochrome *c* is rapid, and fairly specific, under the conditions employed here. A procedure was developed in which a reaction time of one hour, and subsequent purification on an anion exchange column, produced a species with one (± 0.2) $\text{Fe}(\text{CN})_5^{3-}$ group per cytochrome *c* molecule.

The advantage of being able to analyze for bound $\text{Fe}(\text{CN})_5^{3-}$ by a simple spectral analysis was overshadowed by the fact that the analytical procedure derived its utility from the ease with which $\text{Fe}(\text{CN})_5^{3-}$ dissociates from the protein. Within one hour of preparation more than half of the bound $\text{Fe}(\text{CN})_5^{3-}$ is dissociated. The dissociation of attached $\text{Fe}(\text{CN})_5^{3-}$ from cytochrome *c* has been examined more closely in another laboratory.³ Biphasic kinetics were observed, and analyzed in terms of two parallel reactions with $k^d = 8.5 \times 10^{-5} \text{ s}^{-1}$ ($t_{\frac{1}{2}} = 2.3 \text{ h}$) and $6.8 \times 10^{-4} \text{ s}^{-1}$ ($t_{\frac{1}{2}} = 0.28 \text{ h}$) (25°C , 0.025 M phosphate).

Characterization of the $\text{Fe}(\text{CN})_5^{3-}$ -cytochrome *c* derivative obtained here was severely hindered by the inherent lability of the complex. The sites of attachment of $\text{Fe}(\text{CN})_5^{3-}$ were not definitively identified. That more than one site is labeled is suggested by the multiphasic dissociation kinetics discussed above. The dissociation rate constants determined by Toma are similar to those

reported for the model complexes $\text{Fe}(\text{CN})_5\text{Met}^{3-}$ ($k^d = 4.4 \times 10^{-4} \text{ s}^{-1}^2$) and the $\text{Fe}(\text{CN})_5\text{His}^{3-}$ ($k^d = 5.3 \times 10^{-4} \text{ s}^{-1}^1$). These results are in keeping with the originally predicted sites of attachment, namely, Met-65, His-33, and His-26. Additional evidence for coordination of $\text{Fe}(\text{CN})_5^{3-}$ to Met-65 comes from recent cyclic voltammetry results on the $\text{Fe}(\text{CN})_5^{3-}$ -cytochrome *c* species. Toma³ observes a wave corresponding to $E_{\frac{1}{2}} = 0.52 \text{ V}$ (vs. NHE) in addition to the cytochrome *c* wave at $E_{\frac{1}{2}} = 0.26 \text{ V}$ (15°C , gold electrode, in the presence of 4,4'-bipyridyl).

It became clear in the course of this study that additional work on the purification and characterization of the $\text{Fe}(\text{CN})_5^{3-}$ -cytochrome *c* derivative was necessary before electron transfer studies could be attempted. Although anion exchange chromatography effectively removed excess $\text{Fe}(\text{CN})_5^{3-}$ reagent, the solution which was obtained was believed to be a mixture of modified species. Previous chemical modification studies of cytochrome *c* have shown that components of such mixtures can be cleanly separated by the careful application of cation exchange chromatography.⁴⁰ Once separated, the individual species can be characterized with respect to the site of modification. Unless such procedures are carried out on the $\text{Fe}(\text{CN})_5^{3-}$ -cytochrome *c* derivative, any study of its electron transfer reactivity will yield meaningless data. Unfortunately, the amount of time required to carry out these purification and characterization procedures is prohibitively large - a consequence of the instability of the $\text{Fe}(\text{CN})_5^{3-}$ -cytochrome *c* complex.

In view of the limitations discussed, work on the $\text{Fe}(\text{CN})_5^{3-}$ -cytochrome *c* system was discontinued. A system was sought which would exhibit both the specificity and stability of the $\text{Co}(\text{NH}_3)_5(\text{pyr-4-COO})$ -cytochrome *c* system (Chapter 3), and the potential electron transfer reactivity of the $\text{Fe}(\text{CN})_5$ -cytochrome *c* system. The $\text{Ru}(\text{NH}_3)_5$ -cytochrome *c* complex described in Chapter 5 is, in fact, such a system.

REFERENCES AND NOTES

1. Toma, H.E.; Martins, J.M.; Giesbrecht, E. *J. Chem. Soc.*, *Dalton Trans.* 1978, 1610.
2. Batista, A.A.; Toma, H.E. *An. Acad. brasil. Cien.* 1980, 52, 703.
3. Toma, H.E.; Batista, A.A.; Gray, H.B., to be submitted for publication.
4. Dickerson, R.E.; Timkovich, R. In "The Enzymes", 3rd ed.; Boyer, P.D., Ed.; Academic Press: New York, 1975; Vol. 11, Chapter 7.
5. Distances estimated from examination of molecular models of tuna cytochrome *c*.
6. Sutin, N.; Christman, D.R. *J. Am. Chem. Soc.* 1961, 83, 1773.
7. Havsteen, B.H. *Acta Chem. Scand.* 1965, 19, 1227.
8. Brandt, K.G.; Parks, P.C.; Czerlinski, G.H.; Hess, G.P. *J. Biol. Chem.* 1966, 241, 4180.
9. Watt, G.D.; Sturtevant, J.M. *Biochemistry* 1969, 8, 4567.
10. Morton, R.A.; Overnell, J.; Harbury, H.A. *J. Biol. Chem.* 1970, 245, 4653.
11. Margalit, R.; Schejter, A. *FEBS Lett.* 1970, 6, 278.
12. Czerlinski, G.H.; Dar, K. *Biochim. Biophys. Acta* 1971, 234, 57.
13. Stellwagen, E.; Shulman, R.G. *J. Mol. Biol.* 1973, 80, 559.
14. Zabinski, R.M.; Tatti, K.; Czerlinski, G.H. *J. Biol. Chem.* 1974, 249, 6125.

15. Cassatt, J.C.; Marini, C.P. *Biochemistry* 1974, 13, 5323.
16. Creutz, C.; Sutin, N. *J. Biol. Chem.* 1974, 249, 6788.
17. Stellwagen, E.; Cass, R.D. *J. Biol. Chem.* 1975, 250, 2095.
18. Miller, W.G.; Cusanovich, M.A. *Biophys. Struct. Mech.* 1975, 1, 97.
19. Ilan, Y.; Shafferman, A.; Stein, G. *J. Biol. Chem.* 1976, 251, 4336.
20. Ilan, Y.; Shinar, R.; Stein, G. *Biochim. Biophys. Acta* 1977, 461, 15.
21. Potasek, M.J.; Hopfield, J.J. *Proc. Natl. Acad. Sci. USA* 1977, 74, 3817.
22. Kihara, H.; Nakatani, H.; Hiromi, K.; Hon-nami, K.; Oshima, T. *Biochim. Biophys. Acta* 1977, 460, 480.
23. Larroque, C.; Marue, P.; Douzou, P. *Biochim. Biophys. Acta* 1978, 501, 20.
24. Ilan, Y.; Shafferman, A. *Biochim. Biophys. Acta* 1978, 501, 127.
25. McCray, J.A.; Kihara, T. *Biochim. Biophys. Acta* 1979, 548, 417.
26. Ilan, Y.; Shafferman, A. *Biochim. Biophys. Acta* 1979, 548, 565.
27. Goldkorn, T.; Schejter, A. *J. Biol. Chem.* 1979, 254, 12562.
28. Peterman, B.F.; Morton, R.A. *Can. J. Biochem.* 1979, 57, 372.

29. Kihara, H. *Biochim. Biophys. Acta* 1981, *634*, 93.
30. Butler, J.; Davies, D.M.; Sykes, A.G.; Koppenol, W.H.; Osheroff, N.; Margoliash, E. *J. Am. Chem. Soc.* 1981, *103*, 469.
31. Butler, J.; Davies, D.M.; Sykes, A.G. *J. Inorg. Biochem.* 1981, *15*, 41.
32. Toma, H.E.; Creutz, C. *Inorg. Chem.* 1977, *16*, 545.
33. Brauer, G. "Handbook of Preparative Inorganic Chemistry", 2nd ed.; Academic Press: New York, 1965; Vol. 2, p. 1511.
34. Bahner, C.T.; Norton, L.L. *J. Am. Chem. Soc.* 1950, *72*, 2881.
35. Toma, H.E., personal communication, 1979.
36. Borghi, E.B.; Blesa, M.A.; Aymonino, P.J.; Olabe, J.A. *J. Inorg. Nucl. Chem.* 1981, *43*, 1849.
37. Wherland, S.; Gray, H.B. In "Biological Aspects of Inorganic Chemistry"; Addison, A.W.; Cullen, W.; James, B.R.; Dolphin, D., Eds.; Wiley: New York, 1977; p. 289.
38. Toma, H.E.; Malin, J.M. *Inorg. Chem.* 1973, *12*, 1039.
39. Van Gelder, B.F.; Slater, E.C. *Biochim. Biophys. Acta* 1962, *58*, 593.
40. Brautigan, D.L.; Ferguson-Miller, S.; Margoliash, E. *J. Biol. Chem.* 1978, *253*, 130.

CHAPTER 5

SYNTHESIS AND CHARACTERIZATION OF
PENTAAMMINERUTHENIUM(III) COMPLEXES
OF FERRICYTOCHROME *c*

INTRODUCTION

The three most important factors to be considered in the synthesis of a redox reagent-modified metalloprotein are specificity, stability, and electron transfer reactivity. The aquopentaammineruthenium(II) ion is a most attractive metalloprotein modification reagent on all three counts. The basis for such an assertion is rooted in the wealth of information currently available on the chemistry of ruthenium ammines. Similarly to aquopentacyanoferate(II), aquopentaammineruthenium(II) reacts readily with imidazole and thioether ligands.^{1,2} However, unlike the pentacyanoferates, the pentaammineruthenium complexes are reasonably substitution inert in both the Ru(II) and Ru(III) oxidation states.¹⁻⁴ The equilibrium constants (K), as well as the formation (k^f) and dissociation (k^d) constants, for the reactions of interest are presented in Table 5.1. Although the substitution kinetics of $\text{Ru}(\text{NH}_3)_5\text{H}_2\text{O}^{2+}$ with histidine and methionine have not been reported, the amino acid complexes have been prepared and characterized.^{2,5} The latter studies confirm that the imidazole and dimethyl sulfide complexes constitute adequate models for the histidine and methionine complexes, respectively.

Aquopentaammineruthenium(II) has a high affinity for both imidazole ($K = 2.8 \times 10^6 \text{ M}^{-1}$) and thioether ($K \geq 10^5 \text{ M}^{-1}$) groups. Examination of the k^f values indicates

Table 5.1. Reaction of Aquopentaammineruthenium with Imidazole and Dimethyl Sulfide

		$L = \begin{array}{c} \text{HN} \\ \diagup \quad \diagdown \\ \text{C} \quad \text{C} \\ \diagdown \quad \diagup \\ \text{N} \end{array}$	$L = \text{S}(\text{CH}_3)_2$
$\text{Ru}(\text{NH}_3)_5\text{H}_2\text{O}^{2+}$	$+ L$		
K		$2.8 \times 10^6 \text{ M}^{-1}$ ^a	$\geq 10^5 \text{ M}^{-1} \text{ s}^{-1}$ ^e
k^f		$2.0 \times 10^{-1} \text{ M}^{-1} \text{ s}^{-1}$ ^{b,c}	$8.0 \times 10^{-2} \text{ M}^{-1} \text{ s}^{-1}$ ^{e,f}
k^d		$7.1 \times 10^{-8} \text{ s}^{-1}$ ^d	$4.2 \times 10^{-6} \text{ s}^{-1}$ ^{e,g,h}
$\text{Ru}(\text{NH}_3)_5\text{H}_2\text{O}^{3+}$	$+ L$		
K		$1.9 \times 10^6 \text{ M}^{-1}$ ^e	$1.6 \times 10^{-2} \text{ M}^{-1}$ ^e
k^f	—	—	$4.2 \times 10^{-9} \text{ M}^{-1} \text{ s}^{-1}$ ⁱ
k^d	—	—	$2.6 \times 10^{-7} \text{ s}^{-1}$ ^{j,k}

^aRef. 1. ^bRef. 3. ^cpH 7, $\mu = 0.1$ (LiCl), 25°C. ^d k^f/K . ^eRef. 2. ^f0.1 M H⁺, 12-13% EtOH/H₂O, 25°C. ^g0.1 M H⁺, $\mu = 0.1$, 25°C. ^hRepresents rate of dissociation of NH₃ ligand rather than S(CH₃)₂. ⁱK_k^d. ^jRef. 4. ^k₀0.2 M HCl, 0.1 M LiCl, 25°C.

that complex formation must necessarily employ $\text{Ru}(\text{NH}_3)_5\text{H}_2\text{O}^{2+}$ in that $\text{Ru}(\text{NH}_3)_5\text{H}_2\text{O}^{3+}$ is too substitution inert. (No estimate of k^f for $\text{Ru}(\text{NH}_3)_5\text{H}_2\text{O}^{3+}$ /imidazole is available, however, for $\text{Ru}(\text{NH}_3)_5\text{H}_2\text{O}^{3+}$ /pyrazine $k^f < 4 \times 10^{-6} \text{ M}^{-1} \text{ s}^{-1}$.) Once formed, both the $\text{Ru}(\text{NH}_3)_5\text{L}^{2+}$ and $\text{Ru}(\text{NH}_3)_5\text{L}^{3+}$ complexes are relatively substitution inert. Aquation studies of $\text{Ru}(\text{NH}_3)_5\text{S}(\text{CH}_3)_2^{2+}$ show that an NH_3 ligand is lost in preference to the thioether ligand.² The aquation of $\text{Ru}(\text{NH}_3)_5\text{Im}^{2+}$ is acid-catalyzed and competing reactions which involve loss of an NH_3 ligand are also observed (although these are minor).¹ Additional stability with respect to ligand dissociation is gained by oxidation of the $\text{Ru}(\text{NH}_3)_5\text{L}^{2+}$ complexes to the Ru(III) state.

A number of factors contribute to the stabilization of the pentaammineruthenium-imidazole and -thioether complexes. Whereas complexes of Ru(II) with π -acid ligands (e.g., pyridine) are generally stabilized by back-bonding from the low spin d^6 metal center, the π -accepting ability of the pyridine-type nitrogen of imidazole is diminished by the ligand's pyrrole-type nitrogen.¹ The reaction of $\text{Ru}(\text{NH}_3)_5\text{H}_2\text{O}^{2+}$ with imidazole is thus considered to involve mainly σ -type acid-base interactions, and metal-to-ligand back-bonding makes only a small contribution to the stability of the $\text{Ru}(\text{NH}_3)_5\text{Im}^{2+}$ complex.⁷ This is evidenced by the absence of an MLCT band in the electronic spectrum. The low reduction potential of $\text{Ru}(\text{NH}_3)_5\text{Im}^{3+/2+}$ ($E^\circ = 0.11 \text{ V}$)

relative to complexes with better π -acceptor ligands (e.g., $\text{Ru}(\text{NH}_3)_5\text{py}^{3+/2+}$ with $E^\circ = 0.305$ V) also reflects the diminished role of back-bonding in the imidazole complex.¹ $\text{Ru}(\text{III})$ is a stronger σ acid than $\text{Ru}(\text{II})$. Consequently, $\text{Ru}(\text{NH}_3)_5\text{Im}^{3+}$ is also quite stable. Owing to the vacant site in its t_{2g} set of d orbitals, $\text{Ru}(\text{III})$ can also act as a π -acceptor. Stabilization of the $\text{Ru}(\text{III})$ -imidazole complex is believed to be due, in part, to π donation from imidazole to $\text{Ru}(\text{III})$.⁷ The 300-nm band in the absorption spectrum of $\text{Ru}(\text{NH}_3)_5\text{Im}^{3+}$ has been tentatively assigned to an LMCT transition.¹ The spectral and electrochemical properties of $\text{Ru}(\text{NH}_3)_5\text{Im}^{2+/3+}$ and $\text{Ru}(\text{NH}_3)_5\text{His}^{2+/3+}$ are summarized in Table 5.2.

In contrast to $\text{Ru}(\text{NH}_3)_5\text{Im}^{2+}$, back donation from $\text{Ru}(\text{II})$ plays a prominent role in the stabilization of pentaammineruthenium(II)-thioether complexes. The reduction potential of $\text{Ru}(\text{NH}_3)_5\text{S}(\text{CH}_3)_2^{3+/2+}$ ($E^\circ = 0.50$ V²) relative to $\text{Ru}(\text{NH}_3)_6^{3+/2+}$ ($E^\circ = 0.067$ V⁸) reflects the increased stabilization of $\text{Ru}(\text{II})$ by back-bonding in the thioether complex.⁴ Also, the high energy bands in the absorption spectrum of $\text{Ru}(\text{NH}_3)_5\text{S}(\text{CH}_3)_2^{2+}$ are assigned to MLCT transitions.² The identity of the ligand orbitals (sulfur 3d vs. $\text{S}(\text{CH}_3)_2 \sigma^*$) which accept electron density from the metal is a subject of some debate, however.^{4,9} Despite the fact that $\text{S}(\text{CH}_3)_2$ is a weak base, the $\text{Ru}(\text{NH}_3)_5\text{S}(\text{CH}_3)_2^{3+}$ complex is highly substitution inert. The stability of the oxidized

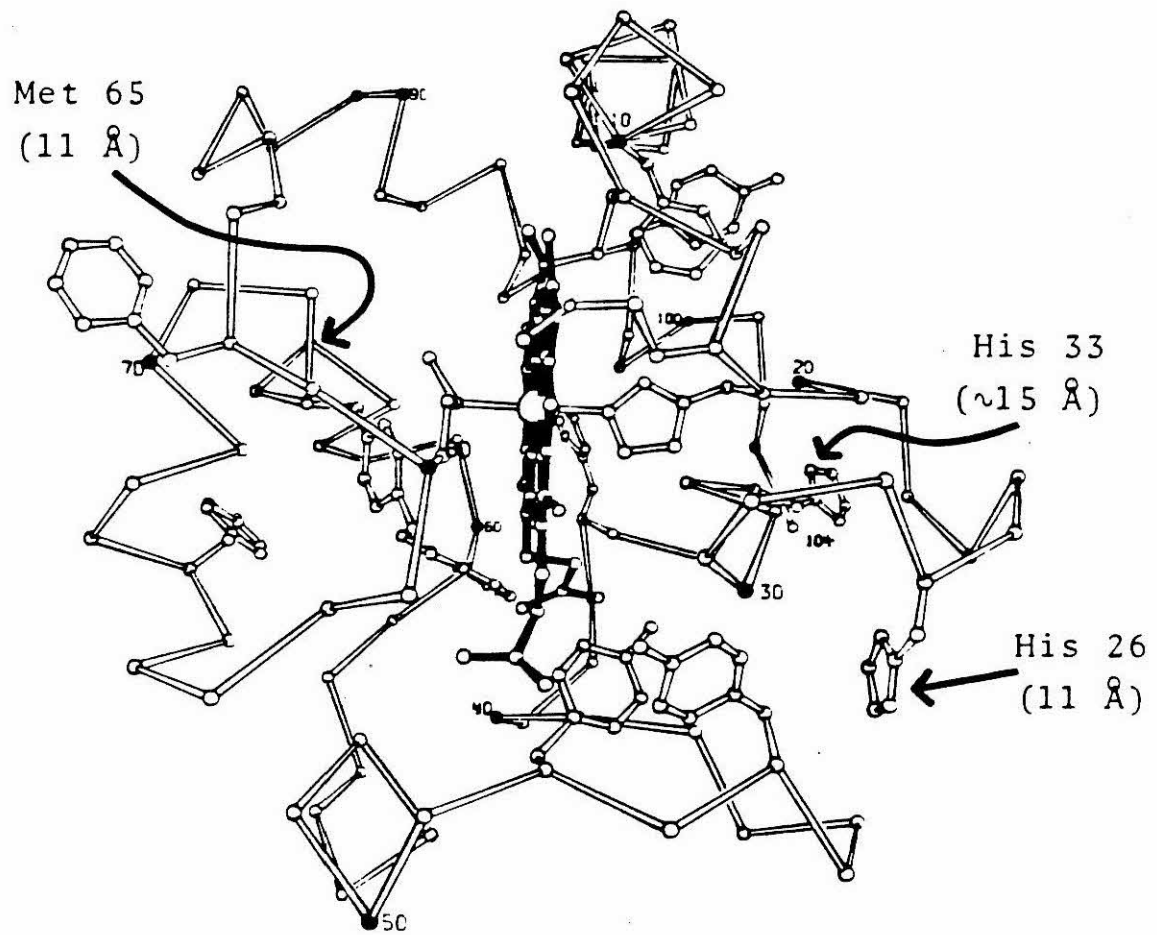
Table 5.2. Spectral and Electrochemical Properties of Imidazole and Thioether Complexes of Pentaammineruthenium

L	Ru(NH ₃) ₅ L ²⁺	Ru(NH ₃) ₅ L ³⁺	Ru(NH ₃) ₅ L ^{3+/2+}	Ref.
Im ≡	255 (2800) 280 sh (2700)	299 (1880) 430 (250)	0.11 —	1
His ≡	260 (3260) 280 (3160)	303 (2100) 450 (290)	— —	5
S(CH ₃) ₂	235 (2050) 258 (2140) 358 (64)	220 (~5000) 285 (930) 310 sh (~800) 453 (300)	0.50 — —	2,4
Met methyl ester ≡ CH ₃ SCH ₂ CH ₂ CH(COOCH ₃) ₂ NH ₃ ⁺	234 (~1000) 255 (~1000)	— —	0.53 —	2

complex is derived from the ability of Ru(III) to accept π electron density from $S(CH_3)_2$. This ligand-to-metal charge transfer also gives rise to the 453 nm band observed in the electronic absorption spectrum of the Ru(III)-thioether complex.⁴ The spectral and electrochemical properties of $Ru(NH_3)_5S(CH_3)_2^{2+/3+}$, and $Ru(NH_3)_5$ methionine methyl ester^{2+/3+}, are summarized in Table 5.2.

Given that $Ru(NH_3)_5H_2O^{2+}$ has a high affinity for, and forms stable complexes with imidazole and thioether groups, successful protein modification then depends on the accessibility of histidine and methionine residues in the protein of choice. Horse heart cytochrome *c* is the protein of choice in these studies. It has a total of three histidines and two methionines. His-18 and Met-80 are coordinated to the heme iron; His-26, His-33, and Met-65 are on the surface of the protein.¹⁰ The positions of the latter three residues relative to the heme *c* group are shown in Figure 5.1. The sulfur of Met-65 lies about 11 \AA from the closest aromatic carbon of the heme.¹¹ His-26 is also located about 11 \AA from the heme, while the His-33 distance is about 15 \AA (imidazole N3 to closest aromatic C of the heme).¹¹ What is not obvious from the skeletal drawing of cytochrome *c* in Figure 5.1 is that His-26 is hydrogen bonded to the carbonyl group of residue 44, rendering it less accessible than it may initially appear.¹² Indeed, in the reaction of horse heart cytochrome *c* with other histidine-specific

Figure 5.1. Structure of horse heart cytochrome *c* (front view). Non-heme-bound histidine and methionine residues are highlighted. Distance from amino acid side chain to closest heme edge is given in parentheses. (Adapted from Reference 59).



reagents (e.g., bromoacetic acid, iodoacetic acid) His-26 is unreactive.¹³

In light of the stated goal of generating a synthetic multisite metalloprotein capable of addressing the role of redox site separation in biological electron transfer reactions, the electron transfer properties of the modification reagent must also be considered. The reaction of the inorganic reagent with the protein must generate a redox site which has inherently high reactivity with the metalloprotein's own metal center, *i.e.*, the thermodynamic driving force for electron transfer between the two sites must be favorable. Model complex studies again support the choice of the pentaammineruthenium reagent. The driving force for the reduction of cytochrome *c* ($E^\circ = 0.26$ V¹⁰) by pentaamminehistidineruthenium(II) is 0.15 V; ΔE° for the oxidation of cytochrome *c* by pentaamminemethionineruthenium(III) is 0.27 V.

The seductive character of pentaammineruthenium(II) as a metalloprotein modification reagent prompted the initiation of the research to be described herein. The reaction of $\text{Ru}(\text{NH}_3)_5\text{H}_2\text{O}^{2+}$ with cytochrome *c*, followed by oxidation, produces several stable $\text{Ru}(\text{NH}_3)_5^{3+}$ -ferricytochrome *c* derivatives. These species have been purified by ion exchange chromatography, and characterized by a variety of techniques, including atomic absorption, high-pressure liquid chromatography, UV-visible absorption spectroscopy, cyclic voltammetry, and spectroelectrochemistry. A preliminary examination of the electron transfer reactivity of a pentaammineruthenium(III)-

histidine complex of cytochrome *c* is reported. A study of the properties and reactivity of the model complexes pentaammineimidazoleruthenium(III) chloride and pentaamminehistidineruthenium(III) chloride is also described.

EXPERIMENTAL SECTIONMaterials

$[\text{Ru}(\text{NH}_3)_5\text{Cl}]\text{Cl}_2$ was prepared from $[\text{Ru}(\text{NH}_3)_6]\text{Cl}_3$ (Matthey Bishop, Inc.) according to Vogt, Katz, and Wiberley,¹⁴ and recrystallized from 0.1 M HCl.¹⁵ $[\text{Ru}(\text{NH}_3)_6]\text{Cl}_2$ was prepared from $\text{RuCl}_3 \cdot 3\text{H}_2\text{O}$ ¹⁶ (Johnson Matthey, through Alfa) and recrystallized as described in Chapter 2. $[\text{Co}(\text{phen})_3](\text{ClO}_4)_3$ was prepared by Emilio Bordignon according to the method of Schlit and Taylor.¹⁷ $\text{Fe}(\text{EDTA})^{2-}$ solutions were made from $(\text{NH}_4)_2\text{FeSO}_4$ and $\text{Na}_2\text{H}_2\text{EDTA}$ as outlined in Chapter 3.

Horse heart cytochrome *c* (type VI) was purchased from Sigma Chemical Co., as were imidazole and L-histidine. Trypsin was from Worthington Biochemical. The acetonitrile used for high-pressure liquid chromatography was J.T. Baker HPLC reagent grade. J.T. Baker was also the supplier of 2,4,6-tris(2'-pyridyl)-s-triazine. Ruthenium atomic absorption standard solutions were obtained from Alfa and Aldrich. 4,4'-bipyridyl·2H₂O was purchased from Aldrich and was recrystallized from water. All other chemicals were reagent grade and were used without further purification.

Materials for column chromatography were obtained from the sources indicated, and were cleaned and equilibrated according to the manufacturers' instructions: AG50W-X2,

200-400 mesh (Bio-Rad); CM52 (Whatman); Sephadex G-25-150 (Sigma). The 3-way plastic stopcocks and medical tubing used in the column chromatography work were obtained from Ace Glass.

Stirred ultrafiltration cells for the concentration of proteins were purchased from Amicon and were used in conjunction with Amicon Diaflo YM5 membranes (m.w. cutoff 5000). Protein solutions (and other particulate-containing solutions) were filtered with disposable Millex-GS 0.22 μ m filter units (Millipore). Tryptic digest solutions were filtered with 0.5 μ m cellulosic membrane filters from Rainin Instrument Co. Spectrapor 1 (m.w. cutoff 6000-8000) dialysis tubing (Spectrum Medical Industries, Inc.) was used with cytochrome *c*. (At low ionic strengths cytochrome *c* tends to stick to dialysis tubing of undefined pore size.) Prior to use the tubing (32 mm diam.) was treated with sulfide and heavy metal removal solutions, also available from Spectrum. Tubing was stored at 4°C in H₂O.

Gas-tight syringes were purchased from Hamilton, as were platinum needles. The carbon paste and gold electrodes used for cyclic voltammetry were obtained from Bioanalytical Systems, Inc.

Serum stoppers were cleaned before use either by boiling in solutions of 1 M NaOH and, subsequently, 1 M HCl, or by soaking in solutions of ethanolic-KOH and ethanolic-HCl. After thorough rinsing the stoppers were stored at 4°C, either dry or in H₂O.

Distilled water was purified by passage through a Barnstead Nanopure water purification system (Model D1794). Argon used in all preparative work was rendered oxygen free by passage through two vanadous scrubbing towers¹⁸ and one H₂O tower. Argon used in kinetics experiments was passed through a MnO/vermiculite column¹⁹ followed by two proflavin/methylviologen towers.²⁰

Methods

Synthesis of Pentaammineimidazoleruthenium(III)

Trichloride and Pentaamminehistidineruthenium(III) Trichloride.

[Ru(NH₃)₅Im]Cl₃·2H₂O was prepared by reacting [Ru(NH₃)₅Cl]Cl₂ and imidazole over zinc amalgam, followed by air oxidation. The procedure employed was that of Sundberg et al.¹ The product was purified by ion exchange chromatography and crystallized from ethanol-water as described. Yield: 61%. The spectrum of the isolated Ru(III) complex, as well as that of the Ru(II) complex (generated by reduction over zinc amalgam), was in good agreement with the published spectral data.¹

[Ru(NH₃)₅His]Cl₃·H₂O was prepared in a manner similar to that of the imidazole complex by the method of Sundberg and Gupta.⁵ The product was purified by ion exchange chromatography and crystallized from acetone-water. Yield: 52%. Again, agreement of the observed spectra of the Ru(III) and Ru(II) complexes with the literature values⁵ was good.

Synthesis of Aquopentaammineruthenium(II) Hexafluorophosphate. $[\text{Ru}(\text{NH}_3)_5\text{H}_2\text{O}](\text{PF}_6)_2 \cdot \text{H}_2\text{O}$ was prepared by the reduction of $[\text{Ru}(\text{NH}_3)_5\text{Cl}]\text{Cl}_2$ over zinc amalgam in 0.1 M sulfuric acid, followed by precipitation with NH_4PF_6 . The procedure used was essentially that of Callahan.²¹ The product was washed with cold, deaerated water, ethanol, and finally, ether. It was dried and stored in a vacuum desiccator and was always used within one day of preparation. The complex exhibits λ_{max} at 415 nm ($\epsilon = 44 \text{ M}^{-1} \text{ cm}^{-1}$) and 268 nm ($\epsilon = 530 \text{ M}^{-1} \text{ cm}^{-1}$).²²

Purification of Commercial Cytochrome *c*. Commercial cytochrome *c* contains significant amounts of deamidated forms of the protein, *i.e.*, species in which several glutamines and/or asparagines have been hydrolyzed to their corresponding acids.²³ These species must be removed prior to protein modification so that they do not interfere with the purification of the $\text{Ru}(\text{NH}_3)_5$ -cytochrome *c* derivatives. Purification of cytochrome *c* is effected by cation exchange chromatography on carboxymethyl cellulose as described by Brautigan.²³ The following purification procedure was used routinely.

A 150-mg sample of type VI horse heart cytochrome *c* was dissolved in 5-10 mL water. A pinch of solid $\text{K}_3\text{Fe}(\text{CN})_6$ was added to the solution to insure complete oxidation of the protein. The solution was applied to a 2 x 60 cm column of CM-cellulose (Whatman CM52). 85 mM phosphate buffer, pH 7.0, was used to equilibrate the column. The same buffer was used

to elute the protein at 30 mL/h. Fractions of 9 mL were collected. The absorbance of the fractions was determined at 360 nm. Fractions corresponding to the major eluting species were pooled and concentrated to \leq 10 mL in an ultrafiltration cell equipped with a YM5 membrane. Typically 100-115 mg of pure cytochrome *c* were obtained. The concentrated solution was stored at 4°C if used within several days. Storage for longer periods was at -10°C.

Reaction of $\text{Ru}(\text{NH}_3)_5\text{H}_2\text{O}^{2+}$ with Cytochrome *c*. The reaction of $\text{Ru}(\text{NH}_3)_5\text{H}_2\text{O}^{2+}$ with horse heart cytochrome *c* was performed at room temperature in 85 mM sodium phosphate buffer, pH 7.0. Each preparation generally employed 100 mg of purified cytochrome *c* at a concentration of *ca.* 0.2 mM, and a 50-fold excess of ruthenium reagent ($[\text{Ru}] \approx 10$ mM). A constant flow of argon was maintained over, or through, the reaction mixture. Two slightly different reaction schemes were employed in the preparation of the $\text{Ru}(\text{NH}_3)_5-$ cytochrome *c* derivatives. The major differences between the two methods relate to the manner in which the $\text{Ru}(\text{NH}_3)_5\text{H}_2\text{O}^{2+}$ reagent was generated. A detailed account of a typical reaction procedure is given below for each of the two methods.

$\text{Ru}(\text{NH}_3)_5\text{Cl}_3/\text{Zn}$ amalgam method. In this method $\text{Ru}(\text{NH}_3)_5\text{H}_2\text{O}^{2+}$ was generated by the reduction of $[\text{Ru}(\text{NH}_3)_5\text{Cl}]\text{Cl}_2$ over zinc-mercury amalgam. The amalgam was prepared by first dissolving 0.72 g HgO in *ca.* 5 mL concentrated HCl . 24 g

mossy zinc (cleaned with dilute HCl) were placed in a beaker along with enough water to cover the zinc. The Hg solution was added slowly to the zinc with stirring. The resulting amalgamated zinc was washed thoroughly with water and towel dried. Zinc amalgam was always freshly prepared prior to use.

A capped serum bottle containing 110 mL buffer, and zinc amalgam, was deoxygenated by bubbling with argon for \geq 30 min, after which 0.33 g $[\text{Ru}(\text{NH}_3)_5\text{Cl}]\text{Cl}_2$ was added. Over the course of one hour the ruthenium complex reduced, and dissolved. 100 mL (1.02 mmol) of the bright yellow ruthenium solution were then transferred via syringe, and Millipore filter, to the deaerated reaction vessel containing several pieces of Zn amalgam. The filter served to get rid of the white precipitate which inevitably formed in the $\text{Ru}(\text{NH}_3)_5\text{Cl}_3/\text{Zn}$ amalgam solution. A spectrum of the $\text{Ru}(\text{NH}_3)_5$ solution taken in a deaerated cell indicated that the $\text{Ru}(\text{NH}_3)_5\text{H}_2\text{O}^{2+}$ solution generated as described was slightly contaminated by $\text{Ru}(\text{NH}_3)_5\text{OH}^{2+}$. The fraction of un-reduced ruthenium was not determined, however.

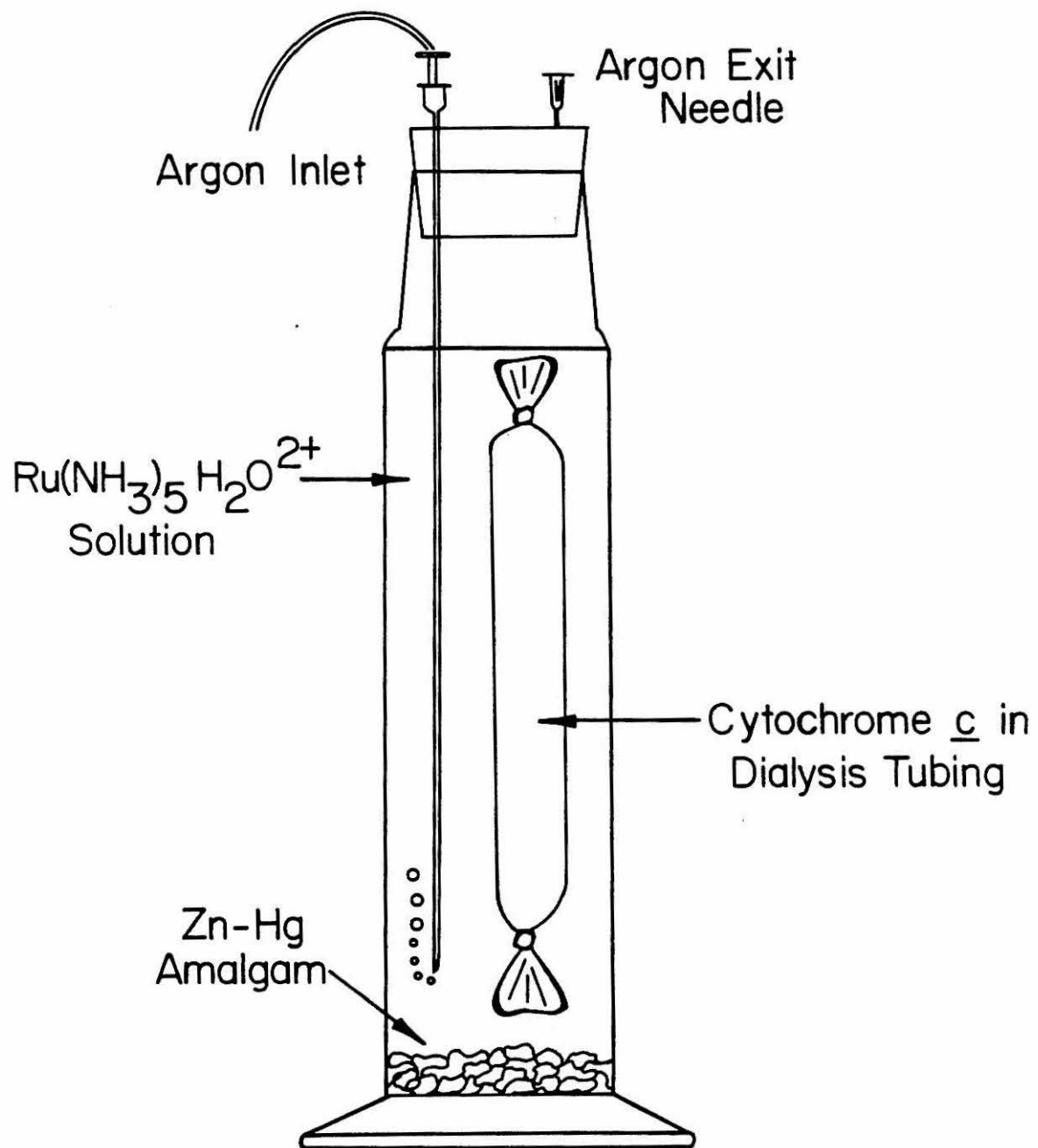
A solution of 100 mg pure native ferricytochrome *c* was diluted to 40 mL with buffer. The solution was placed in dialysis tubing and suspended in deoxygenated buffer. Bubbling of the buffer with argon was continued for \geq 1 hour in order to deoxygenate the protein solution. The dialysis tubing containing the ferricytochrome *c* solution was then

transferred to the reaction vessel containing the $\text{Ru}(\text{NH}_3)_5\text{H}_2\text{O}^{2+}$ solution. The cytochrome *c* solution was kept in the dialysis tubing in order to prevent the protein from coming in contact with the Zn amalgam. This procedure was first employed by Matthews²⁴ for the reaction of $\text{Ru}(\text{NH}_3)_5\text{H}_2\text{O}^{2+}$ with ribonuclease A. As the molecular weight cutoff of the dialysis membrane is 6000-8000, the ruthenium ions diffused readily through the tubing. In less than one hour the ferricytochrome *c* was reduced to ferrocytochrome *c*, as evidenced by the color change in the cytochrome *c* solution (red to pink).

The reaction was allowed to proceed for 69-72 hours at room temperature. Argon was bubbled continuously through the ruthenium solution surrounding the dialysis tubing. Contact of the ruthenium solution with stainless steel needles was avoided. Platinum needles or Teflon tubing-covered needles were used for deoxygenating ruthenium solutions. The reaction setup is illustrated in Figure 5.2.

The reaction was terminated by removing the cytochrome *c* from the dialysis tubing and applying the solution to a Sephadex G-25 column (*ca.* 4 x 25 cm) to remove the excess ruthenium reagent. The protein was eluted with 85 mM phosphate buffer, pH 7. A distinct separation of the pink cytochrome *c* band from the yellow $\text{Ru}(\text{NH}_3)_5\text{H}_2\text{O}^{2+/3+}$ band was observed. The cytochrome *c* band was collected (*ca.* 80 mL) and the solution placed in dialysis tubing. The tubing was suspended in *ca.* 4 L of 85 mM phosphate buffer, pH 7. Air

Figure 5.2. Experimental setup for the reaction of $\text{Ru}(\text{NH}_3)_5\text{O}^{2+}$ with cytochrome *c* by the $\text{Ru}(\text{NH}_3)_5\text{Cl}_3/\text{Zn}$ amalgam method.



was subsequently bubbled through the buffer to effect the oxidation of the bound $\text{Ru}(\text{NH}_3)_5^{2+}$ to the more stable $\text{Ru}(\text{NH}_3)_5^{3+}$ form. The dialysis also served to remove any excess ruthenium reagent not removed by the G-25 column. Dialysis/air oxidation was continued for 48 hours with one change of buffer.

Spectra taken subsequent to air oxidation revealed that this technique was not totally effective in oxidizing the heme iron of cytochrome *c* (% oxidation varied from 60-90%). Whether or not the ruthenium present became totally oxidized could not be determined spectrally as its spectrum is unobservable in the presence of the highly absorbing cytochrome *c*. Thus to complete the oxidation of the cytochrome *c* species (necessary in order to minimize the number of ionic forms present prior to chromatography), one equivalent (based on [cyt *c*]) of $[\text{Co}(\text{phen})_3](\text{ClO}_4)_3$ was added to the cytochrome *c* solution. The solution was then prepared for purification by cation exchange chromatography.

$[\text{Ru}(\text{NH}_3)_5\text{H}_2\text{O}](\text{PF}_6)_2$ method. In this method a solution of $[\text{Ru}(\text{NH}_3)_5\text{H}_2\text{O}](\text{PF}_6)_2$ was added directly to a solution of cytochrome *c*. $[\text{Ru}(\text{NH}_3)_5\text{H}_2\text{O}](\text{PF}_6)_2$ was prepared fresh from 0.3 g $[\text{Ru}(\text{NH}_3)_5\text{Cl}]\text{Cl}_2$. The solid was placed in a capped serum bottle and the bottle was purged with argon. 15 mL deoxygenated buffer was added to the ruthenium solution via syringe. The resultant solution, being slightly cloudy, was transferred via syringe and Millipore filter to a clean,

argon-purged bottle. The concentration of $\text{Ru}(\text{NH}_3)_5\text{H}_2\text{O}^{2+}$ was determined spectrally (in a deoxygenated cell) using $\epsilon(415 \text{ nm}) = 44 \text{ M}^{-1} \text{ cm}^{-1}$ and $\epsilon(268 \text{ nm}) = 530 \text{ M}^{-1} \text{ cm}^{-1}$.²²

A solution containing 100 mg (8.06 μmol) pure cytochrome *c* in 20-25 mL of 85 mM phosphate buffer, pH 7.0, was placed in a stoppered serum bottle and deoxygenated by careful bubbling with argon. After 15 min argon was passed over the solution, rather than through it, to minimize denaturation by frothing. An aliquot of the ruthenium solution containing a 51-fold excess (411 μmol) of $\text{Ru}(\text{NH}_3)_5\text{H}_2\text{O}^{2+}$ was added via syringe to the solution of ferricytochrome *c*. One equivalent of Ru(II) was consumed immediately in the reduction of the cytochrome *c*. Deoxygenated buffer was also added to the reaction mixture to bring the total volume to 40 mL, and thus, the final cytochrome and $\text{Ru}(\text{NH}_3)_5\text{H}_2\text{O}^{2+}$ concentrations to 0.20 mM and 10 mM, respectively.

The reaction was allowed to proceed for 24 hours at room temperature under argon. The reaction was terminated by applying the solution to a Sephadex G-25 column as described above. The subsequent oxidation procedures were also carried out as described for the $\text{Ru}(\text{NH}_3)_5\text{Cl}_3/\text{Zn}$ amalgam method.

Notes on the preparative methods. The samples on which the majority of the subsequent characterization and reactivity studies were done were prepared as described above. However, a number of variations in these methods was investigated in the course of this work. Several had no noticeable effect

on the product distribution, including shortening, or eliminating, the period of air oxidation, provided the sample was subsequently oxidized by $\text{Co}(\text{phen})_3^{3+}$. Generating ferrocytochrome *c* (with $\text{Fe}(\text{EDTA})^{2-}$, followed by G-25 chromatography) prior to mixing with $\text{Ru}(\text{NH}_3)_5\text{H}_2\text{O}^{2+}$, in lieu of allowing the cytochrome *c* to be directly reduced by $\text{Ru}(\text{NH}_3)_5\text{H}_2\text{O}^{2+}$, also had no observable effect on the course of the reaction. Factors which did affect the final products, and in a predictable fashion, included variations in reaction times and in relative reactant concentrations.

On several occasions decomposition in the ruthenium/cytochrome *c* reaction solution became a problem at long reaction times. Decomposition was observed more often in the $\text{Ru}(\text{NH}_3)_5\text{Cl}_3/\text{Zn}$ amalgam reactions than in the $[\text{Ru}(\text{NH}_3)_5\text{H}_2\text{O}]^-(\text{PF}_6)_2$ reactions; however, the latter were not totally immune from the problem. A suspension of a fine black solid in the solution was taken as the criterion that decomposition had occurred. Extreme cases resulted in the plating out of a silvery mirror of ruthenium on the sides of the reaction vessel. In that platinum or Teflon needles were employed in the manipulation of ruthenium solutions, contact with stainless steel needles was clearly not the culprit. The cause of (or the cure for) the decomposition was not found. Providing the contamination was minor, the solution was simply Millipore-filtered upon termination of the reaction. Product distribution was not noticeably affected.

Throughout the course of the preparation, purification, and characterization of the $\text{Ru}(\text{NH}_3)_5$ -cytochrome *c* derivatives it was often necessary to determine the concentration of cytochrome *c*, and/or the relative amounts of oxidized and reduced cytochrome *c*, present in solution. Total cytochrome concentration was determined by adding excess dithionite to a small aliquot of the cytochrome *c* solution and measuring $A_{550 \text{ nm}}$ where $\epsilon = 29.5 \times 10^3 \text{ M}^{-1} \text{ cm}^{-1}^{25}$. $A_{500 \text{ nm}}$ of the totally oxidized protein was determined by adding excess $\text{K}_3\text{Fe}(\text{CN})_6$ to a second aliquot. Knowing A_{550}^{red} , A_{550}^{ox} , and using $\Delta\epsilon = 21.1 \times 10^3 \text{ M}^{-1} \text{ cm}^{-1}^{25}$, the concentration of reduced and oxidized cytochrome species in a given sample could be calculated.

Purification of the $\text{Ru}(\text{NH}_3)_5$ -Cytochrome *c* Reaction Products.

Following oxidation of the reaction solution the components of the mixture were separated by cation exchange chromatography. Whatman CM-cellulose (CM52) was thoroughly equilibrated in 85 mM phosphate buffer, pH 7.0. A column with bed dimensions $2 \times 50\text{--}60 \text{ cm}$ was poured. Equilibration of the column material was considered complete when the pH and conductivity of the effluent buffer was the same as that of the influent buffer. The column was repacked with clean, equilibrated cellulose prior to each purification. All ion exchange chromatography was performed at 4°C .

The $\text{Ru}(\text{NH}_3)_5^{3+}$ -cytochrome *c* reaction solution was prepared for chromatography by first concentrating the solution

to \leq 10 mL in a stirred ultrafiltration cell. The solution was then diluted to *ca.* 50 mL with water and reconcentrated to *ca.* 10 mL. This procedure was effective in reducing the ionic strength of the protein solution to a value below that of the 85 mM equilibration buffer, and thus resulted in a tight band at the top of the ion exchange column upon loading. (This procedure also served to remove added oxidant, and the reduction product thereof, *i.e.*, $\text{Co}(\text{phen})_3^{3+/2+}$.)

The concentrated $\text{Ru}(\text{NH}_3)_5^{3+}$ -ferricytochrome *c* solution was carefully applied to the top of the column bed. After draining the solution to bind the protein to the resin, 85 mM buffer was applied and elution was begun. The protein species were eluted in order of increasing charge by a linear gradient between 1.0 liter each of 85 mM and 150 mM sodium phosphate buffer, pH 7.0. Flow rate was maintained at *ca.* 30 mL/h with a Minipuls 2 peristaltic pump (Gilson). 5-mL fractions were collected with a Gilson MFG Mini-Escargot Fractionator. The absorbance of every other fraction was read at 410 nm with a Cary 219 spectrophotometer.

Although the gradient employed was the most satisfactory of the several which were tested, some tailing of adjacent peaks into one another was still observed. Consequently, each peak was rechromatographed using single ionic strength elution on CM-cellulose. The fractions corresponding to each peak in the initial chromatogram were pooled. One

equivalent of $\text{Co}(\text{phen})_3^{3+}$ (based on [cyt *c*]) was added to each solution to insure oxidation. The solution was concentrated by ultrafiltration, applied to a G-25 column (3 x 20-25 cm), and eluted with 85 mM buffer to remove excess oxidant. The solution was then concentrated, diluted with water, and reconcentrated, as was necessary to reduce the volume and ionic strength for reapplication to a second ion exchange column. The conditions outlined below for rechromatography of peaks A through E are those which were employed when the analogous peaks from four separate preparative procedures ($\text{Ru}(\text{NH}_3)_5\text{Cl}_3/\text{Zn}$ amalgam method) were pooled. The resultant rechromatographed peaks, A' through E', were used in the majority of characterization and reactivity studies reported here (see Results), unless otherwise noted. The procedures used for rechromatography of leaner samples were the same, only the size of the column was scaled down accordingly.

Peak A (*ca.* 32 mg cyt *c*) was rechromatographed on a column (2.3 x 32 cm) of CM52 with 85 mM sodium phosphate buffer, pH 7.0. Peak B (*ca.* 42 mg) was rechromatographed on CM52 with 85 mM buffer; column bed 2.3 x 26 cm. Peak C (*ca.* 48 mg) was also eluted from a CM52 column (2.3 x 19 cm) with 85 mM buffer. Peaks D (*ca.* 24 mg) and E (*ca.* 43 mg) were rechromatographed on CM52 with 100 mM sodium phosphate buffer, pH 7.0. Column beds were 2.3 x 19 cm (peak D) and 2.3 x 17 cm (peak E). In all cases a flow rate of 30 mL/h

was maintained and 5-mL fractions were collected. The absorbance of every other fraction was again read at 410 nm.

The fractions corresponding to each of the major species which eluted upon rechromatography were pooled. These species were designated peaks A' through E'. Each peak was then equilibrated into the buffer of choice (or water) for subsequent experiments by several cycles of concentration by ultrafiltration followed by dilution with the appropriate buffer. Concentrated solutions of the derivatives were kept at 4°C if they were to be used within several days of purification. Otherwise the samples were shell-frozen in liquid nitrogen and stored at -10°C.

Analyses of Ruthenium Content. Owing to the many intense absorption bands in the spectrum of cytochrome *c*, no absorption due to the attached $\text{Ru}(\text{NH}_3)_5$ group could be detected in the spectra of the ruthenium-modified cytochrome *c* species. Analysis for ruthenium in cytochrome *c* samples by other methods is often complicated by the fact that the presence of iron can interfere with the detection of the ruthenium. This is certainly the case for most colorometric procedures for the determination of ruthenium. Although several procedures in the literature claim to overcome iron interferences, reproducible results were not obtained when these procedures were applied to control solutions of cytochrome *c* spiked with known amounts of pure $[\text{Ru}(\text{NH}_3)_5\text{Cl}]\text{Cl}_2$.

The colorometric procedures tested were based on the reaction of ruthenium with o-phenanthroline,²⁶⁻²⁸ and with 2,4,6-tris(2'-pyridyl)-s-triazine.²⁹

Determination of ruthenium by flame atomic absorption (AA) also suffers from interference due to iron. The interference can be suppressed by the addition of cadmium and/or copper salts to the sample solutions.^{30,31} Two different procedures were employed in the determination of ruthenium by AA. Neither was found to be entirely satisfactory. Both required high salt concentrations, which resulted in the deposition of debris on the burner (and larger absorbance errors) when more than a few samples were analyzed at one sitting. In the first procedure the sample solutions, as well as the standard solutions, were made 1% in Na_2SO_4 , 1% in CuSO_4 , and 0.1 M in HCl.³² In the second procedure all solutions were made 0.5% in Cu (as $\text{CuSO}_4 \cdot 5\text{H}_2\text{O}$), 0.5% in Cd (as $3\text{CdSO}_4 \cdot 8\text{H}_2\text{O}$), and 0.1 M in HCl.³⁰

Atomic absorption measurements were carried out on an Instrumentation Laboratories, Inc. Model 151 flame atomic absorption spectrophotometer. The measurements were made either by the staff of the Caltech Analytical Laboratory or by the author. A minimum of four standard solutions in the range 0-15 ppm was used to determine the standard curve. A minimum of ten absorbance readings was taken on each solution and the values averaged. A linear regression program

was used to fit the standard solution data and, subsequently, to determine the ruthenium content of the sample solutions.

The accuracy and precision of the atomic absorption procedures described were monitored by routinely including a sample of $\text{Ru}(\text{NH}_3)_5\text{Cl}_3$ -spiked cytochrome *c* in the samples to be analyzed. On the basis of these controls the estimated error in the values reported is $\pm 15\%$. Such a large error was clearly disturbing, as was the fact that each analysis consumed approximately 5 mg of precious sample. Unfortunately, a more acceptable method of ruthenium analysis was not found.

Prior to analysis by atomic absorption it was necessary to remove the buffer salts from the cytochrome *c* samples. This was done to curtail the precipitation of cadmium and copper phosphates in the analysis solution. The solution was therefore equilibrated into water prior to analysis. Sample solutions for atomic absorption were typically 1×10^{-5} M to 1×10^{-4} M in cytochrome *c*.

The concentration of cytochrome *c* in the atomic absorption samples was determined spectrally (with dithionite) using $\epsilon_{550} = 29.5 \times 10^3 \text{ M}^{-1} \text{ cm}^{-1}$.²⁵ Knowing the ruthenium content as determined by AA, the ratio of ruthenium to cytochrome *c* in a given sample was then calculated.

Tryptic Hydrolyses. In order to identify the sites of $\text{Ru}(\text{NH}_3)_5$ attachment to cytochrome *c*, the protein was digested by trypsin and the resulting peptides were separated by high-pressure liquid chromatography. A 4-mg sample of the

cytochrome *c* species in 2 mL of water was adjusted to pH 8.5 with 0.1 M NaOH. NH_4HCO_3 was added to give a concentration of 0.025 M. At 0 and 6 h, 50 μL of trypsin (2 mg per mL in 0.001 M HCl) were added. The solution was stirred at 37°C for a total of 24 h. The pH of the solution was then lowered to 2.1. After filtration through a 0.5 μm cellulosic membrane filter the solution was lyophilized to dryness. The lyophilized material was dissolved in the chromatography buffer, pH 2.85 phosphate (49 mM KH_2PO_4 , 5.4 mM H_3PO_4), and refiltered.

High-Pressure Liquid Chromatography (HPLC). Chromatographic separations of the tryptic peptides were done on a reversed-phase HPLC column, Ultrasphere ODS, which had been equilibrated with *ca.* 30 mL of starting buffer. The solvent delivery system consisted of two Altex Model 110A pumps, a Rheodyne Model 7125 injector, and an Altex Model 420 Microprocessor Controller. An Altex/Hitachi Model 155-10 UV-Vis Variable Wavelength Detector was used in conjunction with a Linear Instruments single channel recorder.

A 2-mg sample of the digested, filtered cytochrome *c*, dissolved in 0.1 mL of pH 2.85 phosphate buffer, was injected onto the HPLC column. The peptides were eluted with a linear gradient 0-45% in acetonitrile, at a flow rate of 1 mL/min. Absorbance at 220 nm was recorded at 1.0 AUFS (absorbance units full scale); absorbance at 300 nm was recorded at 0.1 AUFS. Chart speed was 40 cm/h. Fraction

size was 0.5 mL. Fractions corresponding to those peaks which were later subjected to amino acid analysis, or examined spectrally, were pooled and blown dry in a 40°C water bath using filtered air.

Amino Acid Analyses. Dried samples were hydrolyzed with *ca.* 2 mL of 6 M HCl. To prevent hydrolytic loss of tyrosine, 2 drops of 0.5% phenol were also added to each sample. Sample tubes were drawn out at the torch, evacuated, and flame-sealed. The tubes were then heated to 110°C for 24 hours.

Hydrolyzed samples were opened and blown dry in a water bath heated to 40°C using filtered air. The sample was dissolved in 0.5 mL of pH 2.2 sodium citrate buffer (0.2 M). The sample solution was then loaded into a manual sample injector and injected onto a column (0.6 x 45 cm) of Beckman spherical resin. Development proceeded with successive sodium citrate buffers of pH 3.1, 4.1, and 7.0. The Na^+ concentration of the first two was 0.2 M; the third was 1.0 M. Buffer was pumped through the column at a flow rate of 40 mL/h and ninhydrin was pumped at 20 mL/h. Detection was at 570 and 440 nm.

The instrument used for these analyses was a Beckman Model 120 amino acid analyzer, modified with a microbore reaction coil and elongated pathlength flow cells. The sensitivity of the instrument was such that yields of amino acids down to 5 nmols could be routinely calculated.

Optical Spectra. The visible and ultraviolet spectrum of each $\text{Ru}(\text{NH}_3)_5$ -cytochrome *c* derivative (peaks A' through E') was taken in a 1-mm cell. The visible spectrum of a dithionite-reduced aliquot of each peak was also recorded. The spectra were taken in phosphate buffer, pH 7, at cytochrome *c* concentrations in the 40-90 μM range. A spectrum of an oxidized sample of each peak was taken in a 1-cm cell in the 800-600 nm region in order to detect whether or not the conformation-sensitive 695-nm band was present. Spectra were taken on a Cary 219 UV-Vis spectrophotometer (Varian) at room temperature.

Spectra of HPLC fractions were recorded on a Hewlett-Packard 8450 UV-Vis spectrophotometer with a 7225A Graphics Plotter. The dried sample corresponding to a given HPLC peak was rediluted with 1 mL water and the spectrum recorded in a small volume, 1-cm cell. The pH of the solutions was approximately 3.

Spectroelectrochemistry. It was first demonstrated by Heineman³³ that the reduction potential (E°) of cytochrome *c* could be rapidly, and accurately, determined by spectroelectrochemistry. Briefly, the technique used here employs an optically transparent thin-layer electrolysis (OTTLE) cell in a nonisothermal configuration. The cell is mounted in a spectrophotometer and a series of potentials are applied sequentially across the cell. The solution is allowed to come to equilibrium at each potential, after which the

absorption spectrum is recorded. A small molecule mediator-titrant facilitates electron transfer between the working electrode and the protein. The ratio of oxidized to reduced protein ($[O]/[R]$) at each potential is determined from the overlay spectra. A Nernst plot of $E(\text{applied})$ *vs.* $\log([O]/[R])$ is used to determine the formal reduction potential. The electron transfer reaction entropy, ΔS_{rc}° , is determined from a plot of E° *vs.* temperature. The experimental details of this technique as it has been applied to metalloproteins in this laboratory, and as it was applied here, are described elsewhere.^{34,35}

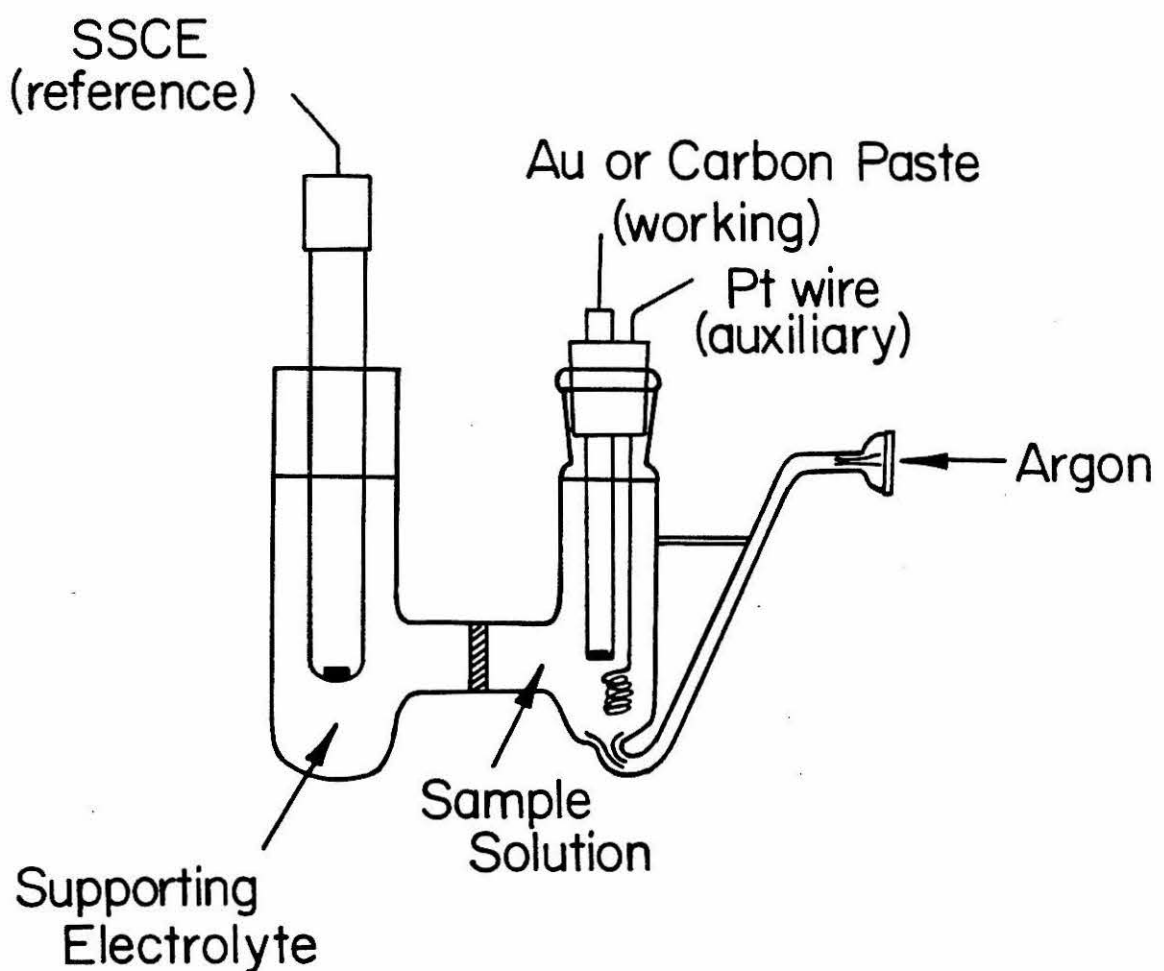
Nonisothermal thin-layer spectroelectrochemistry was utilized here to determine the heme *c* potential of the $\text{Ru}(\text{NH}_3)_5$ -modified cytochrome *c* species corresponding to peak E' . An OTTLE cell containing a gold minigrid electrode was employed. The mediator-titrant was $[\text{Ru}(\text{NH}_3)_5\text{py}](\text{ClO}_4)_3$ (0.8 mM). The cytochrome *c* concentration was 0.16 mM, in pH 7.0 sodium phosphate buffer, $\mu = 0.1$ M. E° 's were determined from Nernst plots at eight different temperatures (9.4 - 40°C). A minimum of seven data points was included in each plot. A linear least squares program was used to calculate E° 's from plots of $E(\text{applied})$ *vs.* $\log([\text{cyt c}^{\text{III}}]/[\text{cyt c}^{\text{II}}])$, and to calculate ΔS_{rc}° from a plot of E° *vs.* temperature.

Cyclic Voltammetry. The procedure used for obtaining cyclic voltammograms of cytochrome *c* was patterned after that described by Hill.³⁶ A PAR 174A potentiostat was used in conjunction with a Hewlett-Packard 7004B X-Y recorder. A Keithley 177 Microvolt DMM voltmeter was used to confirm the starting potential prior to a scan. The all-glass cell consisted of two compartments separated by a sintered glass disk. It was also equipped with a side-arm for degassing the sample. The working electrode was a gold disk, 3 mm in diameter, embedded in the end of a plastic rod so that only one surface was exposed to the solution. Before insertion into each solution the gold surface was polished using a suspension of fine alumina in water, followed by thorough rinsing with water. The auxiliary electrode was a coil of platinum wire. The reference electrode was a saturated NaCl calomel electrode (SSCE). The experimental setup is illustrated in Figure 5.3.

All measurements were made at room temperature. The reported reduction potentials were calculated from the cathodic (E_{pc}) and anodic (E_{pa}) peak potentials using $E_{\frac{1}{2}} = (E_{pc} + E_{pa})/2$. Potentials were measured with respect to SSCE and converted to NHE by adding 0.236 V.³⁷

Cyclics of cytochrome *c*, and derivatives thereof, utilized 1.5 - 2.0 mL of 0.1 - 0.2 mM cytochrome *c*. These solutions were also made 0.01 M in 4,4'-bipyridyl. The supporting electrolyte was 0.1 M NaClO₄ in sodium phosphate

Figure 5.3. Experimental setup for cyclic voltammetry.



buffer, pH 7, $\mu = 0.05$ M. The background was checked periodically with supporting electrolyte (plus 0.01 M 4,4'-bipy) in both compartments. All solutions were deoxygenated by bubbling with argon for several minutes prior to use.

Cyclic voltammograms of $[\text{Ru}(\text{NH}_3)_5\text{Im}]\text{Cl}_3$ and $[\text{Ru}(\text{NH}_3)_5\text{-His}]\text{Cl}_3$ were also obtained with the gold electrode in the presence of 4,4'-bipyridyl using the procedure outlined for cytochrome *c*. Additionally, cyclics of these two model complexes were obtained at a carbon paste electrode (3 mm diameter) in the absence of 4,4'-bipyridyl. The solutions employed in both cases were 0.2 mM in ruthenium. The supporting electrolyte was again 0.1 M NaClO_4 in pH 7.0 sodium phosphate buffer, $\mu = 0.05$ M.

Stopped-Flow Kinetics. The rate of intermolecular reduction of cytochrome *c* by $\text{Ru}(\text{NH}_3)_5\text{Im}^{2+}$, as well as by $\text{Ru}(\text{NH}_3)_5\text{His}^{2+}$, was measured on the Durrum Model D-110 stopped-flow spectrophotometer. The Durrum was also used to monitor the reduction of a $\text{Ru}(\text{NH}_3)_5^{3+}$ -cytochrome *c* derivative (peak E') by $\text{Ru}(\text{NH}_3)_6^{2+}$. The procedures used in making the kinetics measurements, including the method of data collection and analysis, were the same as those described in Chapter 2 and, hence, will not be repeated here. Preparation of the kinetics solutions is described.

Solutions of native ferricytochrome *c* were prepared for kinetics by diluting a concentrated solution of pure horse heart cytochrome *c* (purified on a CM52 column) to 4-6 μM

with a pH 7.0 sodium phosphate buffer, $\mu = 0.1$ M. A solution of $\text{ca. } 4 \mu\text{M}$ $\text{Ru}(\text{NH}_3)_5\text{Im}$ -modified cytochrome *c* (E') was also prepared by diluting a concentrated solution with pH 7.0 phosphate buffer, $\mu = 0.1$ M. The protein solutions were rendered oxygen-free before use by direct bubbling with argon (15 min), followed by maintainence of a flow of argon over the solution.

A stock solution of $\text{Ru}(\text{NH}_3)_5\text{Im}^{2+}$ was made by reducing a solution of 0.8 mM $[\text{Ru}(\text{NH}_3)_5\text{Im}]Cl_3 \cdot 2\text{H}_2\text{O}$ in pH 7.0 phosphate buffer ($\mu = 0.1$ M) over zinc amalgam. The Zn amalgam was added to a deoxygenated solution of the Ru(III) salt and the reduction was allowed to proceed for two hours. Complete reduction was confirmed spectrally. Appropriate aliquots of buffer were pipetted into serum bottles containing several pieces of Zn amalgam each. The buffer was deaerated by continuous bubbling with argon. Just prior to use the appropriate volume of Ru(II) stock solution was transferred via gas-tight syringe, and through a Millipore filter, to the degassed buffer to obtain the desired ruthenium concentrations. The concentration of each ruthenium(II) solution was determined spectrally, in a degassed cell, following completion of that set of kinetics runs. For each $\text{Ru}(\text{NH}_3)_5\text{Im}^{2+}$ solution an average concentration was calculated using $\epsilon (280 \text{ nm}) = 2700 \text{ M}^{-1} \text{ cm}^{-1}$ and $\epsilon (255 \text{ nm}) = 2800 \text{ M}^{-1} \text{ cm}^{-1}$.¹ Solutions of $\text{Ru}(\text{NH}_3)_5\text{His}^{2+}$ were prepared in a strictly

analogous manner. Concentrations were calculated using ϵ (280 nm) = 3160 M⁻¹ cm⁻¹ and ϵ (260 nm) = 3260 M⁻¹ cm⁻¹.⁵ Solutions of $\text{Ru}(\text{NH}_3)_5^{2+}$ were prepared from $[\text{Ru}(\text{NH}_3)_6]\text{Cl}_2$ as described in Chapter 2.

RESULTSSynthesis of Pentaammineruthenium(II) Complexes of Ferricytochrome c

The procedures used in the preparation and purification of $\text{Ru}(\text{NH}_3)_5^{3+}$ -cytochrome *c* derivatives are summarized in Figure 5.4. The reaction of aquopentaammineruthenium with cytochrome *c* was performed using the substitution labile ruthenium(II) complex in a 50-fold molar excess over the cytochrome *c*. The $\text{Ru}(\text{NH}_3)_5\text{H}_2\text{O}^{2+}$ ($E^\circ = 0.10 \text{ V}^2$) quickly reduces the cytochrome *c* ($E^\circ = 0.26 \text{ V}^{10}$) so that the reaction is essentially between $\text{Ru}(\text{NH}_3)_5\text{H}_2\text{O}^{2+}$ and ferrocyanocytocrome *c*. The $\text{Ru}(\text{NH}_3)_5\text{H}_2\text{O}^{2+}$ could be generated either by the reduction of $[\text{Ru}(\text{NH}_3)_5\text{Cl}]\text{Cl}_2$ over zinc amalgam, or more directly by dissolving the ruthenium(II) salt, $[\text{Ru}(\text{NH}_3)_5\text{H}_2\text{O}](\text{PF}_6)_2$. It is important that commercial cytochrome *c* be purified prior to use in order to remove deamidated forms of the protein. Otherwise the reaction with $\text{Ru}(\text{NH}_3)_5\text{H}_2\text{O}^{2+}$ would produce ruthenium-modified native cytochrome *c*, as well as ruthenium-modified, deamidated cytochromes *c*, making subsequent product purification even more difficult.

It was not possible to estimate a rate of reaction of $\text{Ru}(\text{NH}_3)_5\text{H}_2\text{O}^{2+}$ with cytochrome *c* for comparison to the substitution rates of $\text{Ru}(\text{NH}_3)_5\text{H}_2\text{O}^{2+}$ with imidazole or thioether. Due to the number and intensity of absorption

Figure 5.4. Procedure for the synthesis and purification of pentaammineruthenium(III) complexes of ferricytochrome *c*.

Cytochrome *c* (Type VI, Sigma)

↓
CM52 ion exchange
85 mM phosphate, pH 7.0

Cytochrome *c* (Fe^{III}), pure

50 x excess
 $\text{Ru}(\text{NH}_3)_5\text{H}_2\text{O}^{2+}$

$[\text{Ru}(\text{NH}_3)_5\text{Cl}]_{\text{Cl}_2}$
+ Zn/Hg amalgam
or
 $[\text{Ru}(\text{NH}_3)_5\text{H}_2\text{O}](\text{PF}_6)_2$

85 mM phosphate, pH 7.0
r.t.; under argon
rxn. time 1-3 days

Cytochrome *c* (Fe^{II}) - $\text{Ru}(\text{NH}_3)_5^{2+}$ Reaction Mixture

↓
G-25 gel filtration
- excess $\text{Ru}(\text{NH}_3)_5\text{H}_2\text{O}^{2+}$

Cytochrome *c* (Fe^{II}/Fe^{III}) - $\text{Ru}(\text{NH}_3)_5^{2+/3+}$ Products

↓
 O_2 and/or $\text{Co}(\text{phen})_3^{3+}$

Cytochrome *c* (Fe^{III}) - $\text{Ru}(\text{NH}_3)_5^{3+}$ Products

↓
CM52 ion exchange
85→150 mM phosphate, pH 7.0

Cytochrome *c* (Fe^{III})- $\text{Ru}(\text{NH}_3)_5^{3+}$ Products

Peaks A-E

↓
CM52 ion exchange
single ionic strength elutions

Cytochrome *c* (Fe^{III})- $\text{Ru}(\text{NH}_3)_5^{3+}$ Products

Peaks A'-E'

↓
Characterization

bands in the cytochrome *c* spectrum, the progress of the reaction could not be monitored spectrally; no absorption due to the $\text{Ru}(\text{NH}_3)_5\text{L}^{2+/3+}$ complexes formed was detectable. Furthermore, the products obtained represent a mixture of unmodified protein and several different modified species, not a single $\text{Ru}(\text{NH}_3)_5$ -protein complex. Thus a detailed study of the time dependence of ruthenium incorporation into cytochrome *c* was not attempted. Despite the inability to extract a $\text{Ru}(\text{NH}_3)_5$ /cytochrome *c* substitution rate constant, the results do indicate that the reaction is indeed slower than would be anticipated from model complex studies. At the concentrations of ruthenium and cytochrome *c* used here, the comparable reaction between $\text{Ru}(\text{NH}_3)_5\text{H}_2\text{O}^{2+}$ and imidazole would be complete in approximately 15 minutes. In the reaction of $\text{Ru}(\text{NH}_3)_5\text{H}_2\text{O}^{2+}$ with cytochrome *c*, a 24-hour reaction time produces a mixture of products in which the average concentration of bound ruthenium corresponds to less than one ruthenium per cytochrome *c* molecule (determined by atomic absorption). Shorter reaction times, or lower ruthenium concentrations, resulted in yet lower yields of modified cytochrome *c*.

The reaction between $\text{Ru}(\text{NH}_3)_5\text{H}_2\text{O}^{2+}$ and cytochrome *c* was terminated by removing the excess ruthenium reagent on a gel filtration column. The products were subsequently oxidized in order to generate the $\text{Ru}(\text{NH}_3)_5^{3+}$ -cytochrome *c* species, a more stable form with respect to dissociation. Oxygen and/or $\text{Co}(\text{phen})_3^{3+}$ were used as oxidants.

$\text{Co}(\text{phen})_3^{3+}$ ($E^\circ = 0.377$ V³⁴) rapidly oxidized the heme *c* site, whereas oxygen alone did so only very slowly. Complete oxidation of the heme iron is important in order to assure that the species separated by ion exchange chromatography are distinct, *i.e.*, to assure that only one heme redox isomer (the Fe(III) form) of each derivative is present. The oxidation state of the bound pentaammine-ruthenium could not be monitored spectrally. Based on model complex studies it was assumed that the ruthenium site was readily oxidized by O_2 and/or $\text{Co}(\text{phen})_3^{3+}$, provided it was bound to a histidine ($E^\circ = 0.105$ V for $\text{Ru}(\text{NH}_3)_5\text{His}^{3+/2+}$). If bound to methionine, oxidation could not be assumed ($E^\circ = 0.530$ V for $\text{Ru}(\text{NH}_3)_5\text{Met}^{3+/2+}$).

Separation and Purification of $\text{Ru}(\text{NH}_3)_5$ -Cytochromes *c*.

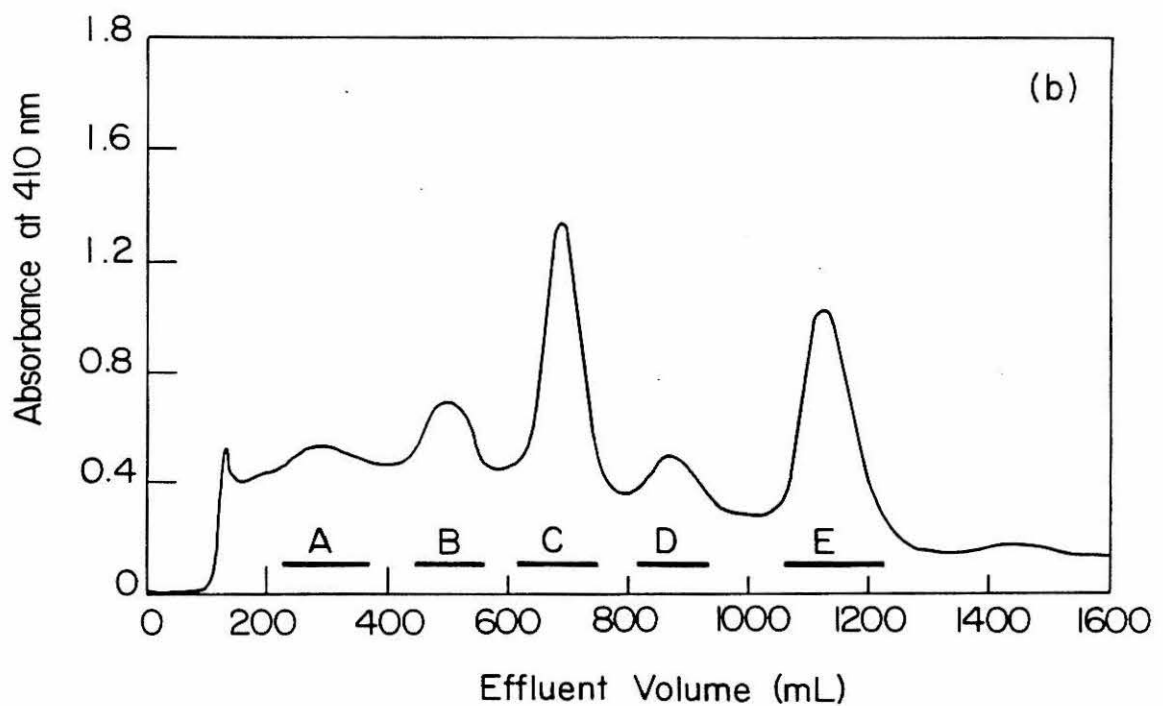
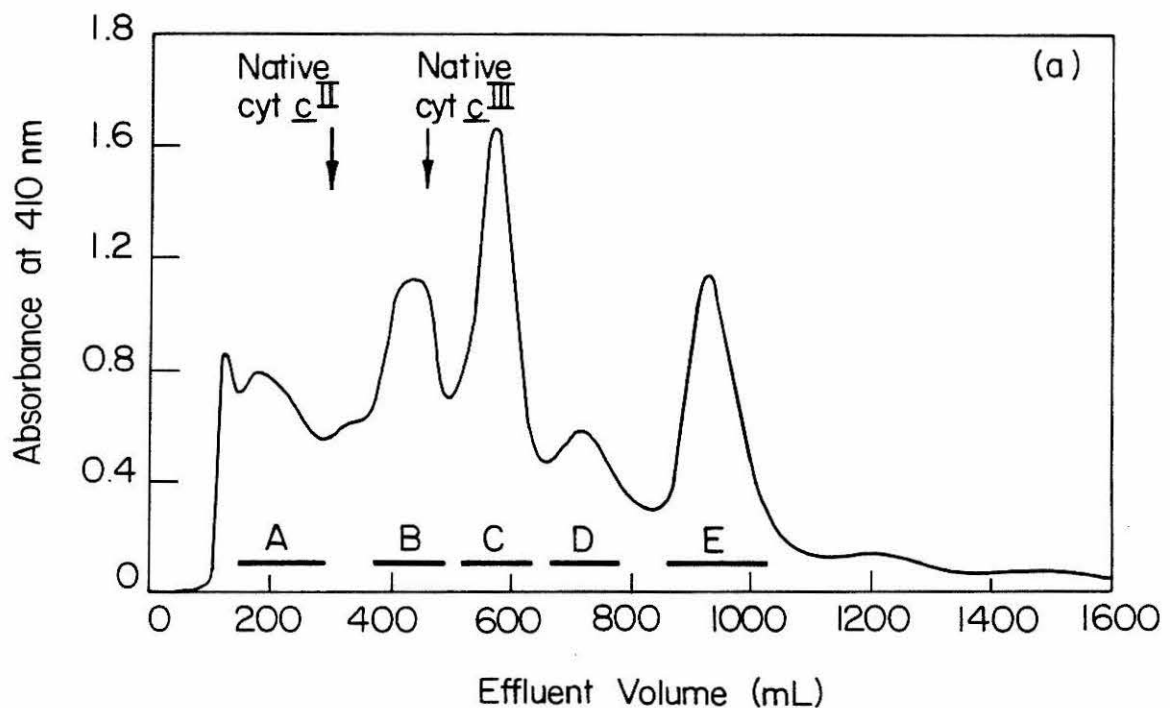
Cation exchange chromatography is an effective method of separating cytochrome *c* modification products when the modification employed changes the charge on the protein. Met-65, His-26, and His-33 are all essentially neutral at pH 7.0 (His-26, pK_a 3.5, is totally deprotonated; His-33, pK_a 6.54, is 74% deprotonated).¹⁰ The attachment of a $\text{Ru}(\text{NH}_3)_5^{3+}$ group to any one of these sites would therefore result in a net +3 charge increase over the native protein. (Native ferricytochrome *c* is +7.5 at pH 7.³⁸) Using a linear gradient of increasing ionic strength, the products should elute in order of increasing positive charge -

unmodified cytochrome *c* first, followed by mono- $\text{Ru}(\text{NH}_3)_5^{3+}$ -cytochromes *c*, di- $\text{Ru}(\text{NH}_3)_5^{3+}$ -cytochromes *c*, etc.

Five major peaks, designated A through E, were obtained when the components of the oxidized product solution were separated on CM-cellulose with a linear phosphate gradient between 85 and 150 mM. Typical, reproducible chromatograms are shown in Figure 5.5. The number and distribution of products was essentially the same regardless of which method was used to generate the $\text{Ru}(\text{NH}_3)_5\text{H}_2\text{O}^{2+}$ reagent.

A preliminary identification of peaks was attempted on the basis of elution volumes. Using the identical chromatographic conditions, a mixture of pure native ferro- and ferricytochrome *c* was eluted from CM-cellulose. The peak maxima for these species were at 300 and 460 mL, respectively, as indicated in Figure 5.5(a). This would suggest that peak B is unmodified ferricytochrome *c*, and the small peak between A and B represents contamination by unmodified ferrocytochrome *c*. (It was often difficult to keep the cytochrome *c* 100% oxidized prior to chromatography once the excess oxidant had been removed.) The spectra of peak fractions between zero and 375 mL confirmed the presence of some reduced protein in the initial peaks. The spectra of peak fractions at elution volumes greater than 375 mL indicated that the cytochrome *c* in this region was always greater than 95% oxidized. Based on the difference in elution volumes between ferro- and ferricytochrome *c*, *i.e.*,

Figure 5.5. CM-cellulose chromatography of $\text{Ru}(\text{NH}_3)_5^-$ -cytochrome *c* reaction products. Elution was with a linear phosphate gradient, pH 7.0. Fractions corresponding to the major eluting species were pooled as indicated by the horizontal bars, and labeled A, B, C, D, E, in order of elution. (a) $\text{Ru}(\text{NH}_3)_5\text{Cl}_3/\text{Zn}$ amalgam synthetic procedure followed. Column bed 2.0 x 54 cm. The elution volumes (peak maxima) of native ferro- and ferricytochrome *c*, determined in a separate experiment but under the same chromatographic conditions, are indicated by the labeled arrows. (b) $[\text{Ru}(\text{NH}_3)_5\text{H}_2\text{O}](\text{PF}_6)_2$ synthetic procedure followed. Column bed 2.0 x 58 cm.



species differing by only one charge unit, a mono- $\text{Ru}(\text{NH}_3)_5^{3+}$ -ferricytochrome *c* derivative should elute at approximately 950 mL. This corresponds to the position of peak E in the chromatogram. In terms of further preliminary identification it could only be stated that peaks C and D represented species with total charges intermediate to B and E, while peak A represented a species slightly more acidic than native ferrocyanocytocrome *c*.

Each of the chromatograms in Figure 5.5 represents the purification of 100 mg of modified cytochrome *c*. Four 100-mg preparations were carried out according to the $\text{Ru}(\text{NH}_3)_5\text{Cl}_3/\text{Zn}$ amalgam method described in the Experimental Section. The chromatogram for each was essentially identical with that in Figure 5.5(a). The fractions corresponding to peaks A through E were pooled as indicated in the figure. The average yield for each peak, calculated from the results on these four preparations, is given in Table 5.3. Peaks A through E account for considerably less than 100% of the initial 100 mg of cytochrome *c*. Incomplete separation of the peaks and irreversible binding of protein material to the top of the column can account for the loss.

Due to the incomplete resolution of the products on the initial cation exchange column, peaks A through E were purified separately by rechromatography on CM-cellulose. The analogous peaks from the four preparations mentioned above were pooled and rechromatographed using single ionic

Table 5.3. Yields of Individual $\text{Ru}(\text{NH}_3)_5$ -Cytochrome *c* Reaction Products^a

Peak	Crude yield (%) ^{b, c}	Peak	Final yield(%) ^{b, d}
A	8.9	A'	4.0
B	11.6	B'	4.3
C	13.5	C'	5.9
D	7.3	D'	2.6
E	12.4	E'	7.2
Unrecovered	46.3	Unrecovered	76.0
Total	100	Total	100

^aYields reported here are for reactions carried out by the $\text{Ru}(\text{NH}_3)_5\text{Cl}_3/\text{Zn}$ amalgam method. The $[\text{Ru}(\text{NH}_3)_5\text{H}_2\text{O}](\text{PF}_6)_2$ preparative procedure gave similar results. ^bYields were

calculated from the spectrally-determined quantity of cytochrome *c* in the pooled fractions of each peak. Yields are based on 100 mg of starting cytochrome *c*. ^cThe crude yield represents the average of four 100-mg preparations.

^dThe final yield represents that obtained when the analogous peaks from four preparations were pooled and rechromatographed.

strength elutions (Figure 5.6). The fractions corresponding to peaks A' through E' (the prime indicating purification by rechromatography) were pooled as indicated in the figure. The asymmetry of the major peaks in the chromatograms of A' and B' suggests that more than one species may still be present in these rechromatographed samples. Further purification was not attempted, however. The final yield of each peak (based on 100 mg of starting protein) is given in Table 5.3.

It should be noted here that the results reported in the remainder of this section were all obtained on aliquots of solutions corresponding to peaks A' through E' in Figure 5.6, unless otherwise noted. Thus comparisons of results obtained by one technique on a given species to those obtained by another technique on the same species are valid. Any discrepancies in the results cannot be attributed to differences in sample preparation or purification.

Ruthenium Content of $\text{Ru}(\text{NH}_3)_5$ -Cytochromes *c*

The amount of ruthenium bound to cytochrome *c* in each of the rechromatographed species (peaks A' through E') was determined by atomic absorption. The results are given in Table 5.4. The values in the first column correspond to samples prepared by the $\text{Ru}(\text{NH}_3)_5\text{Cl}_3/\text{Zn}$ amalgam method and purified as shown in Figures 5.5(a) and 5.6. Values in the second column represent samples prepared by the $[\text{Ru}(\text{NH}_3)_5\text{H}_2\text{O}]$ - $(\text{PF}_6)_2$ method, also purified by chromatography, and

Figure 5.6. Rechromatography of peaks A through E on separate CM-cellulose columns. Analogous peaks from four $\text{Ru}(\text{NH}_3)_5\text{Cl}_3/\text{Zn}$ amalgam preps were pooled prior to rechromatography. Elution was with sodium phosphate buffer, pH 7.0, of the concentration indicated, on a column of the dimensions indicated: peak A, 85 mM, 2.3 x 32 cm; peak B, 85 mM, 2.3 x 26 cm; peak C, 85 mM, 2.3 x 19 cm; peak D, 100 mM, 2.3 x 19 cm; peak E, 100 mM, 2.3 x 17 cm. Fractions corresponding to the major eluting species were pooled as indicated by the horizontal bars and labeled A' through E'.

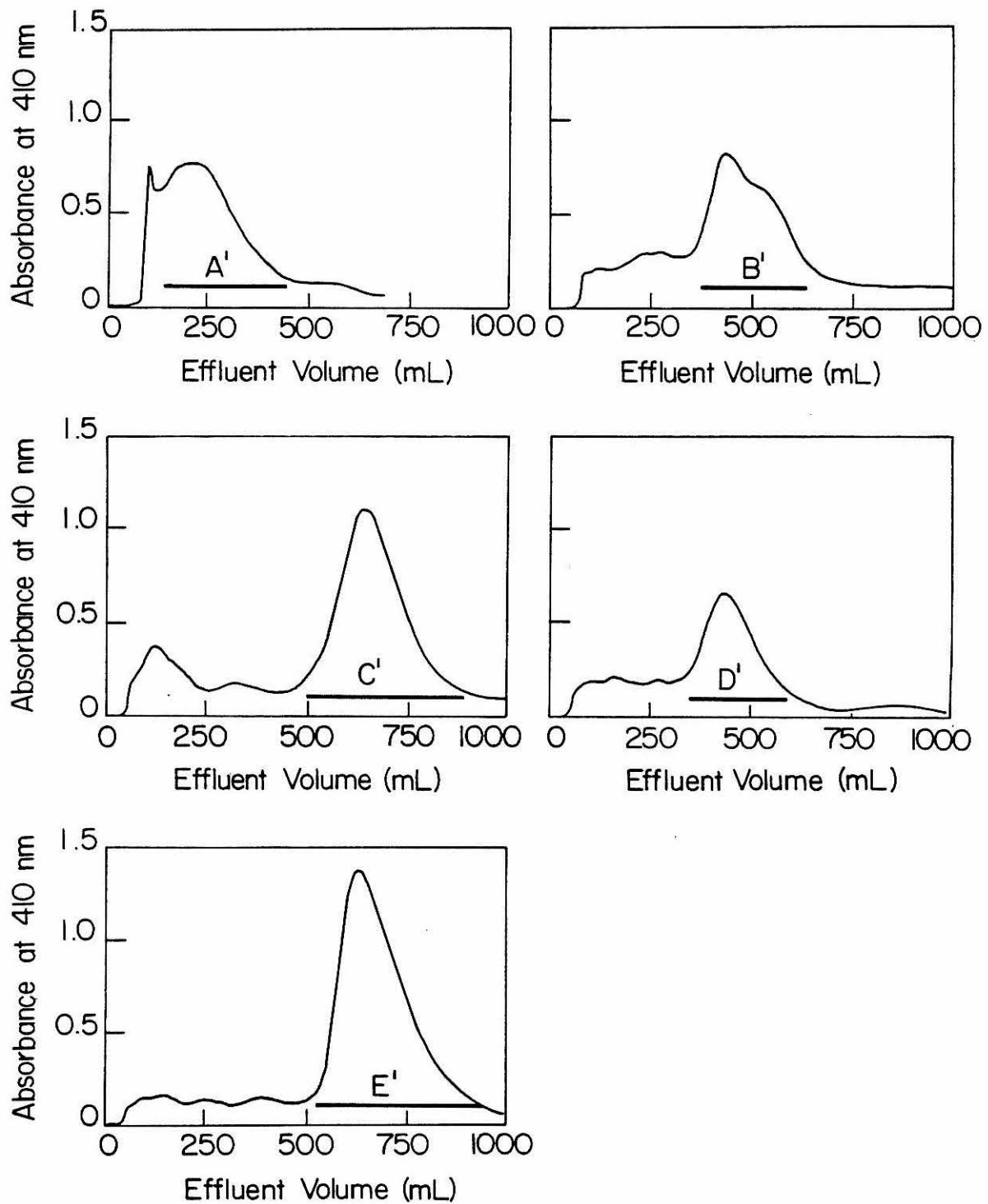


Table 5.4. Ruthenium Content of $\text{Ru}(\text{NH}_3)_5$ -Cytochromes *c*
as Determined by Atomic Absorption

Peak	$\text{Ru}(\text{NH}_3)_5\text{Cl}_3/$ Zn amalgam method	$[\text{Ru}(\text{NH}_3)_5\text{H}_2\text{O}](\text{PF}_6)_2$ method	
	$[\text{Ru}] / [\text{cyt } c]^{a,b}$	$[\text{Ru}] / [\text{cyt } c]^{a,b}$	$[\text{Ru}] / [\text{cyt } c]^{a,c}$
A'	2.5 ± 0.4	2.5 ± 0.4	—
B'	1.5 ± 0.2	1.3 ± 0.2	0.12 ± 0.02
C'	1.3 ± 0.2	1.3 ± 0.2	—
D'	2.2 ± 0.3	2.2 ± 0.3	—
E'	1.3 ± 0.2	1.1 ± 0.2	1.4 ± 0.2

^aConcentration of cytochrome *c* determined spectrally.

^b $[\text{Ru}(\text{NH}_3)_5^{2+}] : [\text{cyt } c]$ in reaction was 50:1. ^c $[\text{Ru}(\text{NH}_3)_5\text{H}_2\text{O}^{2+}] : [\text{cyt } c]$ in reaction was 10:1.

rechromatography, on CM-cellulose. Column three lists the ruthenium content of the two major peaks obtained when the $[\text{Ru}(\text{NH}_3)_5\text{H}_2\text{O}^{2+}]:[\text{cytochrome}]$ ratio in a $[\text{Ru}(\text{NH}_3)_5\text{H}_2\text{O}](\text{PF}_6)_2$ preparation was reduced to 10:1 from the 50:1 ratio normally employed. When chromatographed under the same conditions, the elution volumes of the two peaks corresponded to the positions of peaks B and E in the normal five-peak chromatograms. The two peaks were therefore labeled analogously. Separation of these two peaks in the initial chromatography was good; the peaks were not repurified prior to atomic absorption.

As predicted on the basis of elution volumes, the ruthenium analysis on E' is consistent with it being a mono- $\text{Ru}(\text{NH}_3)_5^{3+}$ -ferricytochrome *c* derivative. The ratios of ruthenium to cytochrome *c* obtained on this peak were often slightly above 1.0, indicating some impurity despite careful chromatographic purification. It has been demonstrated that CM-cellulose chromatography can resolve mono-substituted cytochrome *c* derivatives of the same total charge provided the modifications affect the resin interaction site on the protein differently.³⁹ However, on the basis of the atomic absorption results alone, the possibility that peak E' contains a mixture of mono- $\text{Ru}(\text{NH}_3)_5^{3+}$ -cytochrome *c* species cannot be ruled out.

Recall that peak B elutes at the same position in the initial chromatogram as does native ferricytochrome *c*

under the same conditions (Figure 5.5(a)). However, the ruthenium analyses on peak B' indicate the presence of ruthenium in this species, and in quantities greater than one ruthenium per molecule of cytochrome *c*. But note that when the concentration of ruthenium in the reaction was decreased significantly the major product obtained, eluting in the peak B position, contained only 0.12 ruthenium per cytochrome *c*. The other major peak in this preparation, eluting at position E (but only obtained in one-third the yield of peak B), retained a ruthenium content similar to the other E peaks listed. Assuming no decomposition of the native cytochrome *c*, it appears that the ruthenium contained in peak B has been incorporated in a form or location which does not significantly change the charge on the protein.

The relationship between elution volume and ruthenium content for the remaining species (A', C', and D') is also quite puzzling. A mixture of products containing only $\text{Ru}(\text{NH}_3)_5^{3+}$ -modified cytochromes *c* should elute from CM-cellulose in order of increasing $\text{Ru}(\text{NH}_3)_5^{3+}$ content, *i.e.*, in order of increasing charge. The results in Table 5.4 show no correlation between the order of peak elution and the ruthenium content of the peaks. Therefore, it cannot be assumed that the products obtained are all either unmodified ferricytochrome *c* or simple $\text{Ru}(\text{NH}_3)_5^{3+}$ -ferricytochromes *c*.

Peak E' was the only peak for which both the ruthenium content and chromatographic properties appeared consistent with a mono- $\text{Ru}(\text{NH}_3)_5^{3+}$ -ferricytochrome *c* complex. It was also the peak obtained in the highest final yield. Although the identity of peaks A' through D' was further probed by various techniques (Appendix 5.1), emphasis was placed on characterizing the material corresponding to peak E'.

Atomic absorption was also used to check the long-term stability of E'. A sample of E' was stored at 4°C as a concentrated solution (*ca.* 10^{-4} M) for a total of three weeks. During this time it was used several times for cyclic voltammetric measurements. After three weeks the solution was chromatographed on Sephadex G-25 to remove any ruthenium complex which may have dissociated. Atomic absorption on this sample gave 1.2 (± 0.2) ruthenium per cytochrome *c* *vs.* the original value of 1.3 (± 0.2). Other samples of E' that were stored at 4°C for two months, during which time they were used in several types of experiments, also retained their characteristic chromatographic properties when repurified on CM-cellulose. The observed stability of this $\text{Ru}(\text{NH}_3)_5^{3+}$ -cytochrome *c* complex is consistent with the stability of the simple $\text{Ru}(\text{NH}_3)_5^{3+}\text{L}^{3+}$ model complexes.²

Identification of the $\text{Ru}(\text{NH}_3)_5$ Binding Site

The site of attachment of $\text{Ru}(\text{NH}_3)_5^{3+}$ to the protein in the mono- $\text{Ru}(\text{NH}_3)_5^{3+}$ -ferricytochrome *c* complex, E', was identified by locating and isolating the ruthenium-containing

tryptic peptide. Trypsin is a proteolytic enzyme which catalyzes the hydrolysis of peptide bonds, specifically those bonds whose carbonyl function is donated by arginine or lysine. Thus when cytochrome *c* is digested with trypsin, the peptides that result are those indicated in Figure 5.7. The major peptides are labeled T1 through T18. Note that His-26, His-33, and Met-65 are contained in separate tryptic peptides - T6, T7, and T11, respectively. When separated by HPLC the tryptic peptides give a characteristic elution pattern. A sample of modified cytochrome *c*, when subjected to the same treatment, produces a chromatogram in which the peak corresponding to the modified peptide is shifted from its original position in the native chromatogram. The modified peptide is subsequently identified by amino acid analysis.

The separation of the tryptic digest of native cytochrome *c* on a reversed-phase HPLC column is shown in Figure 5.8. The identity of most of the peaks in the chromatogram was determined by amino acid analyses. The amino acid composition of the native peptides is given in Table 5.5. The chromatogram of the major $\text{Ru}(\text{NH}_3)_5$ -cytochrome *c* derivative (E') is also shown in Figure 5.8. The major difference between the chromatograms of the native and ruthenium-modified proteins is in the position of peptide T7. This His-33-containing peptide shifts to a considerably lower elution volume in the HPLC of the ruthenium-modified

Figure 5.7. The tryptic peptides of horse heart cytochrome *c*. The vertical lines indicate the points of hydrolysis by trypsin. The major resulting peptides are designated T1 through T18. The numbers immediately below the amino acids (10, 20, 30, etc.) are sequence position numbers. His-26, His-33, and Met-65 are highlighted by asterisks. (Adapted from reference 42.)

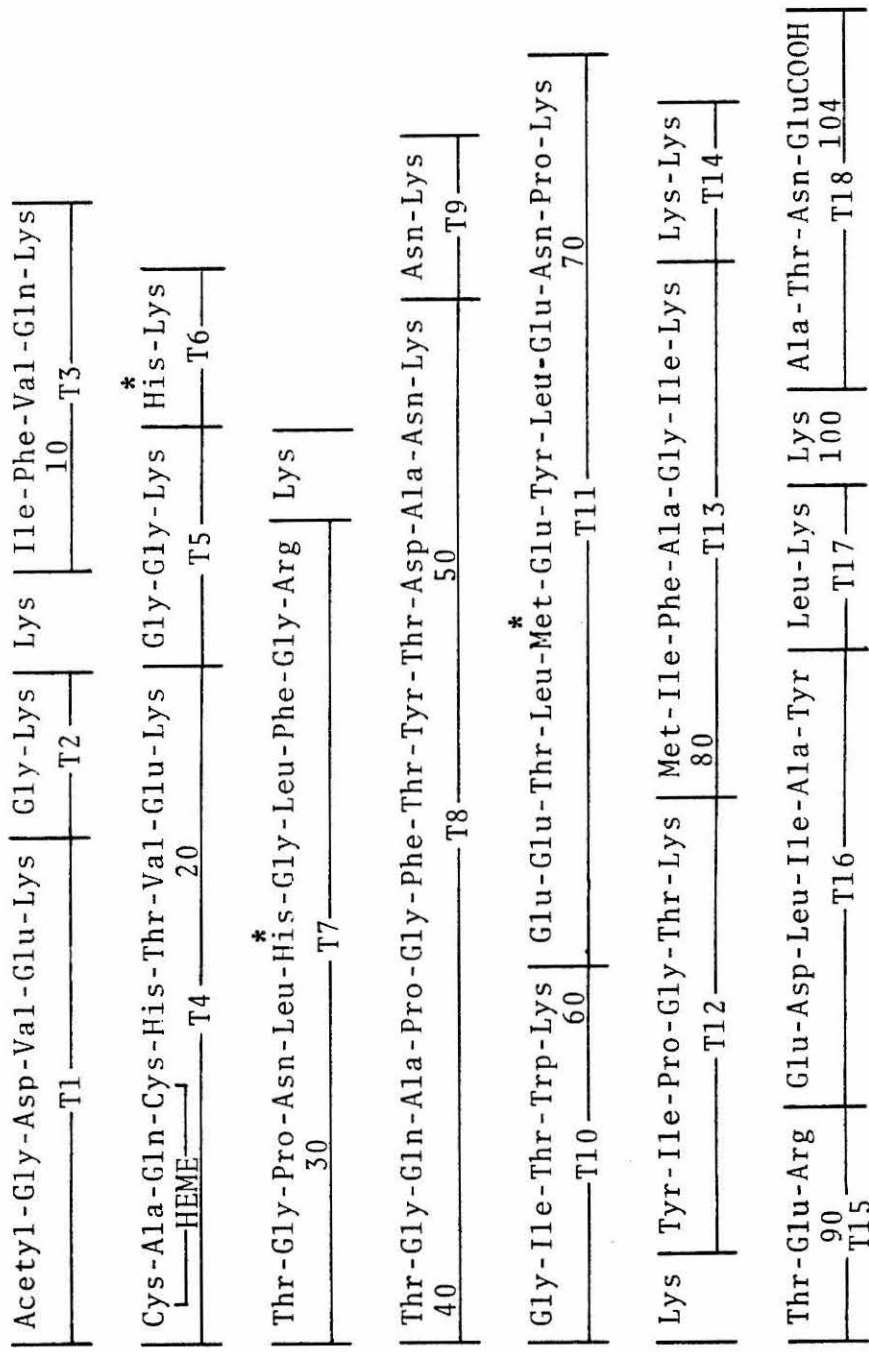


Figure 5.8. Reversed-phase HPLC of tryptic digests of native cytochrome *c* and Ru(NH₃)₅-cytochrome *c* (E') at 220 nm (1.0 AUFS). A 2 mg-sample of hydrolyzed protein was chromatographed with a linear gradient between 0 and 45% acetonitrile in pH 2.85 phosphate buffer. The labeled peaks were identified by amino acid analysis (Tables 5.5 and 5.6).

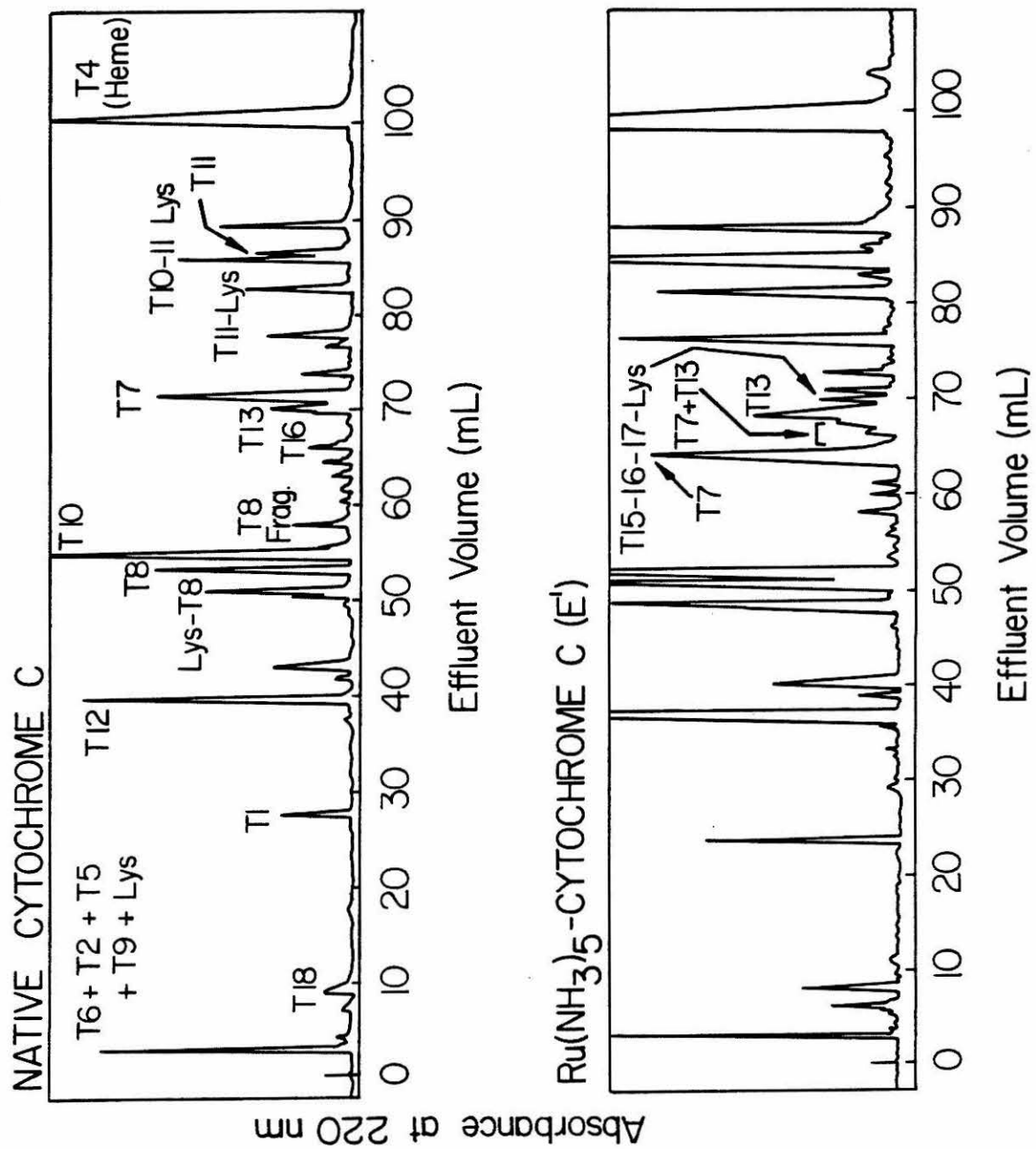


Table 5.5. Amino Acid Composition of Native Cytochrome *c* Tryptic Peptides

Composition of selected peptides in order of elution by HPLC (Fig. 5.8) residues/molecule ^a						
Tryptic peptide: ^b	T2+T5+ T6+T9+ Lys ₁	T18	T1	T12	Lys-T8	T8
Amino Acid:						
Trp						
Lys	+	0.64(1)	0.94(1)	1.27(1)	2.09(2)	1.03(1)
His	+					
Arg						
Asp ^c	+	0.98(1)	1.03(1)	1.01(1)	2.20(2)	2.07(2)
Thr		0.93(1)			2.72(3)	2.77(3)
Ser						
Glue		1.10(1)	1.05(1)		1.56(1)	1.19(1)
Pro					1.07(1)	1.10(1)
Gly	+	0.12	0.99(1)	1.05(1)	2.93(2)	1.91(2)
Ala		1.00(1)			2.30(2)	1.81(2)
Cys						
Val		0.94(1)				
Met					0.94(1)	0.23
Ile						0.37
Leu					0.89(1)	0.34(1)
Tyr						0.92(1)
Phe						0.99(1)
						1.06(1)
Sequence region: ^b	6-7, 23-25, 26-27, 54-55	101-104	1-5	74-79	39-53	40-53

Table 5.5 (cont.)

Tryptic peptide: ^b	T10	T8 Frag.	T16	T13	T7	T11-Lys.	T10-11-Lys.	T11	T4 (Heme)
Amino acid: Trp Lys	0.15(1) 0.97(1)			1.10(1)	0.33 0.94(1)	1.94(2)	2.70(3)	1.10(1)	0.93(1) 0.91(1)
His					0.97(1) 0.93(1)	1.05(1) 0.94(1)	1.26(1) 1.76(2)	1.22(1) 1.00(1)	0.19 1.00(1)
Arg	0.99(1)	1.99(2)	1.08(1)	0.25	0.16 0.30	1.05(1) 0.30	1.26(1) 0.41	1.22(1) 0.41	0.19 0.40
Asp ^c									
Thr	0.99(1)	1.16	0.29		0.23 0.96(1)	4.01(4) 0.96(1)	4.34(4) 1.06(1)	3.97(4) 0.82(1)	2.20(2) 0.72
Ser ^d									
Glue	0.97(1)	1.24(1)	0.21		2.99(3) 0.55	2.99(3) 0.55	1.90(2) 0.56	1.90(2) 0.56	0.27 0.25
Pro	0.71(1)	2.21(2)	0.64	1.20(1)					
Gly	1.13(1)	1.07(1)	1.02(1)	1.09(1)					
Ala									
Cys									
Val									
Met	0.90(1)			0.40(1) 1.86(2)	0.40	0.28(1)	0.54(1)	0.67(1)	
Ile				0.90(1) 1.00(1)	1.92(2)	0.76(1)			
Leu				0.72(1)	1.97(2) 0.51(1)	2.22(2) 1.00(1)	1.93(2) 0.82(1)	0.21	
Tyr	0.57(1)			0.96(1)	1.07(1)				
phe	0.90(1)								
Sequence region: ^b	56-60	40-46	92-97	80-86	28-38	61-73	56-73	61-72	14-22

^aThe numbers in parentheses are the integral number of residues assumed in the assignment of the amino acid composition to the designated tryptic peptide. Contaminants of less than 10% are omitted. ^bNumbering system corresponds to that given in Figure 5.7. ^cBoth Asp and Asn analyze as Asp.

^dCytochrome *c*

contains no serine, however, serine contamination (perhaps from trypsin) was detected in several cases and, hence, is reported. ^eBoth Glu and Gln analyze as Glu. ^fThis mixture of peptides elutes with the solvent front. It analyzed as an equimolar mixture of the indicated peptides: T2, 0.032

μmol; T5, 0.032 μmol, T6, 0.031 μmol; T9, 0.032 μmol; additional Lys, 0.10 μmol. ^gThis number represents a mixture of Cys and Val; these amino acids were unresolved in this particular analysis.

cytochrome *c*. The identity of the "new" peak in the chromatogram of E' as T7 was confirmed by amino acid analysis, as was the fact that very little peptide material corresponding to T7 remains at the original position of the native T7 peptide. Amino acid analyses on the peptides in the region of interest in the chromatogram of $\text{Ru}(\text{NH}_3)_5$ -cytochrome *c* are listed in Table 5.6.

The HPLC results cited thus far are consistent with the identification of peptide T7 as the site of modification in the ruthenium-cytochrome *c* derivative E'. Confirmation that the modification specifically corresponds to the attachment of $\text{Ru}(\text{NH}_3)_5^{3+}$ to His-33 of the T7 peptide was obtained as follows. The HPLC of a native cytochrome *c* tryptic digest was rerun, this time monitoring the absorbance of the eluting peptides at 300 nm. This chromatogram is shown in Figure 5.9. (The chromatograms in Figure 5.8 were monitored at 220 nm.) Peptide bonds, and most amino acid side chains, absorb in the 220-nm region. Very few amino acid side chains have any absorbance in the 300-nm region of the spectrum (only Trp, λ_{max} 280 nm; and to a lesser extent, Tyr, λ_{max} 275 nm; Phe, λ_{max} 267 nm).⁴⁰ The heme-containing peptide, T4, also absorbs at 300 nm. The major peaks in the native cytochrome *c* chromatogram at 300 nm elute at positions corresponding to peptides T10 (contains Trp) and T4 (heme). No peak corresponding to T7 is observed in the 300-nm native cytochrome *c* chromatogram.

Table 5.6. Amino Acid Composition of $\text{Ru}(\text{NH}_3)_5$ -Cytochrome *c* (E') Tryptic Peptides

Composition of selected peptides in order of elution by HPLC (Figure 5.8); residues/molecule ^a					
Tryptic peptide: ^b	T7	T7+T13 ^f	T13	T15-16-17	? ^g
Amino Acid: Trp					
Lys	0.16	+	1.00(1)	1.63(2)	+
His	0.87(1)	+		0.20	+
Arg	0.94(1)	+		1.01(1)	+
Asp ^c	1.27(1)	+		1.18(1)	+
Thr	0.90(1)	+		1.81(1)	+
Ser ^d		+		0.40	+
Glu ^e	0.38	+	0.12	1.97(2)	+
Pro	0.93(1)	+		0.49	+
Gly	2.90(3)	+	1.07(1)	1.52	+
Ala	0.34	+	1.00(1)	1.01(1)	+
Cys					
Val					
Met		+	0.88(1)		
Ile	0.34	+	1.97(2)	0.51(1)	+
Leu	2.24(2)	+	0.13	1.83(2)	+
Tyr	0.31	+		0.71(1)	+
Phe	0.95(1)	+	0.97(1)	0.35	+
Sequence region: ^b	28-38	28-38 80-86	80-86	88-99	

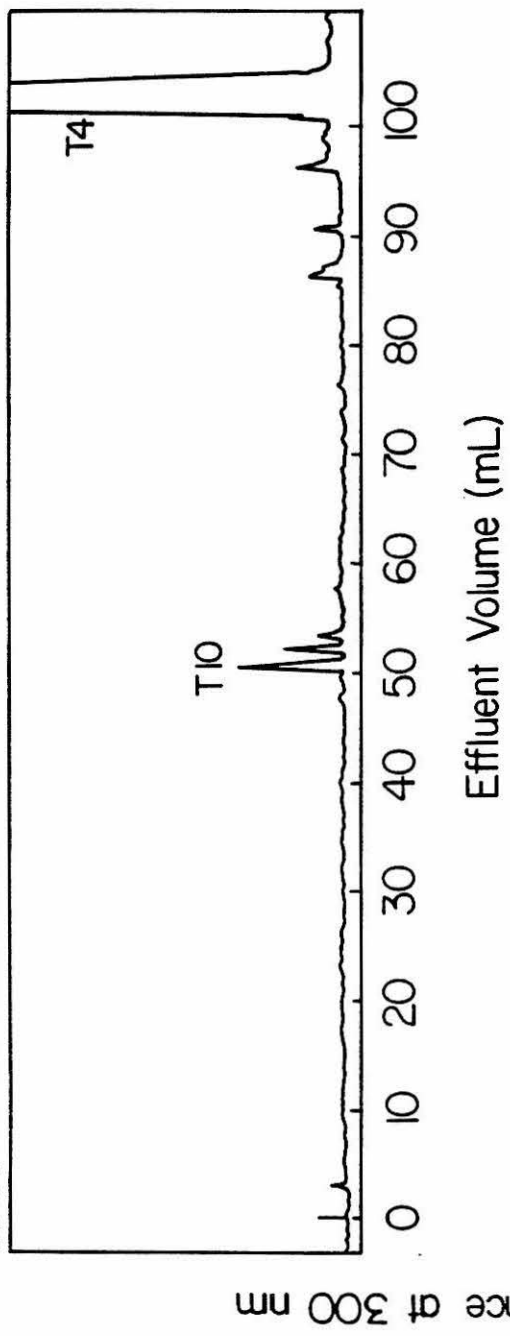
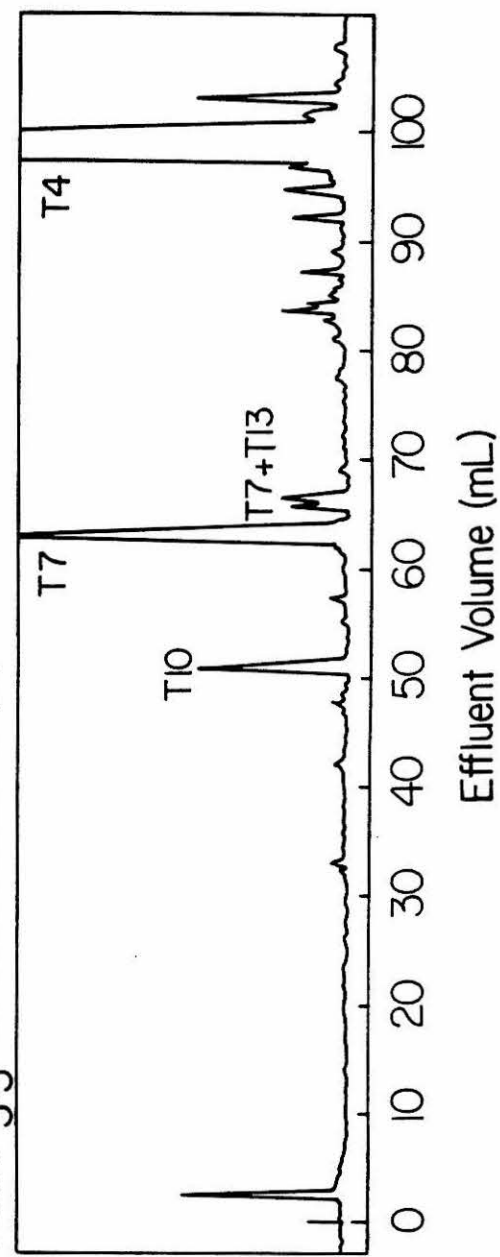
^aThe numbers in parentheses are the integral number of residues assumed in the assignment of the amino acid composition to the designated tryptic peptide. Contaminants of less than 10% are omitted. ^bNumbering system corresponds to that given in Figure 5.7. ^cBoth Asp and Asn analyze as Asp. ^dCytochrome *c*

Table 5.6 (cont.)

contains no serine, however, serine contamination was detected in several cases, and hence, is reported. ^eBoth Glu and Gln analyze as Glu. ^fThis analysis corresponds to two small neighboring peaks in the HPLC. The indicated amino acids are present and the analysis is consistent with a mixture of peptides T7 (0.108 μ mol), T13 (0.075 μ mol), and Lys (0.15 μ mol). The Lys could be associated with T7 and/or T13. ^gAnalysis of this peak showed that the indicated amino acids were present but a fit of the data to a particular peptide, or mixture of peptides, was not realized.

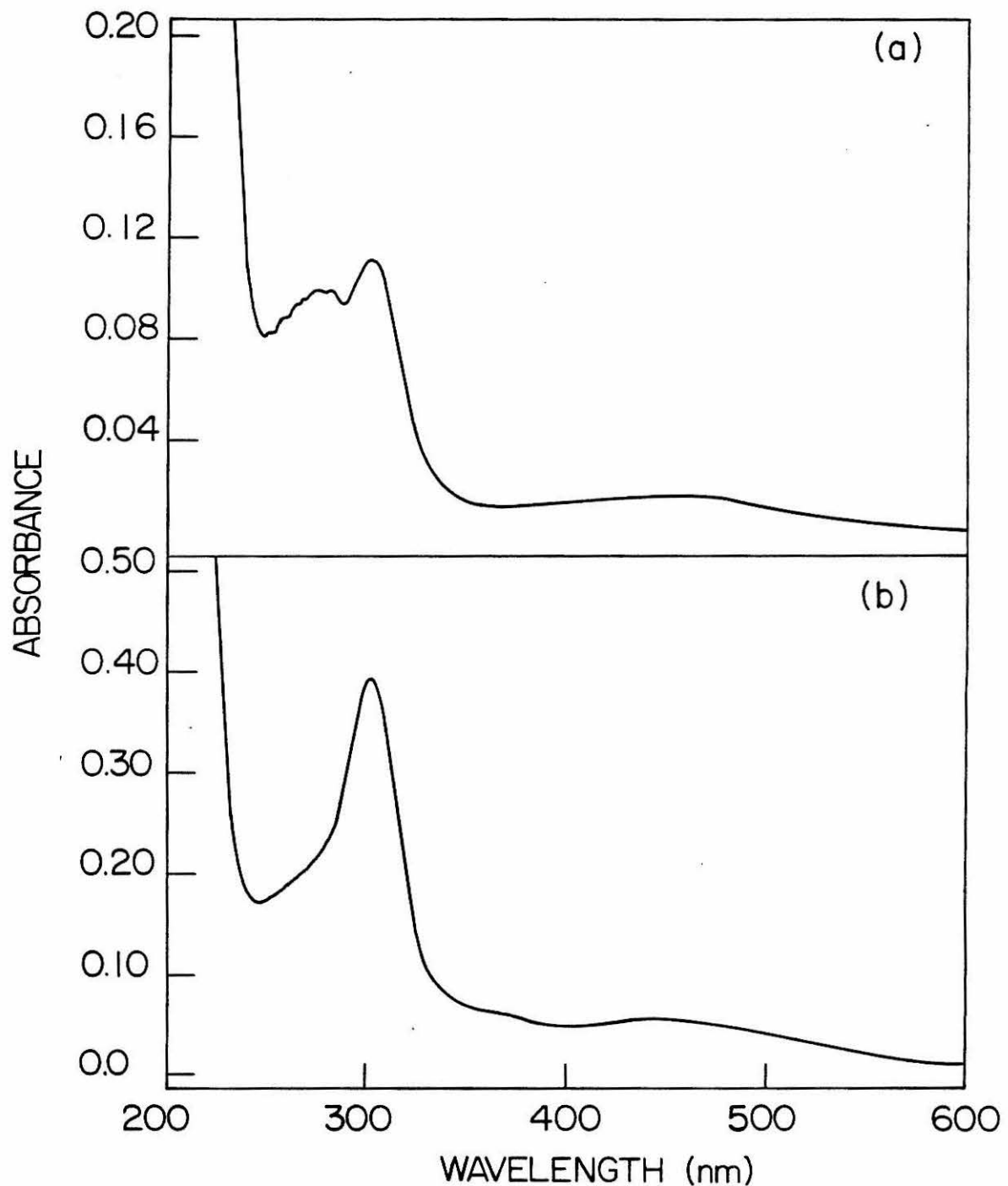
Figure 5.9. Reversed-phase HPLC of tryptic digests of native cytochrome *c* and Ru(NH₃)₅-cytochrome *c* (E') at 300 nm (0.1 AUFS). A 2-mg sample of hydrolyzed protein was chromatographed with a linear gradient between 0 and 45% acetonitrile in pH 2.85 phosphate buffer. The labeled peaks were identified by analogy to the 220-nm chromatograms (Figure 5.8).

NATIVE CYTOCHROME C

Ru(NH₃)₅-CYTOCHROME C (E')

In the chromatogram of ruthenium-modified cytochrome *c* at 300 nm (Figure 5.9) the features corresponding to the T10 and T4 peptides are present, but a new peak at an elution volume of approximately 64 mL is observed. This peak is identified as the T7 peptide by comparison with the 220-nm chromatogram of the $\text{Ru}(\text{NH}_3)_5$ -cytochrome *c* (Figure 5.8). The attachment of $\text{Ru}(\text{NH}_3)_5^{3+}$ to His-33 in the T7 peptide is responsible for the observation of T7 at 300 nm in the modified protein. Recall that the prominent feature in the spectrum of $\text{Ru}(\text{NH}_3)_5\text{His}^{3+}$ is a peak at 303 nm (ϵ 2100 $\text{M}^{-1} \text{cm}^{-1}$).⁵ The spectrum of the fractions corresponding to the T7 peptide in the 300 nm chromatogram of $\text{Ru}(\text{NH}_3)_5$ -cytochrome *c* were collected, dried, and redissolved in water. The UV-visible spectrum of this peak is shown in Figure 5.10(a). For comparison, the spectrum of $\text{Ru}(\text{NH}_3)_5\text{His}^{3+}$ is also shown. The spectrum of the modified T7 peptide is exactly that of $\text{Ru}(\text{NH}_3)_5\text{His}^{3+}$ plus an additional peak at ~ 275 nm attributable to the presence of Phe in the T7 peptide. A spectrum of the smaller peak eluting just after the major T7 peak also exhibited the characteristic $\text{Ru}(\text{NH}_3)_5\text{His}^{3+}$ features. (The tryptic hydrolysis procedure is carried out at pH 8, after which the pH is lowered to 2.85 for HPLC. To confirm that these manipulations do not destroy the $\text{Ru}(\text{NH}_3)_5\text{His}^{3+}$ complex, a sample of $[\text{Ru}(\text{NH}_3)_5\text{His}]\text{Cl}_3$ was subjected to the identical pre-HPLC procedures. The resulting solution retained the characteristic $\text{Ru}(\text{NH}_3)_5\text{His}^{3+}$ spectrum.)

Figure 5.10. (a) UV-visible spectrum of the His-33-containing peptide, T7, of $\text{Ru}(\text{NH}_3)_5$ -cytochrome *c* (E'), isolated by tryptic hydrolysis and HPLC (Figure 5.9); pH 3. (b) UV-visible spectrum of a 0.2 mM solution of $[\text{Ru}(\text{NH}_3)_5\text{His}]\text{Cl}_3$; pH 7.



Recall that the atomic absorption results on the ruthenium-modified cytochrome *c*, E', corresponded to ruthenium to cytochrome *c* ratios of slightly greater than one. No shift in the T11 peptide peak was observed in the high-pressure liquid chromatograms (Figure 5.8), making Met-65 an unlikely second site. The His-26-containing peptide, T6, elutes with the solvent front, however. As a result, the possibility of a minor secondary binding site at His-26 cannot be ruled out on the basis of the HPLC results presented here. Identification of the binding site of the small fraction of "extra" ruthenium was not pursued beyond this point.

These experiments confirm that the $\text{Ru}(\text{NH}_3)_5^{3+}$ moiety is bound to the nitrogen of His-33 in the mono- $\text{Ru}(\text{NH}_3)_5^{3+}$ -cytochrome *c* complex E'. The tryptic hydrolysis, HPLC, and amino acid analysis procedures described above were also performed on the ruthenium-modified species corresponding to peaks A' through D' in an attempt to identify the ruthenium binding site(s) in these derivatives. The results are discussed in Appendix 5.1.

Optical Spectra of $\text{Ru}(\text{NH}_3)_5$ -Cytochromes *c*

The visible and ultraviolet spectra of the $\text{Ru}(\text{NH}_3)_5$ -cytochrome *c* complexes (A' through E'), in both the oxidized $\text{Ru}(\text{III})\text{-cyt } c(\text{III})$ and dithionite-reduced $\text{Ru}(\text{II})\text{-cyt } c(\text{II})$ forms, were indistinguishable from native cytochrome *c* spectra. In the totally oxidized state, no features

attributable to the presence of the $\text{Ru}(\text{NH}_3)_5^{3+}$ group were detectable. In the singly substituted $\text{Ru}(\text{NH}_3)_5^{3+}$ -cytochrome *c* species E' , $\text{Ru}(\text{NH}_3)_5^{3+}$ is present as the $\text{Ru}(\text{NH}_3)_5^{3+}(\text{His-33})^{3+}$ complex (*vide supra*). Although the characteristic spectrum of the ruthenium complex is observed in the isolated tryptic peptide (Figure 5.10), it is obscured by heme absorptions in the total protein spectrum (Figure 5.11). This is not surprising in view of the fact that for the $\text{Ru}(\text{NH}_3)_5^{3+}\text{His}^{3+}$ model complex ϵ (303 nm) = $2.1 \times 10^3 \text{ M}^{-1} \text{ cm}^{-1}$ ⁵ whereas for ferricytochrome ϵ (302 nm) = $1.3 \times 10^4 \text{ M}^{-1} \text{ cm}^{-1}$ ⁴¹.

The conformation-sensitive 695-nm band is retained in all the spectra of the oxidized ruthenium-cytochrome *c* derivatives (E' spectrum shown in Figure 5.11). This band is indicative of the ligation of Met-80 to the heme iron, and is routinely used as evidence that the structure of the native protein is retained in the region of the heme prosthetic group.^{10,42,43}

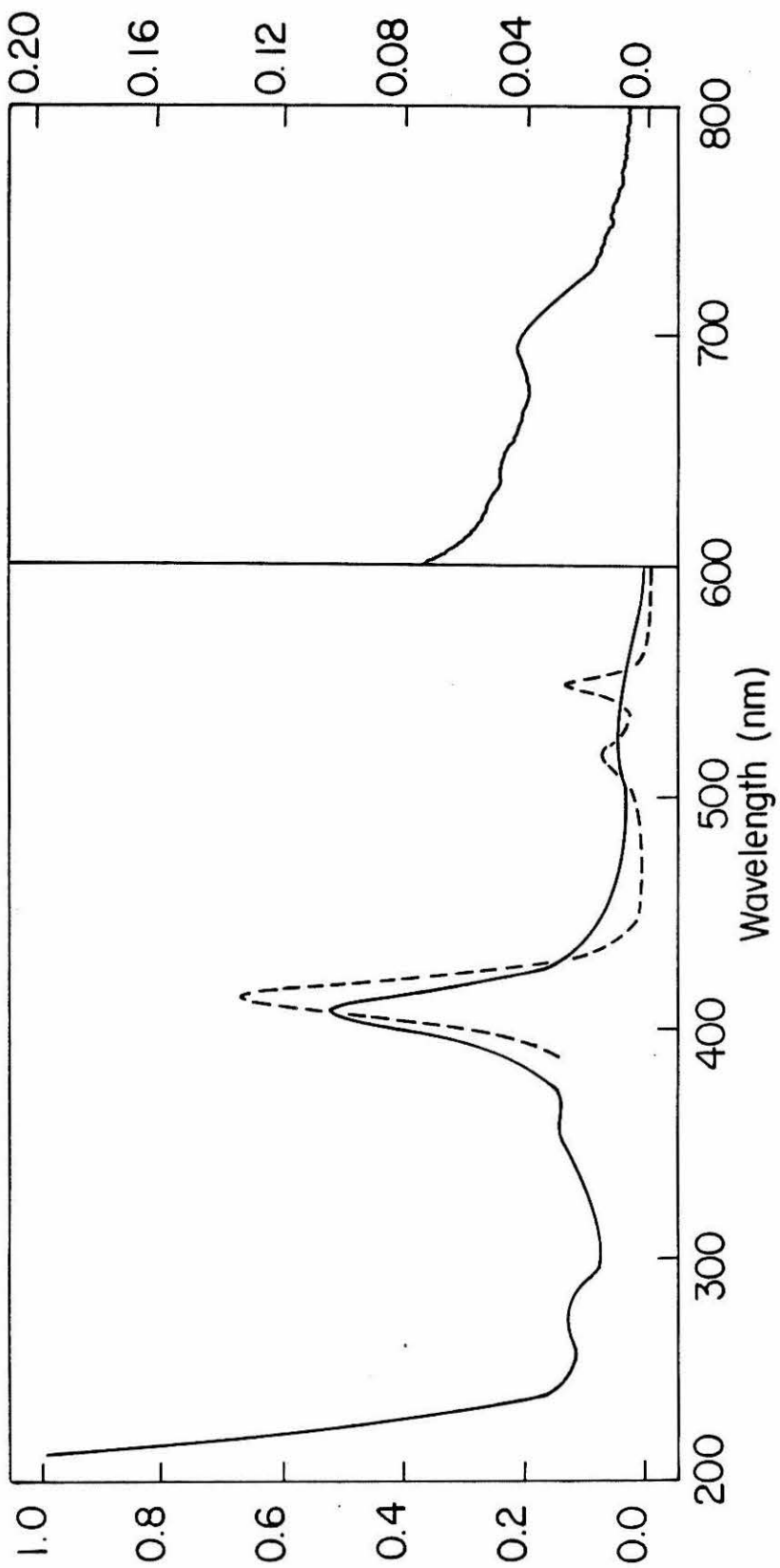
Spectroelectrochemistry of $\text{Ru}(\text{NH}_3)_5$ -Cytochrome *c*

In addition to the 695-nm absorption band, the oxidation-reduction potential of the heme *c* site can be used as test of whether or not the native structure in the region of the active site is retained in the ruthenium-modified protein. Thin-layer spectroelectrochemistry is an accurate method for the determination of metalloprotein redox potentials.³⁴

The heme *c* reduction potential determined at 25°C (pH 7 phosphate buffer, $\mu = 0.1 \text{ M}$) for $\text{Ru}(\text{NH}_3)_5$ -cytochrome *c* (E') is

Figure 5.11. The UV-visible spectra of oxidized (—) and dithionite-reduced (---) $\text{Ru}(\text{NH}_3)_5$ -cytochrome *c* (E').

Spectra in 200 to 600 nm region taken on a 0.05 mM solution (0.1 M phosphate buffer, pH 7) in a 1-mm cell. Spectrum in 600 to 800 nm region taken on same solution in a 1-cm cell.



272 (± 2) mV (vs. NHE). The Nernst plot at 25°C is shown in Figure 5.12. This value is in good agreement with the potential of the native protein, 260 mV.^{33,34}

The potential of the modified protein was also studied as a function of temperature. The results are presented in Table 5.7, and graphically in Figure 5.13. The thermodynamic parameters calculated from the temperature dependence data are presented in Table 5.8 along with the previously determined³⁵ values for native horse heart cytochrome *c*. Although it is difficult to correlate these thermodynamic values with protein properties, it has been suggested that the protein reaction entropies reflect changes in the protein structure in the vicinity of the redox active site.³⁵ It would appear that the ruthenium-modified cytochrome *c* behaves quite similarly to the native protein in this respect.

The reduction potential of the Ru(NH₃)₅(His-33) site in the modified cytochrome *c* was not determined spectroelectrochemically owing to the relative spectral invisibility of the ruthenium site.

Cyclic Voltammetry of Ru(NH₃)₅-Cytochrome *c*

Although rapid electron transfer directly between metalloproteins and electrodes is generally not observed, Hill has shown that cytochrome *c* will undergo electron transfer at a gold electrode in the presence of 4,4'-bipyridyl.^{30,44-48} The cyclics obtained indicate that the process is quasi-reversible and essentially diffusion controlled. The methods

Figure 5.12. Thin-layer spectroelectrochemistry of $\text{Ru}(\text{NH}_3)_5^-$ -cytochrome *c* (E' , 0.16 mM, pH 7 phosphate buffer, $\mu = 0.1$ M, 0.80 mM $[\text{Ru}(\text{NH}_3)_5\text{py}](\text{ClO}_4)_3$ as mediator-titrant). Nernst plot at 25°C.

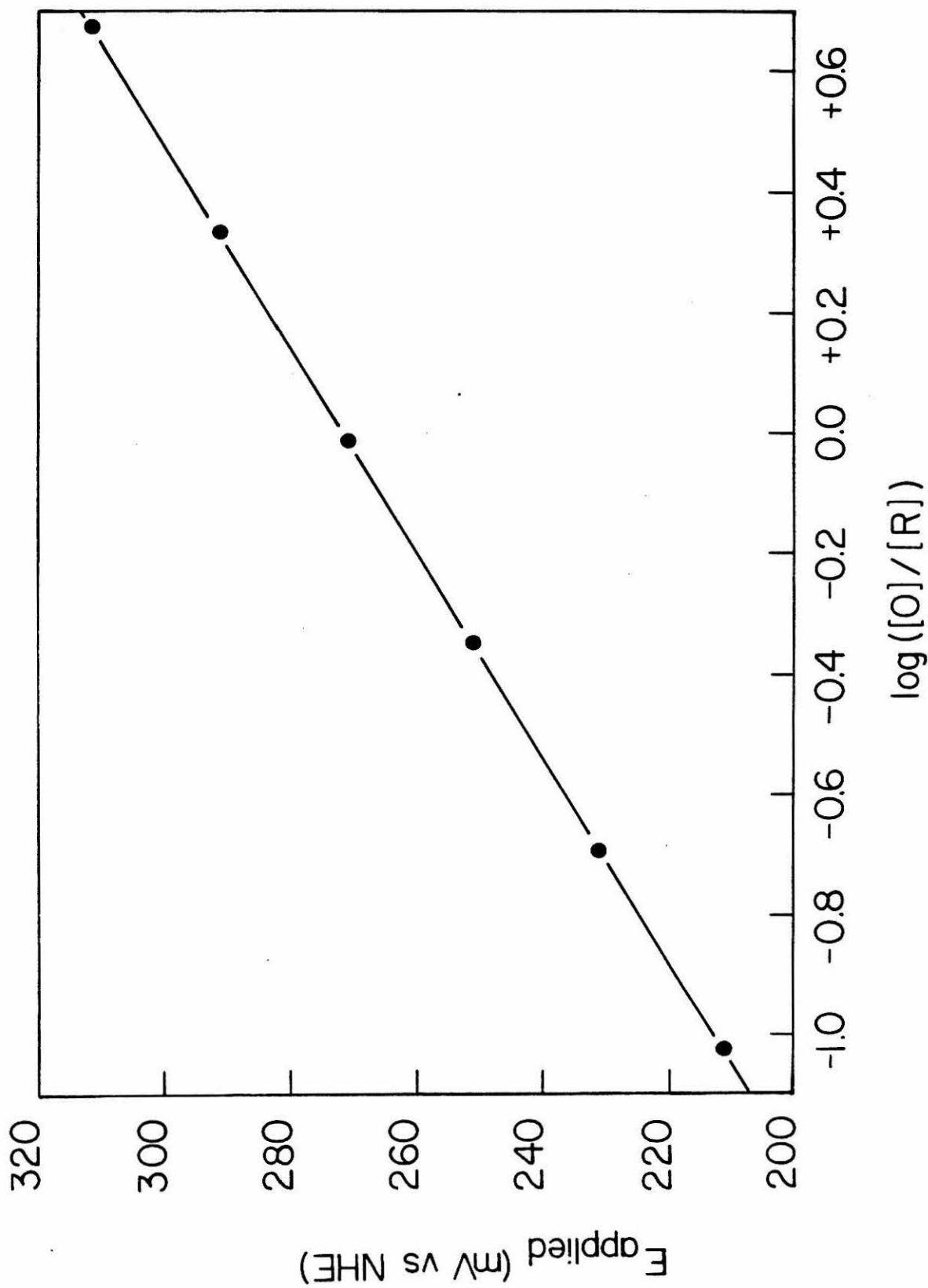


Table 5.7. Temperature Dependence of the Formal Reduction Potential, E° , for the Heme *c* Site of $\text{Ru}(\text{NH}_3)_5$ -Cytochrome *c* Using Nonisothermal Thin-Layer Spectroelectrochemistry^a

T ^b (°C)	E° ^c (mV vs. NHE)	RT/F ^d (mV)	r^2 ^e
9.4	278.6	56	1.000
12.2	277.9	57	1.000
16.0	273.8	59	1.000
20.2	272.2	57	1.000
25.0	271.5	59	1.000
29.9	267.1	60	1.000
35.3	263.7	62	1.000
39.9	260.1	63	1.000

^a $\text{Ru}(\text{NH}_3)_5$ -cytochrome *c* (peak E') was 0.16 mM; sodium phosphate buffer, pH 7, μ = 0.1 M. Mediator-titrant was $[\text{Ru}(\text{NH}_3)_5\text{py}](\text{ClO}_4)_3$ (0.80 mM). ^b $\pm 0.2^\circ\text{C}$. ^c ± 2 mV.

^dExperimental Nernst slope. ^eLinear correlation coefficient.

Figure 5.13. Plot of the temperature dependence of the formal reduction potential, E° , for the heme *c* site of $\text{Ru}(\text{NH}_3)_5$ -cytochrome *c* (E'). Experimental conditions given in Table 5.7.

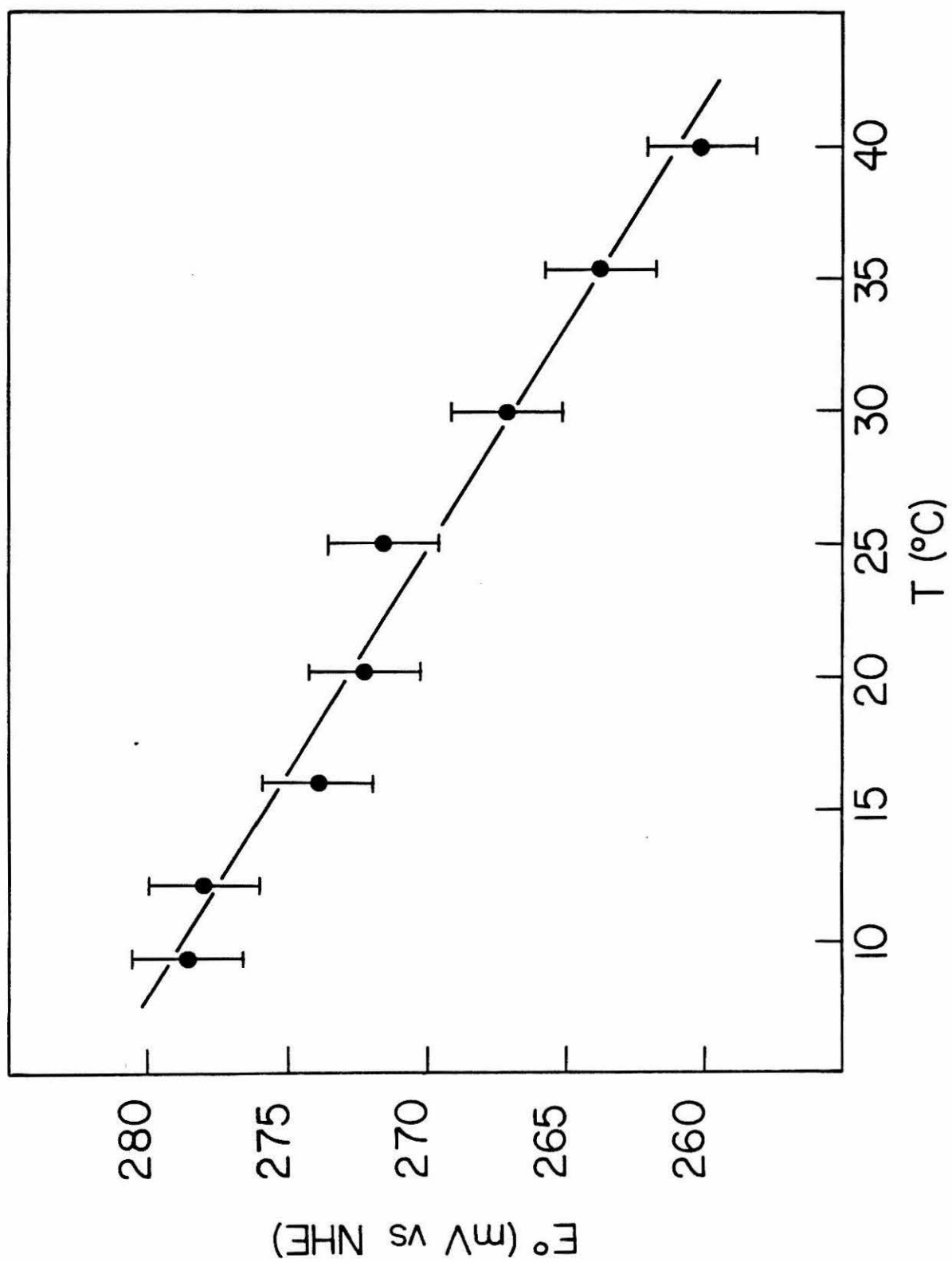


Table 5.8. Comparison of the Thermodynamic Parameters for
 Ru(NH₃)₅-Cytochrome *c* with the Corresponding Native
 Cytochrome *c* Values^a

	Ru(NH ₃) ₅ -Cyt <i>c</i> ^b	Native Cyt <i>c</i> ^c
E°, 25°C (mV <i>vs.</i> NHE) ^e	270 ± 2	260 ± 2
ΔS° (eu)	-29.2 ± 0.8	-28.5 ± 1.2
ΔS° _{rc} (eu) ^d	-13.6 ± 0.8	-12.9 ± 1.2
ΔG° (kcal/mol)	-6.22 ± 0.05	-6.00 ± 0.05
ΔH° (kcal/mol)	-14.9 ± 0.3	-14.5 ± 0.4

^aIn sodium phosphate buffer, pH 7, μ = 0.1 M. ^bPeak E'.
 Values listed correspond to heme *c* site only. ^cReference
 35. ^dΔS°_{rc} = S°_{red}-S°_{ox}. ^eCalculated from the fit to the E°
vs. T data.

developed by Hill were applied here to determine the potentials of the heme *c* and $\text{Ru}(\text{NH}_3)_5(\text{His}-33)$ sites in the modified cytochrome *c* species E' .

Prior to examining the ruthenium-modified cytochrome *c*, the following controls were run. The potentials of the ruthenium model complexes were first determined in the absence of 4,4'-bipyridyl at a carbon paste electrode (Figure 5.14(a,b)). Reversible cyclic voltammograms were obtained with peak separations of 59 ± 2 mV. The $E_{\frac{1}{2}}$ values obtained on solutions of $[\text{Ru}(\text{NH}_3)_5\text{Im}]\text{Cl}_3$ and $[\text{Ru}(\text{NH}_3)_5\text{His}]\text{Cl}_3$ are -138 ± 1 mV *vs.* SSCE (98 ± 1 mV *vs.* NHE) and -135 ± 1 mV *vs.* SSCE (101 ± 1 mV *vs.* NHE), respectively. The model complex potentials were essentially the same in the presence of 4,4'-bipyridyl at a gold electrode. As shown in Figure 5.14(c,d), reversible behavior was again observed ($E_{\text{pa}} - E_{\text{pc}} = 61 \pm 2$ mV) and the following $E_{\frac{1}{2}}$ values were obtained: $[\text{Ru}(\text{NH}_3)_5\text{Im}]\text{Cl}_3$, -131 ± 2 mV *vs.* SSCE (105 ± 2 mV *vs.* NHE); $[\text{Ru}(\text{NH}_3)_5\text{His}]\text{Cl}_3$, -132 ± 1 mV *vs.* SSCE (106 ± 1 mV *vs.* NHE). The potential of $[\text{Ru}(\text{NH}_3)_5\text{Im}]\text{Cl}_3$ reported here is in good agreement with the value of 110 mV *vs.* NHE reported in the literature.¹

A cyclic voltammogram of native cytochrome *c* at a gold electrode, in the presence of 4,4'-bipyridyl, is shown in Figure 5.15(a). In agreement with Hill's results,³⁶ the cytochrome *c* voltammograms obtained here exhibit peak separations of 60 ± 3 mV and $E_{\frac{1}{2}} = 27 \pm 3$ mV *vs.* SSCE (263 ± 3 mV *vs.* NHE). The potential of cytochrome *c* determined by

Figure 5.14. Dc cyclic voltammetry of pentaammineruthenium-imidazole and -histidine complexes. In all cases, $[Ru] = 0.2 \text{ mM}$, in pH 7 phosphate buffer ($\mu = 0.05 \text{ M}$); 0.1 M NaClO_4 . Scan rate 5 mV/sec. (a) $[Ru(NH_3)_5\text{Im}]Cl_3$ at a carbon paste electrode (CPE). (b) $[Ru(NH_3)_5\text{His}]Cl_3$ at CPE. (c) $[Ru(NH_3)_5\text{Im}]Cl_3$ at a gold electrode, in the presence of 0.01 M 4,4'-bipyridyl. (d) $[Ru(NH_3)_5\text{His}]Cl_3$, Au electrode, 0.01 M 4,4'-bipyridyl.

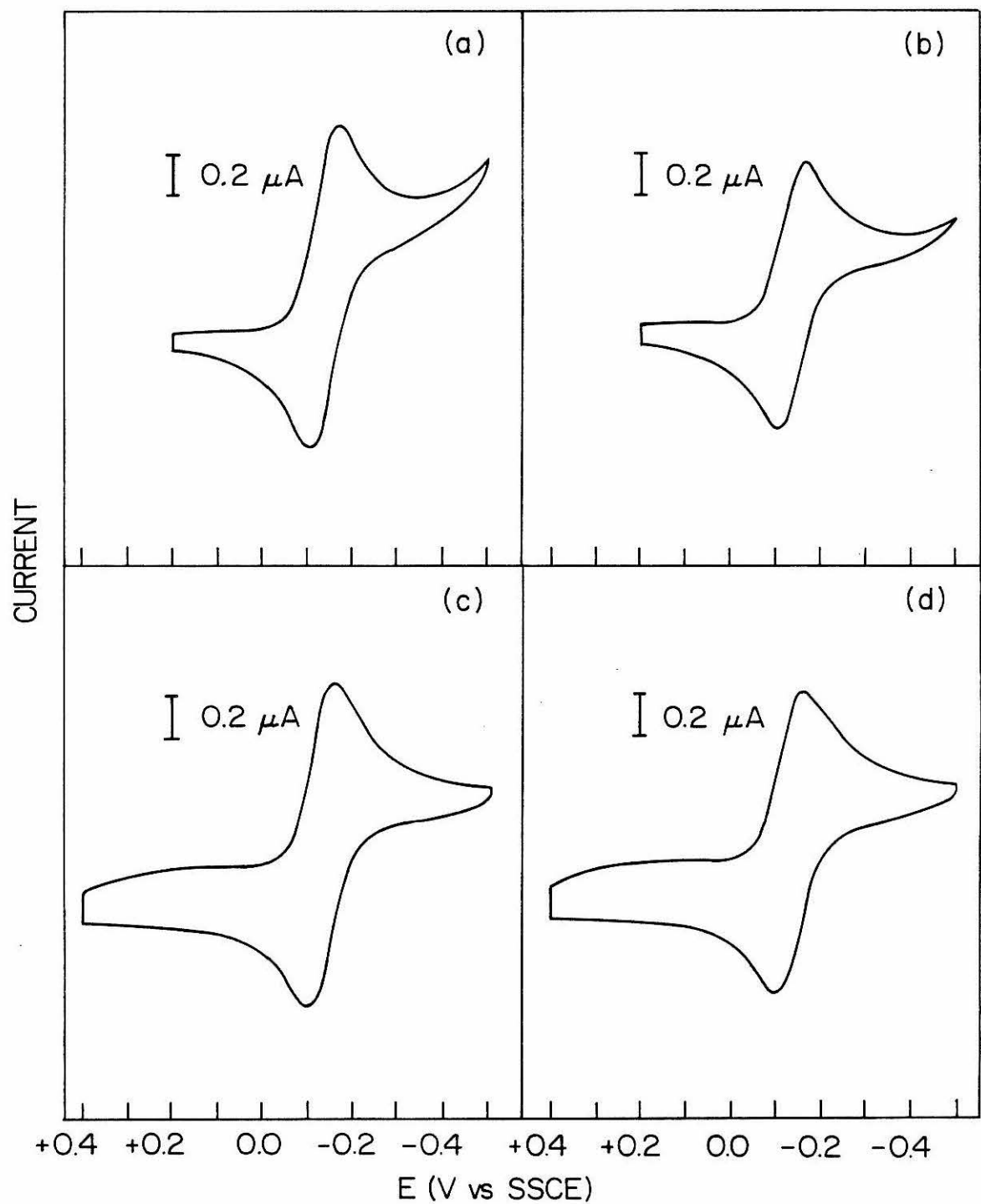
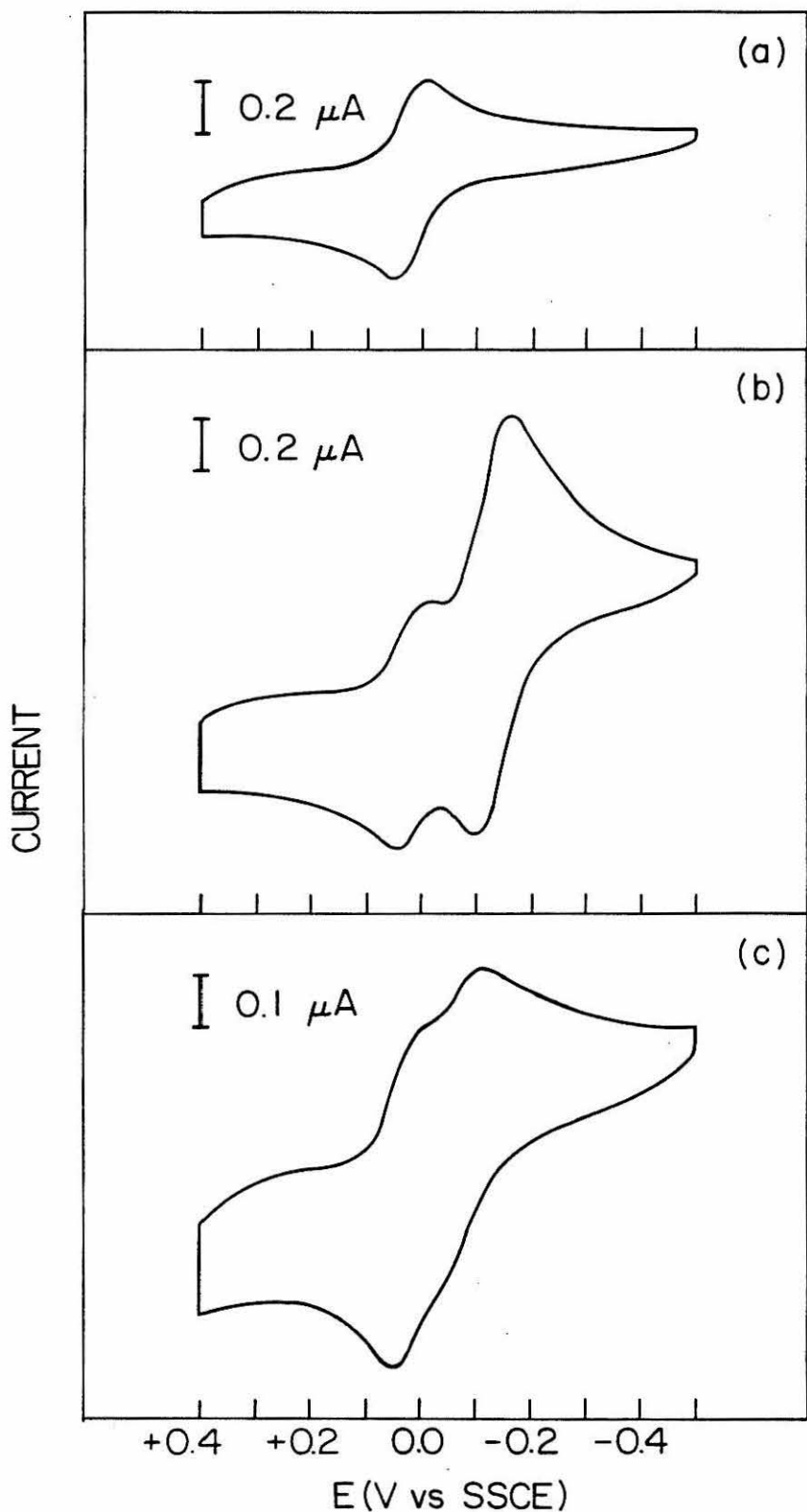


Figure 5.15. Dc cyclic voltammetry of $\text{Ru}(\text{NH}_3)_5$ -cytochrome *c* and related species. All species are in pH 7 phosphate buffer ($\mu = 0.05$ M) at a gold electrode, in the presence of 0.01 M 4,4'-bipyridyl. Scan rate 5 mV/sec. (a) Native cytochrome *c*, 0.21 mM. (b) Native cytochrome *c*, 0.21 mM, plus $[\text{Ru}(\text{NH}_3)_5\text{His}]\text{Cl}_3$, 0.21 mM. (c) $\text{Ru}(\text{NH}_3)_5$ -cytochrome *c* (peak E'), 0.12 mM.



cyclic voltammetry is also in good agreement with values previously determined by other techniques.^{33,34,49-51}

The final set of control experiments carried out prior to the examination of the modified protein employed an equimolar mixture of native cytochrome *c* and pentaammine-ruthenium complex. This was done to confirm that a wave due to a second one-electron species having a potential within 100-200 mV of cytochrome *c* could be resolved in the presence of the protein. A voltammogram of an equimolar mixture of native cytochrome *c* and $[\text{Ru}(\text{NH}_3)_5\text{His}]\text{Cl}_3$ is shown in Figure 5.15(b). The voltammogram shown is typical of a reversible two-component system.⁵² Both waves appear reversible and the individual species retain their characteristic redox potentials: for cytochrome *c*, $E_{\frac{1}{2}} = 19 \pm 1$ mV *vs.* SSCE (255 ± 1 mV *vs.* NHE), $E_{\text{pa}} - E_{\text{pc}} = 59 \pm 2$ mV; for $\text{Ru}(\text{NH}_3)_5\text{His}^{3+/2+}$, $E_{\frac{1}{2}} = -128 \pm 2$ mV *vs.* SSCE (108 ± 2 mV *vs.* NHE), $E_{\text{pa}} - E_{\text{pc}} = 60 \pm 2$ mV. The larger peak current of the $\text{Ru}(\text{NH}_3)_5\text{His}^{3+/2+}$ wave relative to the cytochrome *c* wave is a reflection of the fact that, when free in solution, the small ruthenium complex can diffuse more easily to the electrode than can the large protein molecule.

A cyclic voltammogram of $\text{Ru}(\text{NH}_3)_5$ -cytochrome *c* (E') at a gold electrode, in the presence of 4,4'-bipyridyl, is shown in Figure 5.15(c). Waves corresponding to both redox sites, the heme *c* and the $\text{Ru}(\text{NH}_3)_5(\text{His-33})$, are observed. In that both redox centers are present in equal concentrations, and

both are now protein bound, the peak currents attributable to each wave appear comparable. The midpoint potentials for the two sites obtained from the cyclic shown are: heme *c*, 21 mV *vs.* SSCE (257 mV *vs.* NHE); $\text{Ru}(\text{NH}_3)_5(\text{His-33})$, -85 mV *vs.* SSCE (151 mV *vs.* NHE). Cyclics were obtained on the derivative under varying conditions of current sensitivity and scan rate. The heme potential was in all cases between 18 and 23 mV *vs.* SSCE (255-259 mV *vs.* NHE) while the $\text{Ru}(\text{NH}_3)_5(\text{His-33})^{3+/2+}$ potential varied between -95 and -80 mV *vs.* SSCE (141-156 mV *vs.* NHE). The heme potential appears unperturbed by the presence of the $\text{Ru}(\text{NH}_3)_5$ group on the surface of the protein. The $\text{Ru}(\text{NH}_3)_5(\text{His-33})$ site, however, exhibits a midpoint potential considerably higher (40-50 mV) than the $[\text{Ru}(\text{NH}_3)_5\text{His}]\text{-Cl}_3$ model complex.

The $E_{\frac{1}{2}}$ values for $\text{Ru}(\text{NH}_3)_5$ -cytochrome *c* (*E'*), native cytochrome *c*, and the $\text{Ru}(\text{NH}_3)_5$ model complexes are summarized in Table 5.9. The values listed represent the average value (and standard deviation) obtained for the indicated species over a range of different current sensitivities and scan rates. Cyclic voltammetry was also carried out on the $\text{Ru}(\text{NH}_3)_5$ -cytochrome *c* species corresponding to peaks A' through C'. These results are discussed in Appendix 5.1.

The absence of 4,4'-bipyridyl did not affect the behavior of the ruthenium model complexes at the gold electrode. However, scans on native cytochrome *c* and $\text{Ru}(\text{NH}_3)_5$ -cytochrome *c* at a gold electrode were featureless upon removal of the bipyridyl reagent.

Table 5.9. $E_{1/2}$ Values for $\text{Ru}(\text{NH}_3)_5$ -Cytochrome *c* and Related Model Complexes Determined by Cyclic Voltammetry

Species ^a	$E_{1/2}^b$, (mV vs. NHE)	Cyt <i>c</i>	$E_{1/2}^b$, Ru (mV vs. NHE)
	Au ^c	Au ^c	CPE ^d
$\text{Ru}(\text{NH}_3)_5 \text{Im}^{3+/2+}$ ^e		105 ± 2	98 ± 1
$\text{Ru}(\text{NH}_3)_5 \text{His}^{3+/2+}$ ^e		106 ± 1	101 ± 1
cytochrome <i>c</i> ($\text{Fe}^{3+/2+}$) ^f	263 ± 3		
cytochrome <i>c</i> ^f + $\text{Ru}(\text{NH}_3)_5 \text{His}^{3+/2+}$ ^e	254 ± 1	108 ± 1	
cytochrome <i>c</i> ^f + $\text{Ru}(\text{NH}_3)_5 \text{His}^{3+/2+}$ ^e	255 ± 1	108 ± 1	
$\text{Ru}(\text{NH}_3)_5$ -cytochrome <i>c</i> (E') ^g	256 ± 2	148 ± 5	

^aIn sodium phosphate buffer, pH 7, $\mu = 0.05$ M; 0.1 M NaClO_4 . ^b $E_{1/2} = (E_{pc} + E_{pa})/2$.

^cGold electrode, 3 mm diameter; in the presence of 0.1 M 4,4'-bipyridyl.

^dCarbon paste electrode, 3 mm diameter. ^e[Ru] = 0.2 mM. ^f[cyt *c*] = 0.2 mM.

^g[Ru-Cyt *c*] = 0.12 mM.

Intermolecular Reduction of Ferricytochrome *c* by
 $\text{Ru}(\text{NH}_3)_5\text{Im}^{2+}$ and $\text{Ru}(\text{NH}_3)_5\text{His}^{2+}$

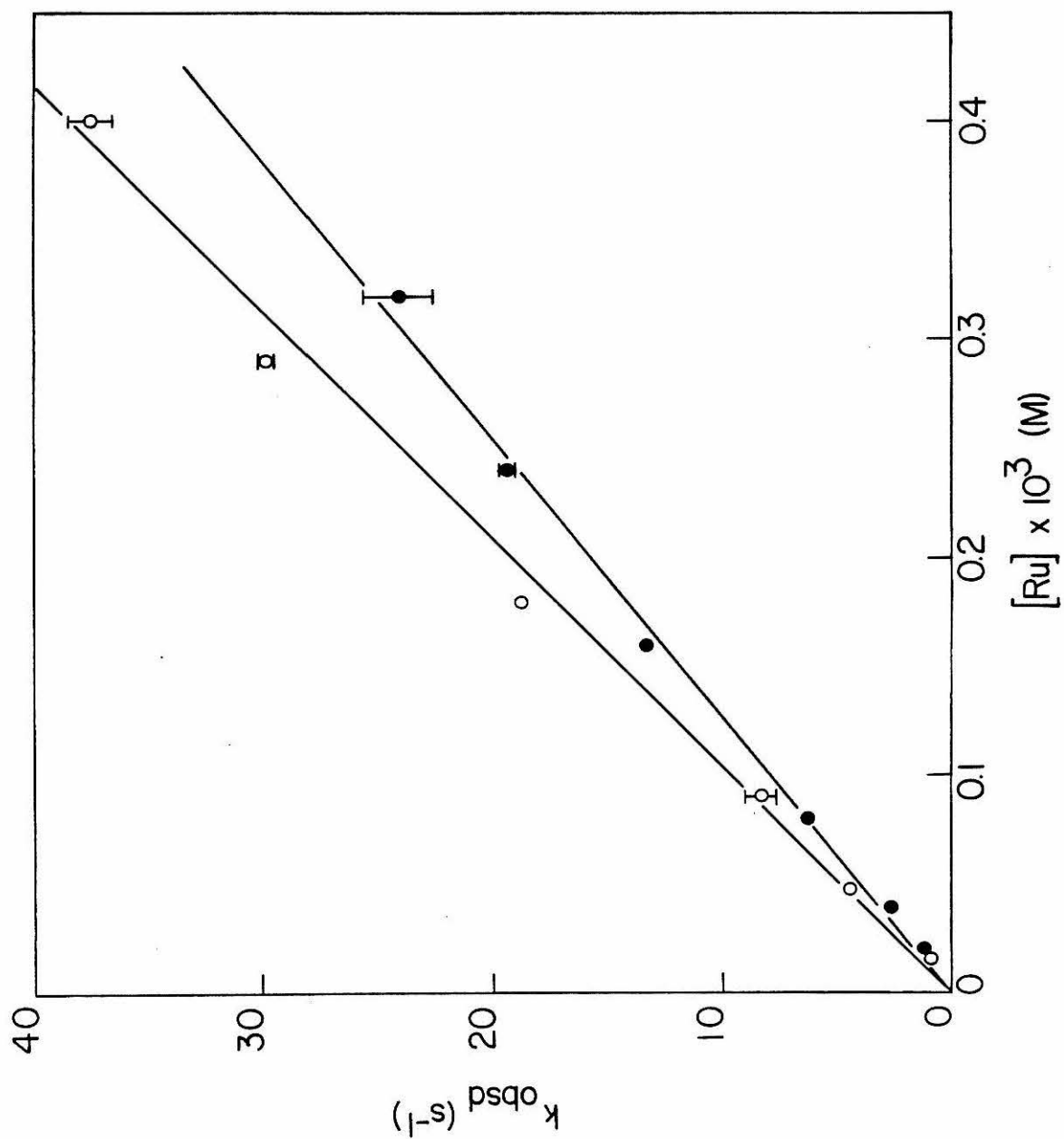
Prior to designing experiments to examine the intramolecular electron transfer reactivity of the $\text{Ru}(\text{NH}_3)_5$ -cytochrome *c* complex, it is important to characterize the intermolecular redox reactivity of the probe reagent with the protein. Although the $\text{Ru}(\text{NH}_3)_5(\text{His-33})$ site in the modified protein has a potential slightly higher than $\text{Ru}(\text{NH}_3)_5\text{Im}^{3+/2+}$ or $\text{Ru}(\text{NH}_3)_5\text{His}^{3+/2+}$, these complexes are still the best models available for studying the intermolecular reduction of cytochrome *c*.

First-order plots of absorbance *vs.* time data for the reduction of ferricytochrome *c* by $\text{Ru}(\text{NH}_3)_5\text{Im}^{2+}$ and $\text{Ru}(\text{NH}_3)_5\text{His}^{2+}$ were linear for greater than 90% of the reaction in all cases. The dependences of the observed first-order rate constants on ruthenium(II) concentration for these two reactions are shown in Figure 5.16. The rate law for the reduction of cytochrome *c* by the model complexes is therefore

$$\frac{-d[\text{cyt } c(\text{III})]}{dt} = k_{12} [\text{Ru}(\text{NH}_3)_5\text{L}^{2+}] [\text{cyt } c(\text{III})]$$

The second order rate constants (k_{12}) calculated from the concentration dependence data for the reduction of native ferricytochrome *c* are: $\text{Ru}(\text{NH}_3)_5\text{Im}^{2+}$, $1.05 (\pm 0.03) \times 10^5 \text{ M}^{-1} \text{ s}^{-1}$; $\text{Ru}(\text{NH}_3)_5\text{His}^{2+}$, $8.51 (\pm 0.10) \times 10^4 \text{ M}^{-1} \text{ s}^{-1}$ (25°C , pH 7 phosphate, $\mu = 0.10 \text{ M}$).

Figure 5.16. The dependences of the observed rate constants for the reduction of ferricytochrome *c* on the concentration of $\text{Ru}(\text{NH}_3)_5\text{L}^{2+}$ at 25°C, $\mu = 0.1$ M, pH 7.0 (phosphate): (o) $\text{Ru}(\text{NH}_3)_5\text{Im}^{2+}$; (●) $\text{Ru}(\text{NH}_3)_5\text{His}^{2+}$.



Eyring plots for these reactions are shown in Figure 5.17.

The activation parameters obtained from the fits of the temperature dependence data are: $\text{Ru}(\text{NH}_3)_5\text{Im}^{2+}$, $\Delta H^\ddagger = 1.3 (\pm 0.7)$ kcal/mol, $\Delta S^\ddagger = -32 (\pm 2)$ eu; $\text{Ru}(\text{NH}_3)_5\text{His}^{2+}$, $\Delta H^\ddagger = 0.19 (\pm 0.22)$ kcal/mol, $\Delta S^\ddagger = -36 (\pm 1)$ eu.

Electron transfer distances were calculated from k_{11}^∞ 's, the electrostatics-corrected protein self-exchange rates, by the methods outlined in Chapter 2. The results are given in Table 5.10, along with the relevant input parameters.

The E° values (vs. NHE) employed were: cytochrome *c*, 260 mV;¹⁰ $\text{Ru}(\text{NH}_3)_5\text{Im}^{3+/2+}$, 105 mV; $\text{Ru}(\text{NH}_3)_5\text{His}^{3+/2+}$, 105 mV. Values of the self-exchange rates for the ruthenium complexes were unavailable from the literature. The value for $\text{Ru}(\text{NH}_3)_6^{3+/2+}$ (similar coordination environment and charge), $3 \times 10^3 \text{ M}^{-1} \text{ s}^{-1}$,⁵³ was used in the calculations. This value probably represents a lower limit on the actual k_{22} in that the imidazole ring could facilitate electron exchange in the model complexes. The radius of the ruthenium complexes was estimated at 3.4 \AA (for $\text{Ru}(\text{NH}_3)_6^{2+}$, $r = 3.3 \text{ \AA}$;⁵³ for $\text{Ru}(\text{NH}_3)_5\text{py}^{3+}$, $r = 3.5 \text{ \AA}$ ⁵⁴).

The total intersite electron transfer distance, R , for these intermolecular reactions can be calculated from $R_p + R_r$.⁵⁵ Taking $R_r = 2 \text{ \AA}$ for the ruthenium complexes, total intersite distances (heme edge to imidazole edge of ruthenium complexes) of 5.2 and 5.4 \AA are estimated for the reduction of ferricytochrome *c* by $\text{Ru}(\text{NH}_3)_5\text{Im}^{2+}$ and $\text{Ru}(\text{NH}_3)_5\text{His}^{2+}$, respectively.

Figures 5.17. Eyring plots of the rate constant data for the reduction of ferricytochrome *c* (pH 7.0 phosphate, μ = 0.1 M): (o) $[\text{Ru}(\text{NH}_3)_5\text{Im}^{2+}] = 4.7 \times 10^{-5}$ M; (●) $[\text{Ru}(\text{NH}_3)_5\text{His}^{2+}] = 4.4 \times 10^{-5}$ M.

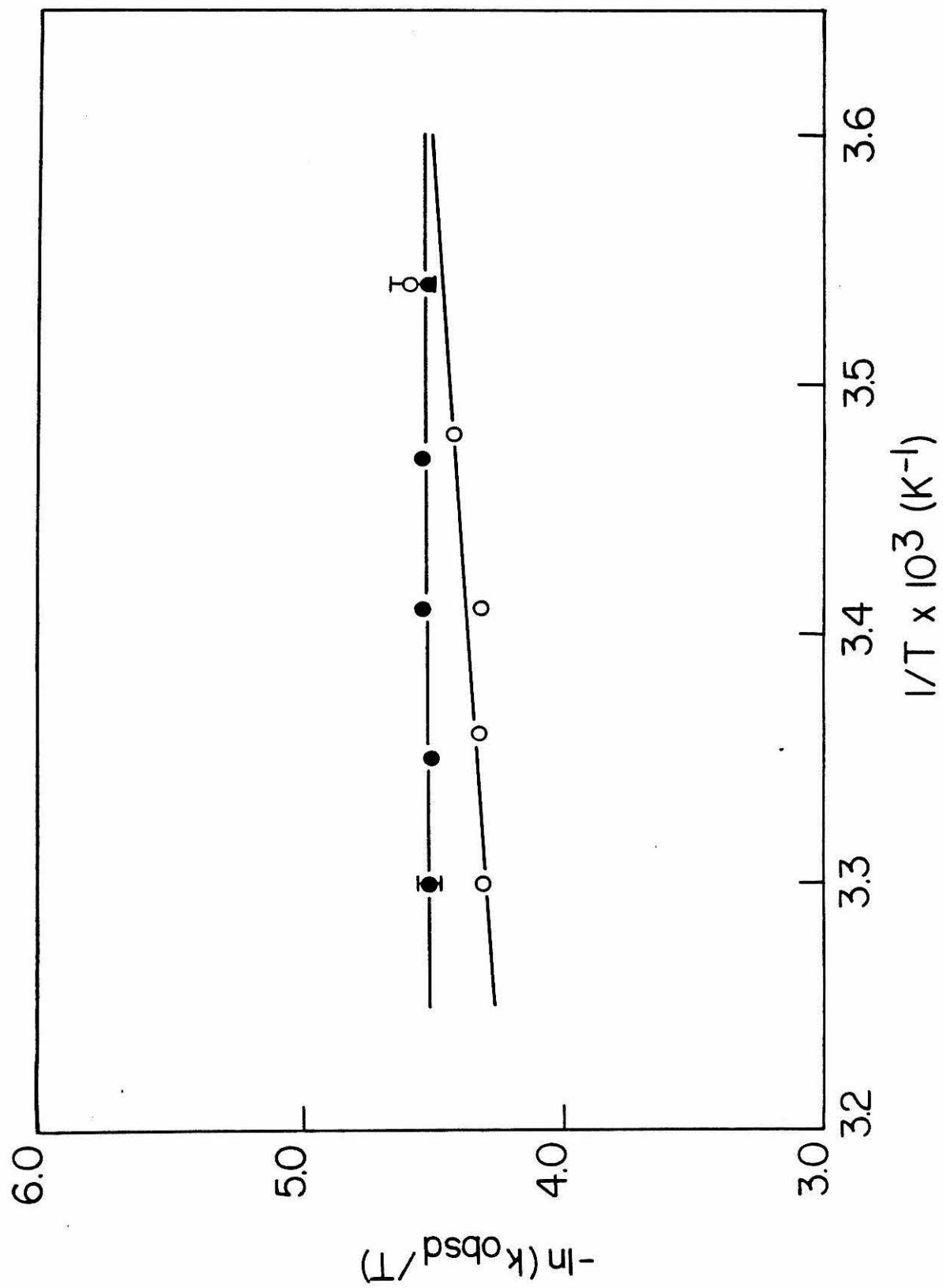


Table 5.10. Calculated Protein Self-Exchange Rate Constants and Electron Transfer Distances for the Reduction of Ferricytochrome *c* by $\text{Ru}(\text{NH}_3)_5\text{Im}^{2+}$ and $\text{Ru}(\text{NH}_3)_5\text{His}^{2+}$ ^a

Reagent	k_{12} ($\text{M}^{-1}\text{s}^{-1}$) ^b	ΔE_{12}° (V)	$R_1(\text{\AA})/R_2(\text{\AA})$	Z_1/Z_1'	Z_2/Z_2'
$\text{Ru}(\text{NH}_3)_5\text{Im}^{2+}$	1.05×10^5	0.155	$16.6/3.4$	$7.5/6.5$	2/3
$\text{Ru}(\text{NH}_3)_5\text{His}^{2+}$	8.51×10^4	0.155	$16.6/3.4$	$7.5/6.5$	2/3
Reagent	k_{12}^∞ ($\text{M}^{-1}\text{s}^{-1}$)	k_{22}^∞ ($\text{M}^{-1}\text{s}^{-1}$)	ΔE_{12}^∞ (V)	k_{11}^∞ ($\text{M}^{-1}\text{s}^{-1}$)	$R_p(\text{\AA})$
$\text{Ru}(\text{NH}_3)_5\text{Im}^{2+}$	2.98×10^5	7.92×10^4	0.147	4.78×10^3	3.2
$\text{Ru}(\text{NH}_3)_5\text{His}^{2+}$	2.41×10^5	7.92×10^4	0.147	3.13×10^3	3.4

^aSubscript 1 refers to protein, 2 to reagent. ^bAt 25°C in pH 7.0 phosphate, $\mu = 0.10$ M.

Intramolecular Reactivity of Ru(NH₃)₅-Cytochrome c

The most stable form of the Ru(NH₃)₅-modified cytochrome *c*, and hence, the form on which the characterization studies were carried out, is the Ru(NH₃)₅³⁺-ferricytochrome *c* species. The derivative designated E' possesses two redox sites, heme *c* and Ru(NH₃)₅(His-33), with reduction potentials of 260 mV and 150 mV (*vs.* NHE), respectively. Thus, in order to observe intramolecular electron transfer within this two-site system the species heme *c*(Fe³⁺)-Ru(NH₃)₅(His-33)²⁺ must be generated. One of several possible approaches to the generation, and subsequent observation, of this species was investigated. The preliminary results are described in Appendix 5.3.

DISCUSSION

The aquopentaammineruthenium(II) ion can be attached directly to the imidazole side chain of histidine-33 on the surface of horse heart cytochrome *c* by means of a simple substitution reaction. The reaction can be carried out under mild conditions-aqueous solution, pH 7, room temperature.

Owing to the incorporation of the +3 charge from $\text{Ru}(\text{NH}_3)_5^{3+}$, the reaction products are readily separated and purified by ion exchange chromatography. The $\text{Ru}(\text{NH}_3)_5\text{H}_2\text{O}^{2+}$ ion exhibited the properties deemed necessary for the production of a synthetic multisite metalloprotein: the modification reaction is specific; the products are stable with respect to dissociation; and the modification leaves intact the ability of the native protein active site, and the attached reagent, to function as redox active metal centers.

Model complex studies indicate that $\text{Ru}(\text{NH}_3)_5\text{H}_2\text{O}^{2+}$ should specifically label histidine and methionine residues on the surface of cytochrome *c*. (Although in other cases cysteine and lysine may be considered as potential ligands, the cysteines in cytochrome *c* are heme-bound, and the lysine side chains are positively charged at pH 7.) The reaction of $\text{Ru}(\text{NH}_3)_5\text{H}_2\text{O}^{2+}$ with horse heart cytochrome *c*, however, appears to be histidine-specific. The site of modification was identified by comparison of the high-pressure liquid chromatograms of the tryptic digests of the ruthenium-modified cytochrome *c* with the chromatogram of native cytochrome *c*. Although the two major mono- $\text{Ru}(\text{NH}_3)_5-$

cytochrome *c* species obtained (C' and E') had distinctly different ion exchange chromatographic properties, the HPLC results indicated that both were modified at His-33. The HPLC techniques used allowed the modified peptides to be isolated and examined by optical spectroscopy. It was thereby established that only one of the singly substituted derivatives (E') corresponded to the desired $\text{Ru}(\text{NH}_3)_5(\text{His-33})^{3+}$ complex of cytochrome *c*. The other singly substituted derivative (C') eluded further identification.

Cytochrome *c* possesses two histidines, His-26 and His-33, in addition to His-18 which acts as an axial ligand to the iron.¹⁰ The HPLC studies established that His-33 is the major site of $\text{Ru}(\text{NH}_3)_5$ modification. The presence of minor products in which His-26 is modified cannot be ruled out on the basis of the results presented, however, it is considered to be unlikely site for two reasons. First, structural studies have shown that His-26 is hydrogen bonded to the carbonyl group of residue 44.¹² The resultant inaccessibility of the imidazole side chain is reflected in its low pK_a (3.5 *vs.* 6.0 for free histidine),¹⁰ and in the fact that it has eluded modification by other histidine-specific reagents.¹³ Second, it has been shown that in phosphate medium, as was employed here, there is a phosphate binding site in the region of His-26-Lys-27.^{39,56} Taken together, these interactions would render His-26 quite unreactive toward $\text{Ru}(\text{NH}_3)_5\text{H}_2\text{O}^{2+}$.

Model complex studies also predict the formation of a stable complex between $\text{Ru}(\text{NH}_3)_5\text{H}_2\text{O}^{2+}$ and the thioether group of methionine.² Met-65 of cytochrome *c* lies on the surface of the protein and is readily modified by other methionine-specific reagents (*e.g.* bromoacetic acid, iodoacetic acid).¹³ In the reaction of cytochrome *c* with $\text{Ru}(\text{NH}_3)_5\text{H}_2\text{O}^{2+}$, however, there was no evidence to support the formation of a $\text{Ru}(\text{NH}_3)_5(\text{Met-65})$ complex. Although surprising, the inability to label methionine with $\text{Ru}(\text{NH}_3)_5\text{H}_2\text{O}^{2+}$ does not appear to be unique to cytochrome *c*. In the modification of the nonmetalloprotein ribonuclease A, Matthews found that $\text{Ru}(\text{NH}_3)_5\text{H}_2\text{O}^{2+}$ is also histidine-specific.^{24,57,58}

The reaction between $\text{Ru}(\text{NH}_3)_5\text{H}_2\text{O}^{2+}$ and imidazole is relatively rapid, $k^f = 2.0 \times 10^{-1} \text{ M}^{-1} \text{ s}^{-1}$.³ Although a rate constant could not be extracted from the modification studies, it was noted that the reaction between $\text{Ru}(\text{NH}_3)_5\text{H}_2\text{O}^{2+}$ and His-33 of cytochrome *c* was considerably slower. Several factors can be seen as contributing to this rate retardation. Histidine, when incorporated in a protein of molecular weight 12,400 is a considerably bulkier ligand than free imidazole. Interaction with only a small percentage of the total protein surface will be effective in producing a $\text{Ru}(\text{NH}_3)_5\text{His}^{2+}$ complex. The other important consideration is charge. Whereas the reaction between $\text{Ru}(\text{NH}_3)_5\text{H}_2\text{O}^{2+}$ and imidazole is between a positively charged species and a neutral ligand,

the reaction of cytochrome *c* with $\text{Ru}(\text{NH}_3)_5\text{H}_2\text{O}^{2+}$ is between two positively charged species. At pH 7 the net charge on ferrocyanocytocrome *c* is +6.5.³⁸ In that the modification reaction was performed at a relatively low ionic strength ($\mu = 0.1 \text{ M}$), the repulsive interactions between reactants could contribute significantly to the observed rate retardation relative to the model complexes. The extent to which charge interactions affect the incorporation of $\text{Ru}(\text{NH}_3)_5^{2+}$ into cytochrome *c* could be determined by studying the modification reaction as a function of ionic strength.

In addition to its specificity, a particularly attractive feature of the $\text{Ru}(\text{NH}_3)_5\text{H}_2\text{O}^{2+}$ ion as a protein modification reagent is the stability of the products which are formed. This feature allowed the oxidized reaction products to be properly separated, purified, and characterized. At pH 7 the purified $\text{Ru}(\text{NH}_3)_5(\text{His-33})^{3+}$ -ferricytochrome *c* complex could be stored for months at 4°C without loss of ruthenium. Furthermore, identification of the site of modification by HPLC was realized only as a result of the stability of the $\text{Ru}(\text{NH}_3)_5\text{His}^{3+}$ complex to the somewhat more demanding conditions of the tryptic hydrolysis procedure (37°C, pH 2-8). Although the long-term stability of the $\text{Ru}(\text{NH}_3)_5^{2+}$ -ferrocyanocytocrome *c* form of the His-33-modified derivative was not determined, it too should be quite stable with respect to dissociation (for $\text{Ru}(\text{NH}_3)_5\text{Im}^{2+}$, $k^d = 7 \times 10^{-8} \text{ s}^{-1}$).^{1,3} The stability of the $\text{Ru}(\text{NH}_3)_5$ -cytochrome *c* system contrasts

sharply with the $\text{Co}(\text{NH}_3)_5$ -cytochrome *c* and $\text{Fe}(\text{CN})_5$ -cytochrome *c* systems examined previously; both these complexes were particularly unstable in the reduced form.

Spectral and electrochemical studies on the $\text{Ru}(\text{NH}_3)_5$ -
(His-33)-cytochrome *c* complex established that both metal centers in this synthetic two-site system retain their redox reactivity. It is indeed unlikely that modification of an amino acid side chain on the surface of cytochrome *c*, 15 Å away from the heme prosthetic group, would disrupt the conformation of the protein in the heme *c* region. And, indeed, the UV-visible spectrum of the ruthenium-modified protein is indistinguishable from that of native cytochrome *c*. In particular, the 695-nm absorption band is observed in the modified species. This band is sensitive not only to the presence of the Met-80-iron linkage, but also to the conformation of the protein in the region of the heme.⁴³ The integrity of the heme redox site in $\text{Ru}(\text{NH}_3)_5^{3+}$ -cytochrome *c* was further established by spectroelectrochemical measurements. The heme redox potential of the modified protein (270 mV *vs.* NHE) is essentially the same as that of the native protein (260 mV¹⁰).

Owing to the inability to detect the low intensity absorption bands of the $\text{Ru}(\text{NH}_3)_5(\text{His-33})^{3+}$ site in the presence of the cytochrome *c* absorptions, it was not possible to determine the redox potential of the ruthenium site spectroelectrochemically. The methodology developed by

Hill³⁶ for obtaining cyclic voltammograms of native cytochrome *c* proved particularly useful for the ruthenium-modified cytochrome *c*. At a gold electrode, in the presence of 4,4'-bipyridyl, the redox potential of the heme site, as well as that of the $\text{Ru}(\text{NH}_3)_5(\text{His-33})^{3+/2+}$ site, was determined. The heme potential of the derivative (255 mV) was in good agreement with the potential of native cytochrome *c* under the same conditions (0.263 V), and in fairly good agreement with the potential of the derivative's heme site determined spectroelectrochemically (270 mV).

A potential of about 150 mV was determined for the ruthenium site by cyclic voltammetry. The model complex $\text{Ru}(\text{NH}_3)_5\text{His}^{3+/2+}$ has a reduction potential of 106 mV under the same conditions. The difference between the model complex potential and the potential of the $\text{Ru}(\text{NH}_3)_5\text{His}^{3+/2+}$ site on cytochrome *c* must arise from the environment imposed on the complex by the protein. The protein environment can have significant effects on the redox potential of a metal center. For example, both horse heart cytochrome *c* and *Rhodospirillum rubrum* cytochrome *c*₂ have a heme chromophore (protoheme IX) with methionine and histidine as axial ligands, yet their redox potentials differ by 60 mV.⁵⁹ There is not total agreement in the literature as to which factors determine the redox potential of a given type of metal center in a protein environment. The hydrophobicity of the environment about the redox site,^{60,61} the extent to

which the metal center is exposed,⁶² and the nature of the hydrogen bonding about the active site^{63,64} are among the factors that have been correlated with variations in the redox potential of heme proteins. Similar considerations could be invoked to explain the difference between the redox potential of the protein-bound $\text{Ru}(\text{NH}_3)_5(\text{His-33})$ group and the simple model complex. The principal determinant of the observed discrepancy cannot be established, however, with the information presently available on this system.

The synthesis and characterization studies presented herein firmly establish the utility of the aquopentaammine-ruthenium(II) ion as a redox active protein modification reagent. In its reaction with cytochrome *c* the major singly substituted $\text{Ru}(\text{NH}_3)_5^{3+}$ -cytochrome *c* derivative is a stable complex with the $\text{Ru}(\text{NH}_3)_5^{3+}$ moiety attached to N-3 of His-33, approximately 15 Å from the heme edge. Both the heme site and the $\text{Ru}(\text{NH}_3)_5(\text{His-33})^{3+/2+}$ site remain redox active in the modified protein. In that the specificity of the modification reaction is derived simply from the strong affinity of $\text{Ru}(\text{NH}_3)_5\text{H}_2\text{O}^{2+}$ for imidazole groups, the utility of this reagent is not limited to the modification of cytochrome *c*. Any metalloprotein possessing surface histidines could conceivably be converted to a well-characterized multisite protein by employing the synthetic, purification, and characterization procedures developed here

for cytochrome *c*. Continuation of the electron transfer studies begun here on the Ru(NH₃)₅-cytochrome *c* system, coupled with similar studies on a variety of new Ru(NH₃)₅³⁺-modified metalloproteins, will make possible a more critical assessment of rate-distant relationships in biological electron transfer.

Appendix 5.1. Further Characterization of the $\text{Ru}(\text{NH}_3)_5^-$ Cytochrome *c* Species Corresponding to Peaks A' through D'

CM-cellulose ion exchange chromatography of the products obtained from the reaction of $\text{Ru}(\text{NH}_3)_5\text{H}_2\text{O}^{2+}$ with cytochrome *c* gave five major species (Figure 5.5). After purification of the individual peaks by rechromatography on CM-cellulose the species were designated A' through E'. The ruthenium content of peaks A' through D', as determined by atomic absorption (Table 5.4), appeared inconsistent with the chromatographic behavior of the species. Peak E', however, appeared well-behaved and was further identified as a mono- $\text{Ru}(\text{NH}_3)_5^{3+}$ -cytochrome *c* species with the $\text{Ru}(\text{NH}_3)_5^{3+}$ group attached to His-33. Herein is reported the HPLC and cyclic voltammetry results obtained on peaks A'-D' in an attempt to further characterize these species.

Peaks A' through D' were digested with trypsin and the resultant peptides separated by HPLC. The separations were monitored at 220 nm and 300 nm; the chromatograms are shown in Figures 5.18 and 5.19, respectively. The chromatograms of native cytochrome *c* and peak E' are included for comparison. In Figure 5.8 the peaks of interest are labeled by the appropriate letter (N = native, A = peak A', etc.) and an HPLC peak number. Peaks with analogous elution positions are given the same peak number throughout. In Figure 5.19 only peaks at positions 1 and 2 are observed at 300 nm and

Figure 5.18. Reversed-phase HPLC of tryptic digests of native cytochrome *c* (N) and Ru(NH₃)₅-cytochromes *c* (A', B', C', D', E') at 220 nm (1.0 AUFS). In each case a 2-mg sample of hydrolyzed protein was chromatographed with a linear gradient between 0 and 45% acetonitrile in pH 2.85 phosphate buffer. Fractions corresponding to peaks in the region of interest were pooled as shown by the horizontal bars and numbered in the order of elution. Peaks with analogous elution positions are given the same peak number throughout.

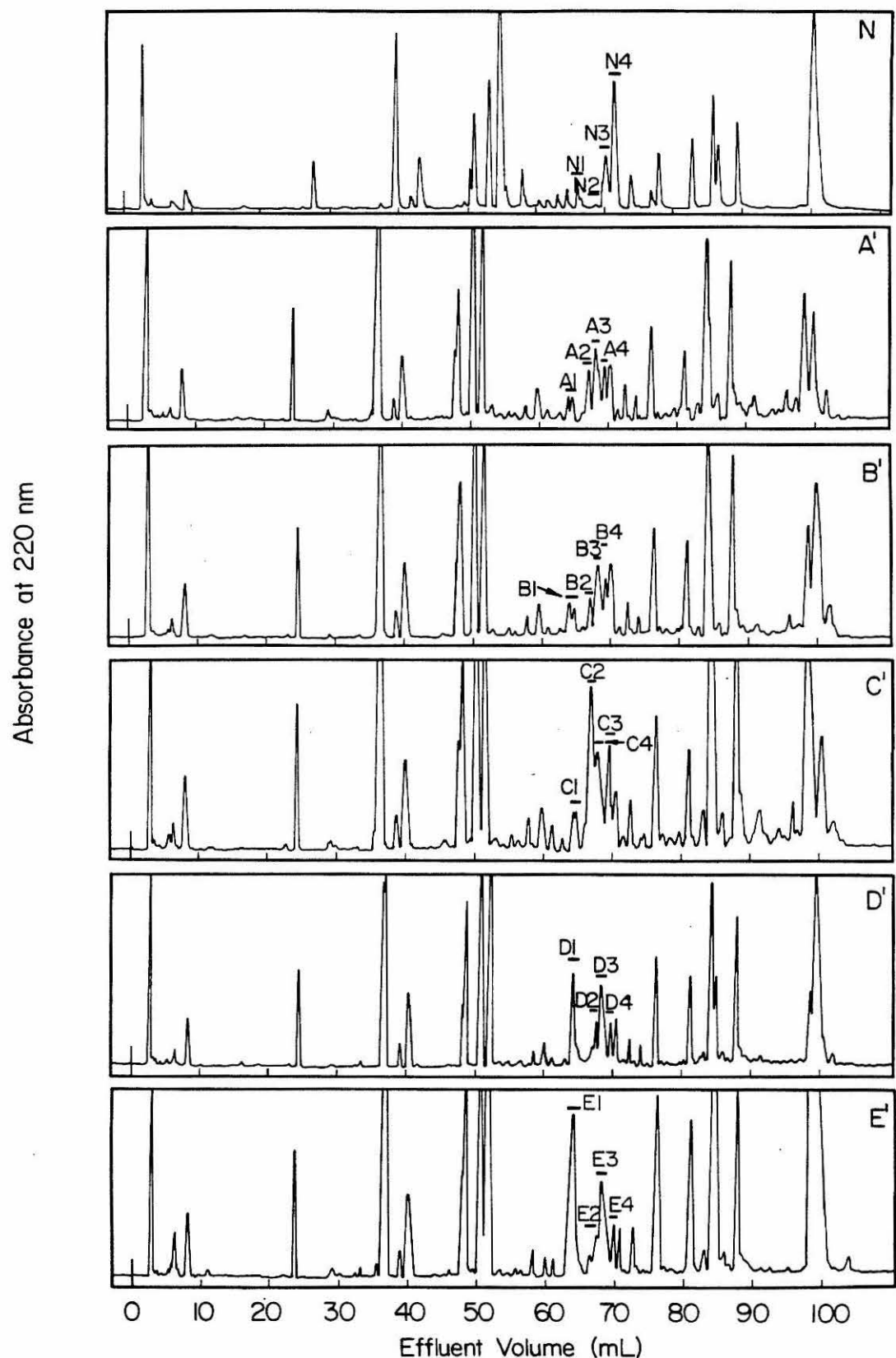
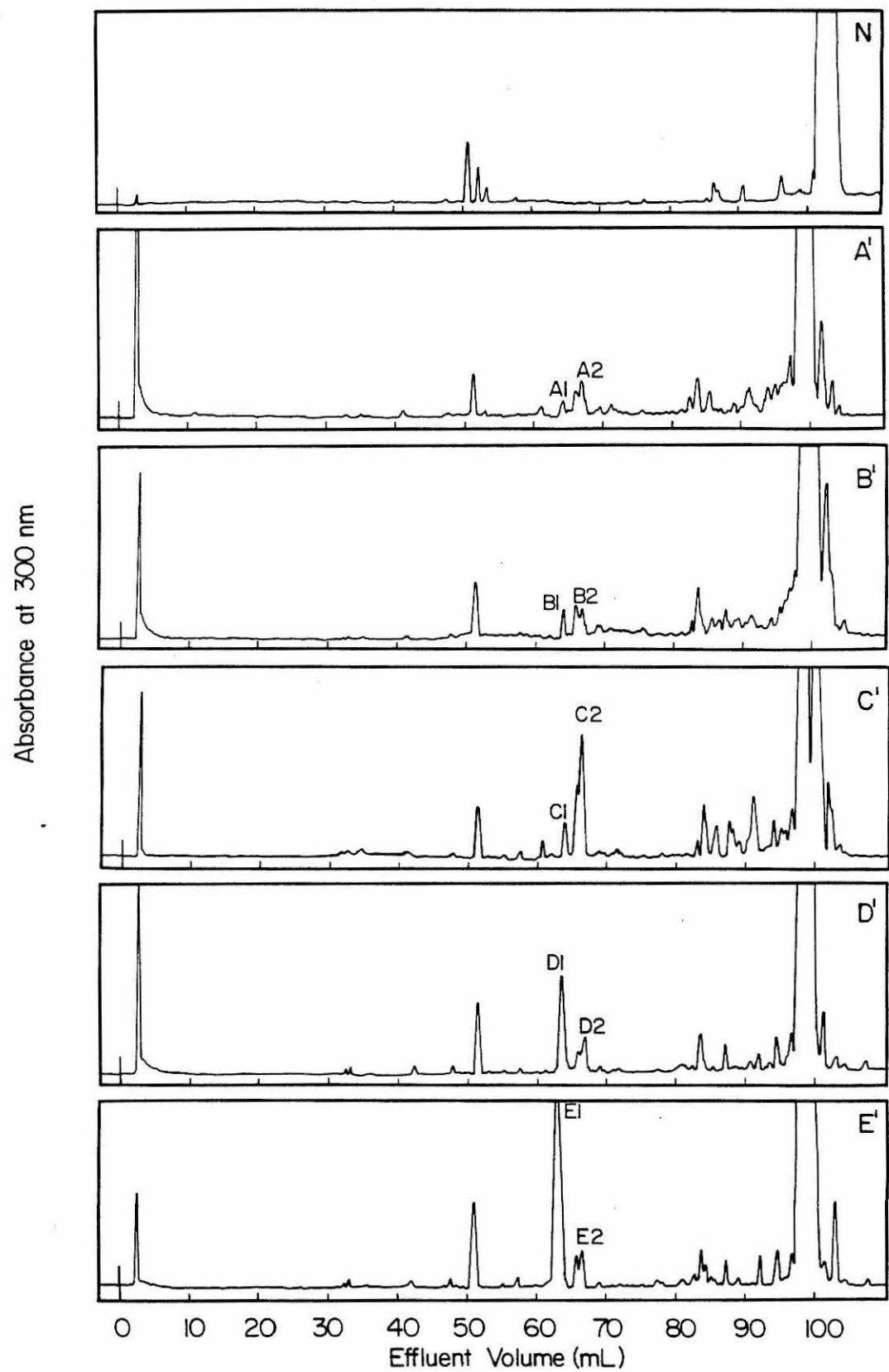


Figure 5.19. Reversed-phase HPLC of tryptic digests of native cytochrome *c* (N) and Ru(NH₃)₅-cytochromes *c* (A', B', C', D', E') at 300 nm (0.1 AUFS). In each case a 2-mg sample of hydrolyzed protein was chromatographed with a linear gradient between 0 and 45% acetonitrile in pH 2.85 phosphate buffer. Peaks of interest are labeled with the designations given to the analogous peaks in the 220-nm chromatograms (Figure 5.18).



are labeled appropriately. Amino acid analyses were carried out on peaks A2-A4 and C1-C4. The peptides found to be present in each peak are summarized in Table 5.11, along with data on the native and E' peaks.

Cyclic voltammograms were obtained on species A', B', and C' at a gold electrode in the presence of 0.01 M 4,4'-bipyridyl (0.1 M NaClO₄, pH 7 phosphate buffer, $\mu = 0.05$ M). In the region examined, -0.4 to +0.5 V *vs.* SSCE, the voltammograms were all indistinguishable from those of native cytochrome *c* under the same conditions.

The HPLC profiles (Figure 5.18 and 5.19), amino acid analyses (Table 5.11), cyclic voltammetry results, and atomic absorption analyses (Table 5.4) taken together still do not allow peaks A' through D' to be definitively identified. These additional characterization studies also fail to provide an explanation for the peculiar relationship between the elution order and ruthenium content of these peaks. The current understanding of the nature of species A'-D' obtained from these studies is, however, summarized below for completeness.

Species A' and B' are only somewhat perturbed in the T7 peptide (His-33) region of the HPLC. The 300-nm chromatograms, as well as the absence of a characteristic Ru(NH₃)₅His^{3+/2+} wave in the cyclic voltammograms, indicates that A' and B' are not significantly modified with Ru(NH₃)₅³⁺ at His-33. Bound ruthenium was found to be

Table 5.11. Identification of Selected HPLC Peaks by Amino Acid Analysis

Identity and quantity (μmol) of tryptic peptides contained in designated HPLC peaks (Figure 5.18) ^a					
Species ^b		1	2	3	4
N	T16 (.006)			T13 (.020)	T7 (.029)
A'		C		T13 (.035)	C
C'	T7-Lys (.005)		T7-Lys (.033)	T13 (.064)	T15-16-17-Lys (.016)
T16 (.008)			T16 (.015)		T7 (.005)
			T13 (.006)		
E'	T7 (.037)		T7 (.011)	T13 (.063)	T15-16-17 (.01)
				T13-Lys (.008)	

^aTryptic peptide numbering system corresponds to that given in Figure 5.7.

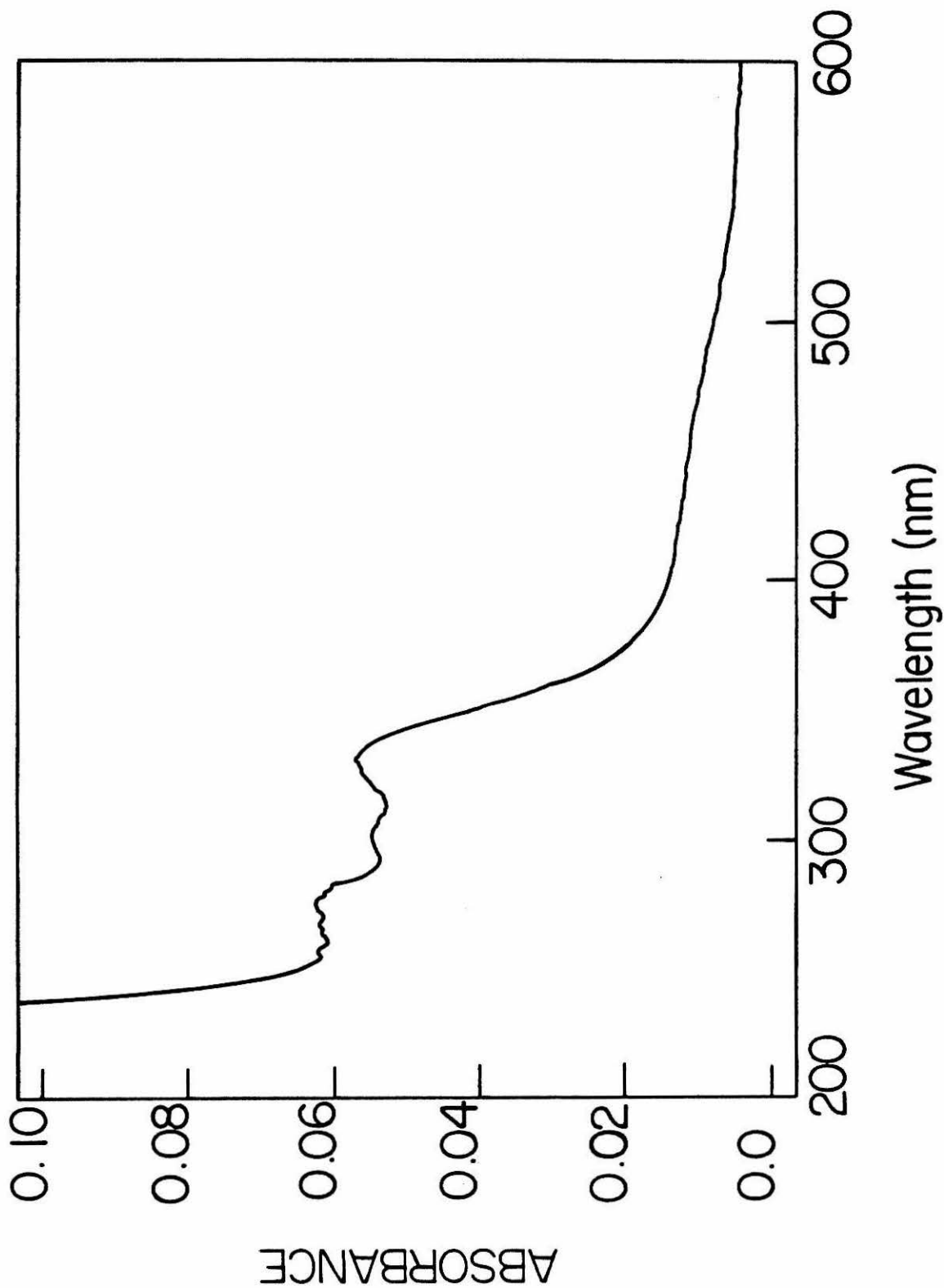
^bN = native cyt c; A', B', C' are Ru-modified species eluted from CM-cellulose (Figures 5.5 and 5.6). Amino acid composition could not be readily fit to a given tryptic peptide or simple mixture of peptides.

present in significant amounts in A' and B' by atomic absorption. The location and form of that bound ruthenium could not be discerned from these experiments. The failure to locate this bound ruthenium could suggest that the interactions between the ruthenium and protein in these species is disrupted by the tryptic hydrolysis procedures, releasing the free ruthenium prior to HPLC. Alternatively, if the ruthenium is attached to one of the small peptides which elutes with the solvent front (T2, T5, T6, T9), the attachment site would go undetected by these procedures.

Species D' is much like E' in that it appears to contain a significant amount of $\text{Ru}(\text{NH}_3)_5^{3+}$ attached to His-33. The UV-visible spectrum of HPLC peak D1 is consistent with this assignment. A cyclic voltammogram of D' was not obtained owing to the low yield. Again, the location and form of the additional bound ruthenium, determined to be present by atomic absorption, could not be identified by these experiments.

Species C' is unique. Atomic absorption indicates that it has slightly greater than one bound ruthenium per cytochrome *c*. The HPLC work shows that T7 is the major site of modification. The remaining evidence, however, is inconsistent with a simple $\text{Ru}(\text{NH}_3)_5(\text{His-33})^{3+}$ -type complex. No waves attributable to the ruthenium species were present in the cyclic voltammogram between -0.4 and +0.5 V *vs.* SSCE. The UV-visible spectrum of HPLC peak C2 is shown in Figure 5.20. Absorption bands are observed at 300 and 450 nm,

Figure 5.20. UV-visible spectrum of the His-33-containing peptide, T7, of $\text{Ru}(\text{NH}_3)_5$ -cytochrome *c* (C'), isolated by tryptic hydrolysis and HPLC (peak C2 in Figure 5.19); pH 3.



as in $\text{Ru}(\text{NH}_3)_5\text{His}^{3+}$, but the predominant feature is a band at 330 nm. Although it appears that the ruthenium may be bound to His-33 in species C', the exact nature of the ruthenium complex which gives rise to the observed properties is not obvious from these experiments.

Appendix 5.2. Supplementary Data. First-Order Rate Constants for the Reduction of Ferricytochrome *c* by $\text{Ru}(\text{NH}_3)_5\text{Im}^{2+}$ and $\text{Ru}(\text{NH}_3)_5\text{His}^{2+}$ ^a

Reagent	T(°C) ^b	[Ru(II)] $\times 10^4$ (M)	k_{obsd} (s ⁻¹) (S.D.)
$\text{Ru}(\text{NH}_3)_5\text{Im}^{2+}$	25.0	0.16	0.78 (0.18)
		0.48	4.37 (0.17)
		0.92	8.23 (0.71)
		1.8	18.7 (0.3)
		2.9	29.8 (0.4)
		4.0	37.5 (1.0)
	30.0	0.47	4.09 (0.12)
	24.9	0.47	3.97 (0.07)
	19.7	0.47	3.92 (0.09)
	14.5	0.47	3.46 (0.09)
	9.4	0.47	2.89 (0.23)
$\text{Ru}(\text{NH}_3)_5\text{His}^{2+}$	25.0	0.21	1.11 (0.03)
		0.40	2.51 (0.08)
		0.81	6.24 (0.02)
		1.6	13.2 (0.2)
		2.4	19.3 (0.4)
		3.2	24.1 (1.6)
	30.1	0.44	3.33 (0.14)
	25.1	0.44	3.31 (0.07)
	19.9	0.44	3.12 (0.08)
	14.7	0.44	3.07 (0.08)
	9.7	0.44	3.08 (0.07)

^aIn pH 7.0 phosphate buffer, $\mu = 0.10$ M. ^b $\pm 0.1^\circ\text{C}$.

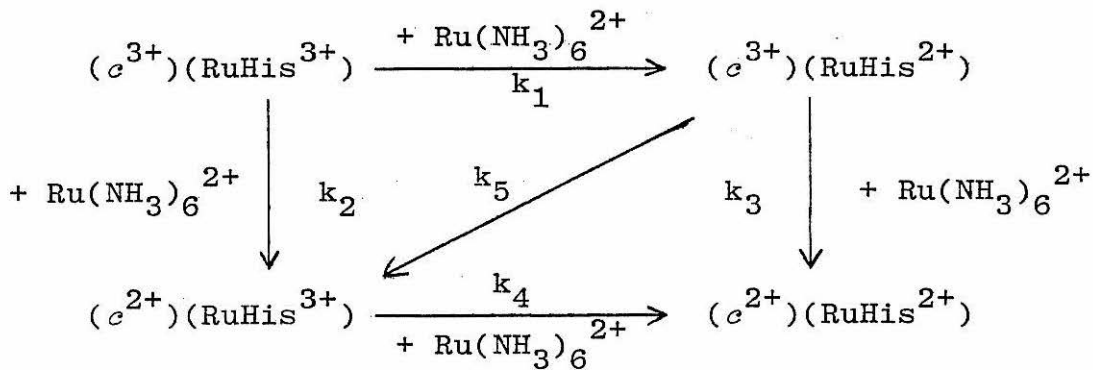
Appendix 5.3. Preliminary Investigation of the Intramolecular Reactivity of $\text{Ru}(\text{NH}_3)_5$ -Cytochrome *c*.

One approach to the generation of the reactive mixed-valence species $\text{Ru}(\text{NH}_3)_5(\text{His-33})^{2+}$ -ferricytochrome *c* (for simplicity, $(\text{c}^{3+})(\text{RuHis}^{2+})$) is the reaction of the totally oxidized derivative with an external reductant. The ideal situation is one in which an external redox reagent is found which will rapidly, and selectively, reduce the RuHis^{3+} site of $(\text{c}^{3+})(\text{RuHis}^{3+})$ to generate $(\text{c}^{3+})(\text{RuHis}^{2+})$. In that such selectivity appeared unattainable, a reductant was sought which reacted significantly faster with the RuHis^{3+} site than the c^{3+} site. Work was initiated on the reduction of $\text{Ru}(\text{NH}_3)_5^{3+}$ -ferricytochrome *c* (E') by $\text{Ru}(\text{NH}_3)_6^{2+}$.

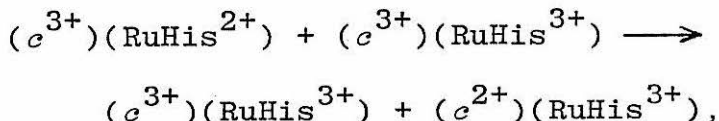
In order to obtain an estimate of the rate of reduction of the $\text{Ru}(\text{NH}_3)_5(\text{His-33})^{3+}$ site by $\text{Ru}(\text{NH}_3)_6^{2+}$, the reduction of the model complexes, $\text{Ru}(\text{NH}_3)_5\text{Im}^{3+}$ and $\text{Ru}(\text{NH}_3)_5\text{His}^{3+}$, by $\text{Ru}(\text{NH}_3)_6^{2+}$ was examined. Although the rates proved too fast for accurate determination with our stopped-flow apparatus, an estimate of $k > 10^4 \text{ M}^{-1} \text{ s}^{-1}$ was obtained. In the case of the protein-bound $\text{Ru}(\text{NH}_3)_5\text{His}^{3+}$ group, the driving force for reduction by $\text{Ru}(\text{NH}_3)_6^{2+}$ is greater than that for the model complexes (81 mV *vs.* 38 mV). On the other hand, the protein-bound $\text{Ru}(\text{NH}_3)_5\text{His}^{3+}$ group has reduced accessibility and increased positive charge (from the surrounding protein) working against it. Although

unpredictable, it is unlikely that the rate of reduction of the $\text{Ru}(\text{NH}_3)_5(\text{His-33})^{3+}$ site by $\text{Ru}(\text{NH}_3)_6^{2+}$ is significantly faster than the heme reduction rate, as desired. Recall the rate of native cytochrome *c* reduction by $\text{Ru}(\text{NH}_3)_6^{2+}$ is $6.7 \times 10^4 \text{ M}^{-1} \text{ s}^{-1}$. This rate should apply to modified cytochrome *c* as well, in that the heme site appears unperturbed.

The scheme shown below summarizes the processes involved in the $\text{Ru}(\text{NH}_3)_6^{2+}$ reduction of $\text{Ru}(\text{NH}_3)_5^{3+}$ -ferricytochrome *c*:



In addition to the reactions shown, intermolecular reactions between modified protein molecules must also be considered, *i.e.*,



etc. The reaction between the model complex, $\text{Ru}(\text{NH}_3)_5\text{His}^{2+}$ and ferricytochrome *c* establishes an upper limit on the rate constant for this process, *i.e.*, $k = 8.5 \times 10^4 \text{ M}^{-1} \text{ s}^{-1}$.

The interprotein reaction should be slower than this owing to the fact that, once protein-bound, the $\text{Ru}(\text{NH}_3)_5(\text{His-33})^{2+}$ site is in a less accessible, more highly charged environment, and also has a higher redox potential. Furthermore, the rate of interprotein reactions can be minimized by working at low protein concentrations.

The reduction of $\text{Ru}(\text{NH}_3)_5^{3+}$ -ferricytochrome *c* by $\text{Ru}(\text{NH}_3)_6^{2+}$ was studied as a function of $\text{Ru}(\text{NH}_3)_6^{2+}$ concentration (0.025 - 0.20 mM) at a modified protein concentration of 0.004 mM (pH 7.0, μ = 0.10 M, 25°C). Using the stopped-flow spectrophotometer the reduction of the heme *c* site was monitored at 550 nm. Under pseudo-first-order conditions, the observed rate of reduction of the heme site should be essentially the same as that observed for native cytochrome *c* in the event that the reduction of the $\text{Ru}(\text{NH}_3)_5(\text{His-33})^{3+}$ site has no perturbing influence on the system. If, however, the reduction of $\text{Ru}(\text{NH}_3)_5(\text{His-33})^{3+}$ affects the redox properties of the heme, or if the intra- and/or intermolecular electron transfer between $\text{Ru}(\text{NH}_3)_5(\text{His-33})^{2+}$ and heme *c*³⁺ is relatively rapid, the observed reduction of the heme *c* site will not be strictly first-order.

First-order plots of the absorbance *vs.* time data for the reduction of $\text{Ru}(\text{NH}_3)_5^{3+}$ -ferricytochrome *c* by $\text{Ru}(\text{NH}_3)_6^{2+}$ were nonlinear. The observed reduction process was rapid. Based on half-lives alone, at a given concentration of

$\text{Ru}(\text{NH}_3)_6^{2+}$, the reduction of the modified protein was approximately five times more rapid than the reduction of native cytochrome *c*. Although the rate of reduction was consistently higher than that of native cytochrome *c*, the day-to-day reproducibility of the data for the ruthenium-modified protein was not good. This was due, in part, to the low signal-to-noise ratio obtained for these rapid reactions. Further manipulation of the kinetic data was precluded on the basis of its poor quality.

No conclusions concerning the intramolecular rate of electron transfer in the $\text{Ru}(\text{NH}_3)_5$ -cytochrome *c* system can be drawn on the basis of this cursory examination of its reactivity. It is encouraging, however, that the presence of the attached $\text{Ru}(\text{NH}_3)_6^{3+}$ center significantly alters the reactivity of the cytochrome *c*. The kinetic scheme applicable to this system is admittedly complex. $\text{Ru}(\text{NH}_3)_6^{2+}$ is clearly not the ideal reagent for pursual of this approach. Reagents should be sought which tend to favor the kinetic pathways leading to the generation of $(c^{3+})(\text{RuHis}^{2+})$. The reduction of $\text{Ru}(\text{NH}_3)_5^{3+}$ -ferricytochrome *c* could be further probed with reagents such as $\text{Ru}(\text{EDTA})^{2-}$ and $\text{Fe}(\text{HEDTA})^-$. Alternatively, the oxidation of the fully reduced $\text{Ru}(\text{NH}_3)_5^{2+}$ -ferrocytochrome *c* species by external oxidants (*e.g.*, $\text{Co}(\text{phen})_3^{3+}$, $\text{Ru}(\text{NH}_3)_5\text{py}^{3+}$) could be examined.

REFERENCES AND NOTES

1. Sundberg, R.J.; Bryan, R.F.; Taylor, I.F., Jr.; Taube, H. *J. Am. Chem. Soc.* 1974, 96, 381.
2. Kuehn, C.G.; Taube, H. *J. Am. Chem. Soc.* 1976, 98, 689.
3. Shepherd, R.E.; Taube, H. *Inorg. Chem.* 1973, 12, 1392.
4. Stein, C.A.; Taube, H. *Inorg. Chem.* 1979, 18, 1168.
5. Sundberg, R.J.; Gupta, G. *Bioinorg. Chem.* 1973, 3, 39.
6. Matsurbara, T.; Creutz, C. *Inorg. Chem.* 1979, 18, 1956.
7. Brown, G.M.; Sutton, J.E.; Taube, H. *J. Am. Chem. Soc.* 1978, 100, 2767.
8. Yee, E.L.; Cave, R.J.; Guyer, K.L.; Tyma, P.D.; Weaver, M.J. *J. Am. Chem. Soc.* 1979, 101, 1131.
9. Kuehn, C.G.; Isied, S.S. *Prog. Inorg. Chem.* 1980, 27, 153.
10. Dickerson, R.E.; Timkovich, R. In "The Enzymes", 3rd ed.; Boyer, P.D., Ed.; Academic Press: New York, 1975; Vol. 11, Chapter 7.
11. Distances estimated from examination of molecular models of tuna cytochrome *c*.
12. Dickerson, R.E.; Takano, T.; Eisenberg, D.; Kallai, O.B.; Samson, L.; Cooper, A.; Margoliash, E. *J. Biol. Chem.* 1971, 246, 1511.
13. Ferguson-Miller, S.; Brautigan, D.L.; Margoliash, E. In "The Porphyrins"; Dolphin, D., Ed.; Academic Press: New York, 1979; Vol. VII, Chapter 4.
14. Vogt, L.H., Jr.; Katz, J.L.; Wiberley, S.E. *Inorg. Chem.* 1965, 4, 1157.

15. Ford, P.; Rudd, D.P.; Gaunder, R.; Taube, H. *J. Am. Chem. Soc.* 1968, 90, 1187.
16. Lever, F.M.; Powell, A.R. *J. Chem. Soc. (A)* 1969, 1477.
17. Schlit, A.A.; Taylor, R.C. *J. Inorg. Nucl. Chem.* 1959, 9, 211.
18. Meites, L.; Meites, T. *Anal. Chem.* 1948, 20, 984.
19. Shriver, D.F. "The Manipulation of Air Sensitive Compounds"; McGraw-Hill: New York, 1969; p. 199.
20. Sweetser, P.B. *Anal. Chem.* 1967, 39, 979.
21. Callahan, R.W.; Brown, G.M.; Meyer, T.J. *Inorg. Chem.* 1975, 14, 1443.
22. Ford, P.C.; Kuempel, J.R.; Taube, H. *Inorg. Chem.* 1968, 7, 1976.
23. Brautigan, D.L.; Ferguson-Miller, S.; Margoliash, E. *Methods Enzymol.* 1978, 53, 128.
24. Matthews, C.R.; Erickson, P.M.; Van Vliet, D.L.; Perersheim, M. *J. Am. Chem. Soc.* 1978, 100, 2260.
25. Van Gelder, B.F.; Slater, E.C. *Biochim. Biophys. Acta* 1962, 58, 593.
26. Adler, A.D.; George, P. *Anal. Biochem.* 1965, 11, 159.
27. Cameron, B.F. *Anal. Biochem.* 1965, 11, 164.
28. Kodama, K. "Methods of Qualitative Inorganic Analysis"; Wiley: New York, 1963; p. 240.
29. Sasak, Y. *Anal. Chim. Acta* 1978, 98, 335.
30. Rowston, W.B.; Ottaway, J.M. *Anal. Lett.* 1970, 3, 411.

31. Mallett, R.C.; Pearson, D.C.G.; Ring, E.J.; Steele, T.W. *Talanta* 1972, 19, 181.
32. Stanford University Analytical Laboratory, personal communication, 1980.
33. Heineman, W.R.; Norris, B.J.; Goelz, J.F. *Anal. Chem.* 1975, 47, 79.
34. Taniguchi, V.T.; Sailasuta-Scott, N.; Anson, F.C.; Gray, H.B. *Pure & Appl. Chem.* 1980, 52, 2275.
35. Taniguchi, V.T.; Ellis, W.R., Jr.; Camarata, V.; Webb, J.; Anson, F.C.; Gray, H.B. In "Electrochemistry and Spectrochemistry of Biological Redox Components"; Kadish, K., Ed.; Advances in Chemistry Series; American Chemical Society: Washington, D.C., in press.
36. Eddowes, M.J.; Hill, H.A.O. *J. Am. Chem. Soc.* 1979, 101, 4461.
37. Ives, D.J.G.; Janz, G.F. "Reference Electrodes"; Academic Press: New York, 1961.
38. Wherland, S.; Gray, H.B. In "Biological Aspects of Inorganic Chemistry"; Dolphin, D., Ed.; Wiley: New York, 1977, Chapter 10.
39. Brautigan, D.L.; Ferguson-Miller, S.; Margoliash, E. *J. Biol. Chem.* 1978, 253, 130.
40. Weast, R.C., Ed. "CRC Handbook of Chemistry and Physics", 55th ed.; CRC Press: Cleveland, 1974.
41. Margoliash, E.; Frohwirt, N. *Biochem. J.* 1959, 71, 570.

42. Brautigan, D.L.; Ferguson-Miller, S.; Tarr, G.E.; Margoliash, E. *J. Biol. Chem.* 1978, 253, 140.
43. Myer, Y.P.; McDonald, L.H.; Verma, B.C.; Pande, A. *Biochemistry* 1980, 19, 199.
44. Eddowes, M.J.; Hill, H.A.O. *J. Chem. Soc., Chem. Commun.* 1977, 21, 771.
45. Eddowes, M.J.; Hill, H.A.O.; Uosaki, K. *J. Am. Chem. Soc.* 1979, 101, 7113.
46. Eddowes, M.J.; Hill, H.A.O.; Uosaki, K. *J. Electroanal. Chem.* 1980, 116, 527.
47. Uosaki, K.; Hill, H.A.O. *J. Electroanal. Chem.* 1981, 122, 321.
48. Albery, W.J.; Eddowes, M.J.; Hill, H.A.O. *J. Am. Chem. Soc.* 1981, 103, 3904.
49. Henderson, R.W.; Rawlinson, W.A. *Biochem. J.* 1956, 62, 21.
50. Hawkridge, F.M.; Kuwana, T. *Anal. Chem.* 1973, 45, 1021.
51. Margalit, R.; Schejter, A. *Eur. J. Biochem.* 1973, 32, 492.
52. Bard, A.J.; Faulkner, L.R. "Electrochemical Methods: Fundamentals and Applications"; Wiley: New York, 1980; p. 232.
53. Brown, G.M.; Sutin, N. *J. Am. Chem. Soc.* 1979, 101, 883.
54. Cummins, D.; Gray, H.B. *J. Am. Chem. Soc.* 1977, 99, 5158.
55. Mauk, A.G.; Scott, R.A.; Gray, H.B. *J. Am. Chem. Soc.* 1980, 102, 4360.
56. Stellwagen, E.; Shulman, R.G. *J. Mol. Biol.* 1973, 75, 683.

57. Matthews, C.R.; Erickson, P.M.; Froebe, C.L. *Biochim. Biophys. Acta* 1980, 624, 499.
58. Matthews, C.R.; Recchia, J.; Froebe, C.L. *Anal. Biochem.* 1981, 112, 329.
59. Cusanovich, M.A. In "Bioorganic Chemistry"; Academic Press: New York, 1978; Vol. IV, Chapter 4.
60. Kassner, R.J. *Proc. Natl. Acad. Sci. USA* 1972, 69, 2263.
61. Kassner, R.J. *J. Am. Chem. Soc.* 1973, 95, 2674.
62. Stellwagen, E. *Nature* 1978, 275, 73.
63. Valentine, J.S.; Sheridan, R.P.; Allen, L.C.; Kahn, P.C. *Proc. Natl. Acad. Sci. USA* 1979, 76, 1009.
64. Sheridan, R.P.; Allen, L.C. *Chem. Phys. Lett.* 1980, 69, 600.